# ANALYSIS OF SPACECRAFT TRAJECTORIES ON THE POLAR AXIS OVER THE EVENT HORIZON OF A STELLAR ORIGINATED ROTATING KERR BLACK HOLE

**BY**


**Seetesh PANDE**

**(P500013232)**


**SUBMITTED**

**IN PARTIAL FULFILMENT OF THE REQUIREMENT OF THE DEGREE OF DOCTOR OF PHILOSOPHY**

**TO**


**UNIVERSITY OF PETROLEUM AND ENERGY STUDIES**

**DEHRADUN**


**Apsril 15, 2013**

**UNIVERSITY OF PETROLEUM AND ENERGY STUDIES**

COLLEGE OF ENGINEERING

THESIS COMPLETION CERTIFICATE

THIS IS TO CERTIFY THAT THE THESIS ON Analysis of Spacecraft Trajectories on the Polar Orbit over the Event Horizon of a Stellar Originated Rotating Kerr Black Hole BY Seetesh Pande IN PARTIAL COMPLETION OF THE REQUIREMENTS FOR THE AWARD OF THE DEGREE OF DOCTOR OF PHILOSOPHY (SCIENCE) IS AN ORIGINAL WORK CARRIED OUT BY HIM UNDER OUR JOINT SUPERVISION AND GUIDANCE.

IT IS CERTIFIED THAT THE WORK HAS NOT BEEN SUBMITTED ANYWHERE ELSE FOR THE AWARD OF ANY OTHER DIPLOMA OR DEGREE OF THIS OR ANY OTHER UNIVERSITY.

Prof. Dr. Ugur GUVEN

(Internal Guide)

# ABSTRACT

Astrodynamic study of a body in the strong gravitating region of a stellar originated rotating Kerr black hole is the objective of this research work. An analysis of particle trajectory in the spacetime of a rotating Kerr black hole is performed and applied for designing an orbit for a spacecraft in these regions. Spherical Polar orbits are considered favorable for a realistic spacecraft approaching a black hole. Such orbits are found to be stable for lower altitudes for a particle approaching near the black hole. Spherical polar orbits at different radii are studied and the corresponding features of these orbits are computed using analytical and numerical techniques. Dragging of spherical polar orbits in the sense of the rotating black hole is calculated for stellar originated rotating Kerr black holes. The effect of frame dragging is studied for a gyroscope following an orbit in Kerr field. The dragging of stellar spherical polar orbits in the Galactic black hole Sgr A* is estimated using similar equations of geodesics in Kerr spacetime. The analogy of a spacecraft in the gravitating region of a stellar black hole with a star orbiting close to a supermassive black hole is established and seen to be two distinct but alike cases of the governing particle trajectory equations in Kerr spacetime. An effort has been made to understand the tidal forces near the rotating black holes by forming an orthonormal tetrad and employing the equations of parallel transport of a tetrad along a general Kerr geodesic and the tidal tensor is calculated for the first time for the specific case of a spherical polar orbit by identifying the set of parallel propagated vectors in these orbits.

# ACKNOWLEDGEMENTS

I gratefully acknowledge the help, guidance and support of my thesis supervisor Prof. Ugur GUVEN for leading me to this research topic. I also acknowledge the University of Petroleum and Energy Studies for providing me the opportunity to pursue my research career.

I would like to thankfully mention Dr. Shantanu Mukherjee, Post Doctoral Fellow at the prestigious Niels Bohr Institute, Denmark, for numerous Skype discussions, during the phase of this thesis, on Physics, Fortran, and Mathematica, whenever required. We have been classmates and friends for more than a decade and together share the unceasing, ever increasing, enthusiasm for Physics since our college days.

A whole lot of credit goes to my mother Smt. Krishna Pande for her thorough support to help me realize this project. Even though far from any scientific background, I truly admire her keen interest and faith towards Science.

Last but not the least let me take this opportunity to thank my teachers and guides at various stages of my education, from Delhi University, Indian Institute of Technology, Delhi, ENS Lyon, Observatoire de Lyon, especially Prof. Ajoy Ghatak ( M.Sc Project Supervisor), Prof. N. Panchapakeshan (B.Sc. Project Guide), Prof. Dilip Ranganathan, Prof. Bruno Guiderdoni ( Observatoire de Lyon, France ) and Prof. David Polarsky (Universite de Montpellier 2, France) , who may appear far, but continue to guide in many ways, through their exemplary acts.

**CERTIFICATE OF EXAMINATION** ..... **i**
**ABSTRACT** ..... **ii**
**ACKNOWLEDGEMENT** ..... **iii**
**TABLE OF CONTENTS** ..... **iv**
**LIST OF SYMBOLS AND ABBREVIATIONS** ..... **vi**
**LIST OF FIGURES** ..... **viii**
**LIST OF TABLES** ..... **xi**
**1. INTRODUCTION TO BLACK HOLES** ..... **1**
1.1 History of Black holes ..... **Error! Bookmark not defined.**
1.2 Mathematical Theory of Black holes ..... 5
1.2.1 Schwarzschild Black holes ..... 6
1.2.2 Kerr Black holes ..... 9
1.3 Properties of Black holes ..... 10
1.3.1 Event Horizon ..... 10
1.3.2 Ergosphere and the Static Limit ..... 11
1.3.3 Laws of Black hole Dynamics ..... 13
1.4 Types of Black holes ..... 16
1.4.1 Stellar Black holes ..... 17
1.4.2 Supermassive Black holes ..... 19
1.4.3 Premordial Black holes ..... **Error! Bookmark not defined.**1
**2. SPACECRAFT TRAJECTORY ANALYSIS** ..... Error! Bookmark not defined.**2**
2.1 General ..... **Error! Bookmark not defined.**3
2.2 The Two Body Problem ..... **Error! Bookmark not defined.**5
2.2.1 Energy Equation ..... 29
2.2.2 Circular Orbits ..... 30
2.2.3 Elliptical Orbits ..... 31
2.2.4 Parabolic Trajectories ..... 33
2.2.5 Hyperbolic Trajectories ..... 35
2.2.6 Perifocal Frames ..... 37
2.2.7 The Lagrange Coefficients ..... 39
2.3 Restricted Three Body Problem ..... 42
**3. ROTATING KERR BLACK HOLES** ..... **46**
3.1 Kerr Geometry ..... 47
3.2 Properties of Kerr Metric ..... 50
3.2.1 The Event Horizon ..... 51
3.2.2 Frame Dragging ..... 52
3.2.3 Ergosphere and Static Limit ..... 53
3.3 Effect on Outer Bodies ..... 56

**4. PARTICLE TRAJECTORY IN KERR SPACETIME ..... 57**
4.1 Constants of Motion in Kerr spacetime ..... 58
4.2 Equatorial Geodesics in Kerr spacetime ..... 60
4.3 The General Equations of Geodesics in Kerr spacetime ..... 64
4.4 Keplerian Orbits in Kerr spacetime ..... 68
**5. POLAR ORBITS IN KERR SPACETIME ..... 74**
5.1 Spherical Polar orbits in Kerr spacetime ..... 76
5.2 Frame Dragging of Polar Orbits ..... 79
5.3 Non Spherical Polar Orbits ..... 80
5.4 Precission of Gyroscopes ..... 82
5.5 Numerical Simulation of Spherical Polar Orbits ..... 86
**6. RELATIVISTIC EFFECTS ON SPACECRAFT IN KERR SPACETIME . 91**
6.1 Parallel Transport in Kerr Geometry ..... 91
6.2 Tidal Tensor ..... 96
6.3 Tidal Tensor on the Symettry Axis ..... 98
6.4 Tidal Tensor along the Spherical Polar Orbit ..... 101
6.5 Time Dilation in Spherical Polar Orbits ..... 105
**7. STELLAR ORBITS AROUND THE SMBH AT MILKYWAY CENTER . 108**
7.1 Stellar Orbits in the Central Arc Second ..... 108
7.2 Dragging Effect in Stellar Shpherical Polar Orbit ..... 111
**CONCLUSION ..... 114**
**REFERENCES ..... 115**
**APPENDICES ..... 120**
**CV ..... 128**

# LIST OF SYMBOLS AND ABBREVIATIONS

| | |
|---|---|
| $\mu, \nu$ | *4-coordinate indices*, 0,1,2,3. |
| $i, j$ | *spatial coordinate indices*,1,2,3. |
| $g_{\mu\nu}$ | *spacetime metric* |
| $c$ | *speed of light* |
| $M_{\odot}$ | *Solar mass* |
| $x_{\mu}$ | *event, greek indices* 0,1,2,3 |
| $u_i$ | *space components of four velocity* |
| $\eta_{\mu\nu}$ | *metric in flat spacetime* = diag(-1,1,1,1) |
| $\Gamma^{\mu}_{\nu\rho}$ | *Christoffel symbols* |
| $t$ | *Coordinate time* |
| $\tau$ | *Proper time* |
| $r$ | *Spherical Radial coordinate* |
| $\theta$ | *Spherical Angular coordinate* |
| $\phi$ | *Spherical Azimuth coordinate* |
| $E$ | *Energy, Constant of Motion* |
| $L, \Phi$ | *Angular Momentum, Constant of Motion* |
| $C$,$K$ | *Carter's Constant* |

| | |
|---|---|
| $G$ | *Gravitation Constant* |
| $R_{abcd}$ | *Riemann curvature Tensor* |
| $G_{\mu\nu}$ | *Einstein Tensor* |
| $T_{\mu\nu}$ | *Energy Momentum Tensor* |
| $\Delta$ | $= r^2 - 2Mr + a^2$ |
| $\rho^2, \Sigma$ | $= r^2 + a^2 \cos^2\theta$ |
| $A$ | $= (r^2 + a^2)^2 - \Delta a^2 \sin^2\theta$ |
| $e$ | *Eccentricity of orbit* |
| $T_\tau$ | *Time period of orbit in spacecraft frame* |
| $T_t$ | *Time period of orbit in asymptotic Lorentz frame* |
| $S^{\hat{\imath}}$ | *Gyroscope spin* |
| $S$ | *Classical Action function* |
| $C_{ij}$ | *Tidal Tensor* |
| $R(r)$ | $\Delta[-C + r^2 - (L - aE)^2] + [E(r^2 + a^2) - La]^2$ |
| $\Theta(\theta)$ | $C + \cos^2\theta \left[(1 + E^2)a^2 - \frac{1}{\sin^2\theta} L^2\right]$ |
| $\Gamma$ | $= (1 - E^2)^{1/2}$ |
| $Q$ | $= K - a^2E^2$ |
| $k$ | $= a\Gamma/Q^{1/2}$ |

# LIST OF FIGURES

Fig 1.1: Effective potential of Schwarzschild Black hole $\widetilde{V}(r)$ vs log(r/M.)……7

Fig 2.1: Differential area swept by vector **r** during interval dt…….28

Fig 2.2: Illustration of Restricted Three Body Problem……42

Fig 4.1: Trajectory of a particle in the Kerr spacetime at a distance of $1000M$ and eccentricity 0 ($a = 0.5$)…….68

Fig 4.2: Trajectory of a particle in the Kerr spacetime at a distance of $1000M$ and eccentricity 0.1 ($a = 0.5$)……..69

Fig 4.3: Trajectory of a particle in the Kerr spacetime at a distance of $1000M$ and eccentricity 0.2 ($a = 0.$)……...70

Fig 4.4: Trajectory of a particle in the Kerr spacetime at a distance of $1000M$ and eccentricity 0.3 ($a = 0.5$)……..70

Fig 4.5: Trajectory of a particle in the Kerr spacetime at a distance of $1000M$ and eccentricity 0.4 ($a = 0.5$)……..71

Fig 4.6: Trajectory of a particle in the Kerr spacetime at a distance of $1000M$ and eccentricity 0.5 ($a = 0.5$)……..71

Fig 4.7: Trajectory of a particle in the Kerr spacetime at a distance of $1000M$ and eccentricity 0.6 ($a = 0.5$)……..72

Fig 4.8: Trajectory of a particle in the Kerr spacetime at a distance of $1000M$ and eccentricity 0.7 ($a = 0.5$)……..72

Fig 4.9: Trajectory of a particle in the Kerr spacetime at a distance of $1000M$ and eccentricity 0.8 ($a = 0.5$)……..73

Fig 4.10: Trajectory of a particle in the Kerr spacetime at a distance of $1000M$ and eccentricity 0.9 ($a = 0.5$)……73

Fig 5.1: Effective potential *vs* log *r/M* for Kerr spacetime, for four different values of Carter's constant……76

Fig 5.2a: Temporal evolution of a spherical polar orbit in the x-y-z space……...77

Fig 5.2b: Spherical polar orbits in the x-y plane……78

Fig 5.3 : Variation of $\theta, \phi$ coordinates with respect to $\tau$ for an orbit of radius $10M$……78

Fig 5.4a: The plots show variation of $\theta$ and $\phi$ coordinates of the Boyer Lindquist coordinate system and trajectory of a particle in spherical polar orbit at $r = 5M_{\odot}$……87

Fig 5.4b: The plots show variation of $\theta$ and $\phi$ coordinates of the Boyer Lindquist coordinate system and trajectory of a particle in spherical polar orbit at $r = 10M_{\odot}$…….....87

Fig 5.4c: The plots show variation of $\theta$ and $\phi$ coordinates of the Boyer Lindquist coordinate system and trajectory of a particle in spherical polar orbit at $r = 10M_{\odot}$ ……88

Fig 5.4d: The plots show variation of $\theta$ and $\phi$ coordinates of the Boyer Lindquist coordinate system and trajectory of a particle in spherical polar orbit at $r = 100M_{\odot}$ ……..89

Fig 5.4e: The plots show variation of $\theta$ and $\phi$ coordinates of the Boyer Lindquist coordinate system and trajectory of a particle spherical polar orbit at $r = 500M_{\odot}$……...89

Fig 5.4f: The plots show variation of $\theta$ and $\phi$ coordinates of the Boyer Lindquist coordinate system and trajectory of a particle in spherical polar orbit at $r = 1000M_{\odot}$. ……..……..90

Fig 7.1: Stellar orbits in the central arc second of the Milky Way. (*Courtesy Keck/UCLA Galactic Center Group.*)……110

Fig 7.2: Image of stars in the Sgr A* region. (*Courtesy Keck/UCLA Galactic Center Group.*)…….111

# LIST OF TABLES

Table 6.1 Energy, Carter's constant, $\delta\phi$ and Time Periods $T_t, T_\tau$ for spherical orbits of different radii for a Kerr black hole with $a = 0.8M_\odot$ ……106

Table 7.1 Orbital Periods of S stars in the galactic central arc second……110

Table 7.2 Energy associated and the corresponding frame dragging effect for different radii for a SMBH of mass $4.06 \times 10^6 M_\odot$ and Kerr parameter $a = 0.52M_\odot$……112

Table 7.3 Energy associated and the corresponding frame dragging effect for different radii for a SMBH of mass $4.06 \times 10^6 M_\odot$ and Kerr parameter $a = 0.75M_\odot$……113

Table 7.4 Energy associated and the corresponding frame dragging effect for different radii for a SMBH of mass $4.06 \times 10^6 M_\odot$ and Kerr parameter $a = 0.95M_\odot$……113

# Chapter 1

# Introduction to Black Holes

Since the advent of the General Theory of Relativity by Albert Einstein by 1915, the concepts of singularity and the concept of infinite curvature as a black hole has become a widely discussed concept. For many years, astronomers and astrophysicists have discussed the possibility of existence of such objects. Theoretical as well as observational work has been conducted on the subject. In fact, many eminent scientists such as Schwarzchild, Kerr, Penrose, Hawking have explored the concept of black holes and all that it pertains. Even with the scientific and observational capabilities of the 21$^{st}$ century, the concept of black holes still remains a mystery to some extent.

An object with highly strong gravitational field such that even light cannot escape from its surface and with a singularity at its centre is termed as a black hole. Here we discuss the spatial aspects related to these black holes, the theoretical developments on the subject, nature of the space-time around black holes as predicted by the mathematical theory of black holes, and also, the observational advancements in this field to date.

Black holes have been seen gaining ever more attention since the recent discoveries of black holes at the centre of galaxies like our own. Now it is widely starting to be believed that the supermassive black holes in galactic centers are the central engines for any and all of galactic formations. Black holes have finally started to enjoy the attention that they long deserved. They are no more the hidden monsters feeding away stellar companions, but on the contrary, they are now the objects closely related to the origin of galaxies and to the large scale structure formation in the universe.

In case of stellar black holes, it is now known that it is the result of a gravitational collapse of a star (with mass $M > 3\,M_{sun}$) at the end of its evolution. Such a

continuous gravitational collapse leads to an implosion and subsequent formation of a subspace called the event horizon of the black hole. A limiting radius $r_g = 2GM/c^2$, called the gravitational radius or the *event horizon,* for a black hole of mass M exists such that the escape velocity of any particle leaving its boundary is equal to the speed of light. Thus no signal or particles can ever leave the boundary of the black hole. This makes it a challenge to identify a black hole in space, since it does not reflect or produce any signals to directly detect its presence.

Einstein's theory of Gravitation has successfully provided a framework to study the nature of space-time around black holes. We would intend to have a close look at the physical characteristics of space-time in the vicinity of stellar black holes and calculate the spacecraft trajectories in such extremely curved spacetimes. We conduct a numerical and computational study of the geodesics in strongly curved spacetime using the appropriate mathematical equations describing motion in these spacetimes as elaborated in the black hole theory.

## 1.1 History of Black Holes

The term *black hole* was coined first by John A. Wheeler in 1967 [1], however the object existed in theory long before. The first formal theoretical description of these objects was given by Karl Schwarzschild when he found the exact solutions of Einstein equations for spherically symmetric distribution of mass in vacuum [2]. The physical existence of such objects remained as an open forum of discussion since the Schwarzschild solutions were discovered, and even Einstein did not approve the fact that the nature could be hiding objects of the size of gravitational radius.

The work of Subramanian Chandrasekhar [3] on white dwarf stars in the thirties brought light to compact objects. Chandrasekhar's work showed that a star less massive than 1.4 $M_{sun}$, at the end of its evolution, could balance the gravitational collapse by its electron degeneracy pressure and thus exist as a highly dense compact object termed as white dwarf stars.

Subsequent theoretical work by Landau in 1932 [4], Baade and Zwicky in 1934 [5], Oppenheimer and Volkoff in 1939 [6] showed us that the neutron stars could also exist in nature and interestingly the limits on their radii was only a few times of the order of the gravitational radius $r_g$. Without much of a delay, appeared the first paper by Oppenheimer and Snyder in 1939 [7] on the continuous gravitational collapse of massive stars to gravitational radius.

The final stage of the massive stars were termed as *frozen* or *collapsed stars* and considered to be more of dead objects in space than object of any promising research. The scenario changed a decade later with contributions majorly from Kruskal [8], who obtained the complete solution of the Schwarzschild problem and removed the '*spherical singularity'* at $r = r_g$ and presented a maximal singularity free extension of the Schwarzschild metric.

The next astonishing development in the field of black holes was the work by Roy Kerr in 1965 [9] in which he introduced the Kerr metric describing the space-time around the more general *rotating black hole*. Kerr's paper was a sensation in the physics community as even Einstein had doubts that such solutions could exist. This was a major breakthrough for relativists working on black holes as it provided complete solutions to rotating spacetime and give the equations of motion in rotating space-time using the principles of general relativity.

Kerr's solution was a milestone in the development of the theory of black holes. A few years later the term *black hole* was coined and apart from some hesitations it was widely accepted by the theoreticians. A substantial amount of work on black holes was developed in the following years. What was considered as an exotic object came to the main stream research, with theories developing on the formation, evolution, properties of black holes, its interactions with matter and classical fields, to two black holes collision, and black hole dynamics, which were all discussed at full length in the scientific community now. A Black hole no longer remained a strange dubious character but took the form of an entity

describing the ultimate form of compressed matter and extreme spacetime curvature.

A black hole has been proven to be described by only three parameters, its mass, angular momentum and its charge. The famous theorem 'black hole has no hair' stated this fact that a black hole has only three attributes required for its complete description [10]. Now the black hole theory been substantially developed, a search for black holes in the outer space was an obvious longing among both relativists and astrophysicists.

Neutron stars were discovered in the end of the sixties [11] and theoreticians like Zel'dovich and Zwicky were proven correct with these new findings. They further suggested that matter accretion onto black holes would be a powerful source of X-ray emission [12] and with the advent of X-ray astronomy and X-ray satellites in parallel, technology was at hand to verify these predictions. Many galactic X-ray sources were starting to be identified by the 1970's and supported the hypothesis that black hole binary systems could be the source behind such X-ray detections.

Many X-ray sources were now discovered by the spatial satellites, the first being Sco X1 in the constellation Scorpio by a team led by Riccardo Giaconni [13] in 1962. The powerful X-ray source near the constellation Cygnus, termed as Cygnus X-1, was first discovered in 1964 and is now considered as a strong candidate of a black hole binary system. It consists of an X-ray source and a companion star HD226868 with masses estimated 16 $M_{solar}$ and 20 $M_{solar}$ respectively [14]. Presently there are a number of such binaries with dark companions found in our galaxy [14], and advanced X-ray telescopes such as Chandra [15] are in the continuous search for such valuable discoveries.

The discovery of stellar black hole candidates in the galaxy was a strong observational evidence of the black hole theory which was getting developed throughout sixties and seventies. Much advancement in the black hole theory were done during and after this period and a theoretical formulation of black hole

physics hence paved its way to the contemporary mainstream astrophysics research.

## 1.2 Mathematical Theory of Black Holes

The Black hole theory is an important extension of the Einstein's General Theory of Relativity [10], where the space-time curvature $R_{\mu\nu}$ and the Energy Momentum $T_{\mu\nu}$ tensor are unified to give the Einstein's Equation's which in turn give the complete set of equations of motion in the particular space-time geometry given by the metric $g_{\mu\nu}$. Einstein equation can be expressed as ($G = c = 1$)

$$G_{\mu\nu} = 8\pi T_{\mu\nu} \tag{1.1}$$

Where, $G_{\mu\nu}$ is the Einstein tensor dervied by contracting the Riemann curvature tensor $R_{\mu\nu\alpha\beta}$.

The curvature tensor is calculated using the Christoffel symbols ($\Gamma^{\alpha}_{\beta\gamma}$) which are functions of the metric $g_{\mu\nu}$:

$$R^{\mu}_{\nu\alpha\beta} = \frac{\partial \Gamma^{\mu}_{\nu\beta}}{\partial x^{\alpha}} - \frac{\partial \Gamma^{\mu}_{\nu\alpha}}{\partial x^{\beta}} + \Gamma^{\mu}_{\rho\alpha}\Gamma^{\rho}_{\nu\beta} - \Gamma^{\mu}_{\rho\beta}\Gamma^{\rho}_{\nu\alpha} \tag{1.2}$$

where the Christoffel symbols for the metric are given as:

$$\Gamma^{\sigma}_{\lambda\mu} = \frac{1}{2} g^{\nu\alpha}\left(\frac{\partial g_{\mu\nu}}{\partial x^{\lambda}} + \frac{\partial g_{\lambda\nu}}{\partial x^{\mu}} - \frac{\partial g_{\mu\nu}}{\partial x^{\nu}}\right) \tag{1.3}$$

and the invariant line element is expressed as

$$ds^2 = g_{\mu\nu} dx^{\mu} dx^{\nu} \tag{1.4}$$

The form of line elements related to the study of black holes are the Schwarzschild line element expressed in Schwarzschild coordinates $(t, r, \theta, \phi)$ and the more general Kerr line element in the Boyer Lindquist coordinates $(t, r, \theta, \phi)$ discussed in the following subsections.

### 1.2.1 Schwarzschild Black Holes

Karl Schwarzschild solved the Einstein's equations for a spherical distribution of matter of mass M to obtain the space-time geometry which is given in the form of Schwarzschild metric (G = c = 1):

$$ds^2 = -\left(1-\frac{2M}{r}\right)dt^2 + \left(1-\frac{2M}{r}\right)^{-1}dr^2 + r^2(\,d\theta^2 + \sin^2\theta d\phi^2) \qquad (1.5)$$

In case of a gravitational collapse of the above spherical distribution of mass to a size less than $r_g$, in absence of any outward pressure, a black hole is expected to be formed. A Schwarzschild black hole is the typical case of a more general charged and rotating black hole. The gravitational field outside the Schwarzschild black hole asymptotically reaches the Newtonian field. However near the Schwarzschild radius the space-time is strongly curved and the equations of motion are no more purely Newtonian and are described by the general relativistic equations.

The Schwarzschild line element (1.2) is independent in $t$ and $\phi$ coordinates, in other words the line element is *cyclic* in $t$ and $\phi$, therefore the corresponding conjugate momenta $p_t \equiv -E$ and $p_\phi = \pm L$ are conserved along the trajectories. If we consider motion along the equator such that $p^\theta = \frac{d\theta}{d\lambda} = 0$, in this particular choice of coordinates we find the **4**–vector of energy momentum as given by the rest mass of the particle,

$$g_{\alpha\beta}p^\alpha p^\beta + \mu^2 = g^{\alpha\beta}p_\alpha p_\beta + \mu^2 = 0 \qquad (1.6)$$

gives,

$$-\frac{E^2}{\left(1-\frac{2M}{r}\right)} + \frac{1}{\left(1-\frac{2M}{r}\right)}\left(\frac{dr}{d\lambda}\right)^2 + \frac{L^2}{r^2} + \mu^2 = 0 \qquad (1.7)$$

By the equivalence principle, we know that regardless of mass all test particles follow the same world lines, so we consider the quantities in terms of per unit mass, $\check{E} = E/\mu$ , $\tilde{L} = L/\mu$ and $\lambda = \tau/\mu$ . With these substitutions we deduce the change of $r$ coordinate with respect to proper time without the rest mass appearing in the equation,

$$\left(\frac{dr}{d\tau}\right)^2 = \tilde{E}^2 - (1 - 2M/r)\left(1 + \tilde{L}^2/r^2\right) \qquad (1.8)$$

$$= \tilde{E}^2 - \tilde{V}^2(r) \qquad (1.9)$$

where

$$\tilde{V}(r) = \left[\left(1 - \frac{2M}{r}\right)\left(1 + \frac{\tilde{L}^2}{r^2}\right)\right]^{1/2} \qquad (1.10)$$

is the *effective potential* in the Schwarzschild space-time .

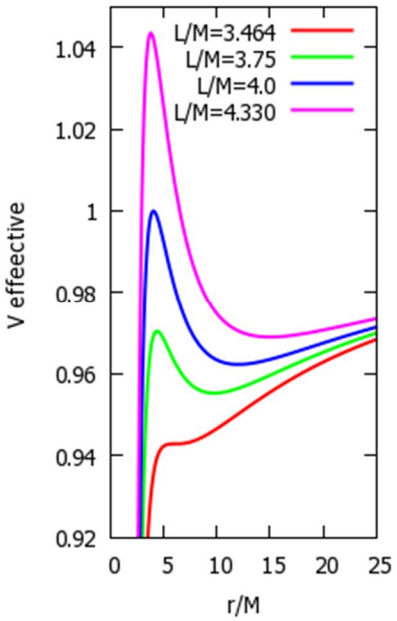


**Fig 1.1** *Effective potential of Schwarzschild Black hole* $\tilde{V}(r)$ vs log(*r/M.*)

Fig.1 shows the variation of effective potential for different $\tilde{L}/M$ values, here x-axis is $\log r/M$ and plotted on the y-axis is the effective potential $\tilde{V}$

Newtonian limit ($\left|\tilde{E}-1\right| \ll 1, M/r \ll 1, \tilde{L}/r \ll 1$) , the particle orbits are Keplerian and depending on their energies are either reflected off by the effective potential or are trapped in the effective potential well and move back and forth between periastron and apastron.

In the case of relativistic orbits:

**a)** Orbits with periastron at $r \gg M$ are Keplerian in form except for the periastron shift as observed in Mercury's orbit.

**b)** Orbits with periastron at $r \leq 10M$ differ significantly from Keplerian orbits.

**c)** As seen from **Fig 1** for $\tilde{L} \leq 2\sqrt{3}\,M$ , there is no periastron and any particle will get pulled into the region $r = 2M$ .

**d)** For $2\sqrt{3} \leq \tilde{L}/M \leq 4$ there are orbits in which the particle moves between the periastron and apastron and any particle with $\tilde{E}^2 \geq 1$ coming from $r = \infty$ gets pulled into the region $r = 2M$.

**e)** For $\tilde{L}/M > 4$ there are bound orbits with and moreover particles coming from $r = \infty$ with energies less than $\tilde{V}_{max}$ will reach a periastron and return to $r = \infty$, and particles with energies greater than $\tilde{V}_{max}$ coming in from $r = \infty$ will eventually get pulled into the region $r = 2M$.

**f)** The stable orbits exist at the minimum of the effective potential and the most tightly bound stable orbit exist for $\tilde{L}/M = 2\sqrt{3}$ at $r = 6M$ , these inner-most stable circular orbits are also studied closely for the accretion of matter around compact objects such as Neutron stars.

Another key feature of the motion in Schwarzschild spacetime is that even though an incoming particle takes a finite amount of proper time $\tau$ to reach the surface $r = 2M$, of a Schwarzschild black hole, the coordinate time $t$ elapsed in this journey comes out to be infinite [10,16].This however is a manifestation of the singularity inherent of the Schwarzschild coordinates and it can be removed with a proper choice of coordinate system such as the one given by Kruskal [8].

### 1.2.2 Kerr Black Holes

The more general case, a rotating black holes is described by the Kerr Metric, discovered by Roy Kerr in 1963 [9]. Kerr metric is an analytic description of the spacetime around a rotating black hole and provides framework for developing equations of motion in a rotating geometry. Many new facets and properties of these objects and the related spacetime are distinctly identified with the aid of Kerr metric. The metric written in Boyer Lindquist coordinates [17], a generalization of Schwarzschild coordinates, for a black hole of mass $\boldsymbol{M}$, angular momentum $\boldsymbol{S}$ and charge $\boldsymbol{Q}$, is as follows,

$$ds^2 = -\frac{\Delta}{\rho^2}[dt - \text{asin}^2\,\theta\ d\phi]^2 + \frac{\sin^2\theta}{\rho^2}[(r^2 + a^2)d\phi - adt]^2 + \frac{\rho^2}{\Delta}dr^2 + \rho^2 d\theta^2 \qquad (1.11)$$

where,

$$\Delta \equiv r^2 - 2Mr + a^2 + Q^2 \qquad (1.12)$$

$$\rho^2 \equiv r^2 + a^2\cos^2\theta \qquad (1.13)$$

$$a \equiv S/M \equiv \text{angular momentum per unit mass} \qquad (1.14)$$

As discussed in the previous section, the smooth gravitational collapse of a non rotating mass would result in a stationary and spherically symmetric black hole as the radius of the collapsing body becomes less than the gravitational radius $r_g$. If the mass is initially rotating, then the laws of physics will require the body to conserve its angular momentum, and the gravitational pull would produce a black hole rotating even more rapidly along with the gravitational shrink. Another property that can be attributed to this system is the charge of the body which can be non zero and will also be preserved during the collapse. These three quantities, mass, angular momentum and the charge, are the only quantities which are necessary and sufficient to describe the most general type of black holes that can be found in nature.

A detailed study on the Kerr metric, its derivation, the spacetime structure around Kerr black hole and the subsequent equations of motions of particles in Kerr Spacetime are presented in chapter 3 of the thesis.

## 1.3 Properties of Black Holes

A black hole of sufficient generality is a charged and rotating black hole and is mathematically described by the Kerr metric given in the previous section. The Kerr metric reveals a number of interesting properties on the spacetime around these objects and brings insight to many new phenomenon previously unknown to the realm of physics. What follows from the metric in a straightforward manner are the concepts of event horizon, ergosphere, frame dragging, static limit and singularity, which are concepts related purely to the spacetime of rotating black holes.

### 1.3.1 Event Horizon

The event horizon of a black hole is in other words the boundary of the black hole beyond which it is impossible to extract any information about the fate of an object pulled by the gravity of the black hole. Since not even light can escape from this region any information once gone inside the event horizon is permanently lost to the universe and can never be retrieved, therefore it is termed as event horizon as the events beyond this region are undetectable are and cut-off from the outer world.

For a Schwarzschild black hole the event horizon is a perfect sphere, of radius $r_g = 2M$, which is the gravitational radius of the black hole. However for a rotating black hole there are two different such horizons which are described by the vanishing of the quantity $\Delta$, i.e.

$$\Delta \equiv r^2 - 2Mr + a^2 + Q^2 = 0 \qquad (1.15)$$

giving roots, $r_+ = M + \sqrt{M^2 - a^2 - Q^2}$, termed as the event horizon, and in addition $r_- = M - \sqrt{M^2 - a^2 - Q^2}$ termed as the Cauchy horizon. We will be concerned about the event horizon $r_+$ as the Cauchy horizon is beyond the scope of this work.

The area of the black hole $A$ plays an important role in the black hole dynamics and is given as the area enclosed by the surface of the event horizon of the black hole.

area of Schwarzschild black hole is thus,

$$A = 4\pi(2M)^2 \qquad (1.16)$$

Whereas the area of a Kerr black hole is given as,

$$A = 4\pi(r_+ + a^2) = 4\pi(M + \sqrt{M^2 - a^2 - Q^2} + a^2) \qquad (1.17)$$

Area of a black hole is an irreducible property and once an area has been attained it can never be decreased.

### 1.3.2 Ergosphere and the Static Limit

One difference between the Schwarzschild and Kerr spacetime is that in the case of Kerr metric the event horizon given by $r_+$ does not coincide with the surface $g_{tt} = 0$. The Kerr metric which can also be written in the following form:

$$ds^2 = -\frac{1}{\rho^2}[\Delta - a^2 \sin^2\theta]dt^2 + \frac{\sin^2\theta}{\rho^2}[-\Delta a^2 \sin^2\theta + (r^2 + a^2)^2]d\phi^2 - 2\frac{(2Mr - Q^2)a \sin^2\theta}{\rho^2}dtd\phi + \frac{\rho^2}{\Delta}dr^2 + \rho^2 d\theta^2 \qquad (1.18)$$

has

$$g_{tt} = \frac{1}{\rho^2}[\Delta - a^2 \sin^2\theta] \qquad (1.19)$$

which vanishes when,

$$[\Delta - a^2 \sin^2 \theta] = 0 \qquad (1.20)$$

or,

$$r^2 - 2Mr + a^2 \cos^2 \theta + Q^2 = 0, \qquad (1.21)$$

i.e. at the surface,

$$r = r_e(\theta) = M + \sqrt{M^2 - Q^2 - a^2 \cos^2 \theta} \qquad (1.22)$$

This surface touches the event horizon only at the poles ( $\theta = 0, \pi$). The region between the surface $r_e$ and the event horizon $r_+$, is known as the ergosphere ( $r_e < r < r_+$). It has very important consequences that though the $g_{tt}$ changes sign beyond the ergosphere, metric becoming timelike to spacelike, it is still possible for a particle or light to cross the ergosphere boundary, experience the spacelike region ($g_{tt} > 0$) and still escape from this region and reach infinity. Roger Penrose [18] used this concept to suggest that it is possible to extract energy from a black hole by exploiting this region.

If an observer in Kerr spacetime moves in an orbit with fixed ( $r, \theta$) with a uniform angular velocity with respect to the asymptotic Lorentz frame, he will observe no change in the local neighborhood and will be *stationary* relative to the local geometry. If we want to calculate the angular velocity of this stationary observer in the asymptotic Lorentz frame, we can define

$$\Omega \equiv \frac{d\phi}{dt} = \frac{d\phi/d\tau}{dt/d\tau} = \frac{u^\phi}{u^t} \qquad (1.23)$$

The 4-velovity $\boldsymbol{u}$ of this stationary observer in terms of the Killing vectors associated with the symmetries in $t$ and $\phi$ coordinates, will then be

$$\boldsymbol{u} = u^t \left(\frac{\partial}{\partial t} + \frac{\Omega\, \partial}{\partial \phi}\right) = \frac{\xi_t + \Omega \xi_\phi}{|\xi_t + \Omega \xi_\phi|} \qquad (1.24)$$

$$= \frac{\xi_t + \Omega \xi_\phi}{\left(-g_{tt} - 2\Omega g_{t\phi} - \Omega^2 g_{\phi\phi}\right)^{1/2}} \qquad (1.25)$$

The above expression for the 4-velocity $\boldsymbol{u}$ will be timelike only when,

$$g_{tt} + 2\Omega g_{t\phi} + \Omega^2 g_{\phi\phi} < 0 \qquad (1.26)$$

Hence the angular velocity of the stationary observer will have only certain values which lie between the roots of the above equation, viz:

$$\Omega_{min} < \Omega < \Omega_{max} \qquad (1.27)$$

where,

$$\Omega_{min} = \omega - \sqrt{\omega^2 - g_{tt}/g_{\phi\phi}} \qquad (1.28)$$

$$\Omega_{max} = \omega + \sqrt{\omega^2 - g_{tt}/g_{\phi\phi}} \qquad (1.29)$$

$$\omega \equiv \frac{1}{2}(\Omega_{min} + \Omega_{max}) = -\frac{g_{\phi t}}{g_{\phi\phi}} = \frac{(2Mr - Q^2)a}{(r^2+a^2)^2 - \Delta a^2 \sin^2\theta} \qquad (1.30)$$

At the surface of the ergosphere, where $g_{tt}$ vanishes, one observes from the above equation that $\Omega_{min}$ becomes zero, implying that the locally stationary observer at the surface of the ergosphere must also rotate with the black hole. Thus the surface of the ergosphere is also known as the *static limit*, as the local observer can never be static with respect to the asymptotic Lorentz frame. Since the local inertial frames are essentially dragged with the spacetime of the black hole the effect is termed as *frame dragging*.

### 1.3.3 Laws of Black Hole Dynamics

The two important laws concerning black hole physics are stated as the first and the second law of black hole dynamics. These laws were given the name *laws of black hole dynamics* by Werner Israel [19] and are analogous to the laws of

thermodynamic as expounded by Stephen Hawking in his original research on the thermodynamics of black holes [20,21].

The analogy of black hole physics with thermodynamics is carried out as follows; the quantities surface gravity, area and mass of the black hole play the roles of temperature, entropy and the internal energy respectively, and mathematically denoted as ( $\hbar = c = k = 1$ ):

$\theta \equiv \kappa$ , the temperature of the black hole corresponds to the surface gravity of the black hole.

$S \equiv A$ , the entropy of the black hole corresponds to the area of the black hole

$E \equiv M$ , the internal energy corresponds to the mass of the black hole.

The ***Zeroth law of black hole dynamics*** states that: *The surface gravity κ of a stationary black hole is constant everywhere on the surface of the event horizon.* Just as the thermodynamics does not allow equilibrium for a system if different parts of the system are at different temperature, so does the zeroth law of black hole dynamics does not allow different surface gravities at different regions of the event horizon.

The ***First law of black hole dynamics*** is simply the restatement of the laws of conservation of total energy, 4-momentum and the angular momentum of the black holes in addition to the law of conservation of total charge of the black hole. It has been stated in literature as: *When a black hole chances from one stationary state to another, its mass changes by*

$$dM = \theta dS + \Omega\, dJ + \Phi dQ + \delta E_{gw} \qquad (1.31)$$

*where dJ and dQ are the changes in total angular momentum and charge of the black hole and $\delta E_{gw}$ is the energy radiated by the black hole in the form of gravitational radiation.*

For example if we consider the specialized case when two black holes collide and coalesce, then the first law says that

$$\boldsymbol{P}_1 + \boldsymbol{P}_2 = \boldsymbol{P}_3 + \boldsymbol{P}_{gw} \quad (1.32)$$

and

$$\boldsymbol{J}_1 + \boldsymbol{J}_2 = \boldsymbol{J}_3 + \boldsymbol{J}_{gw} \quad (1.33)$$

where $\boldsymbol{P}_1(\boldsymbol{J}_1), \boldsymbol{P}_2(\boldsymbol{J}_2), \boldsymbol{P}_3(\boldsymbol{J}_3)$, are the 4-momenta (total angular momentum tensors) of the first, second and final black hole and $\boldsymbol{P}_{gw}(\boldsymbol{J}_{gw})$ is the total 4-momentum (angular momentum) radiated as gravitational waves.

The ***Second law of black hole dynamics*** is stated in many different forms in literature and it primarily exploits the second law of thermodynamics which prohibits the decrease of entropy in any system in nature. It states that *in any process involving black holes such as matter falling in a black hole or collision or scattering of two or several black holes, the sum of the surface areas of all the black holes involved can never decrease.*

i.e.

$$\Delta A \geq 0 \quad (1.34)$$

The surface area of a black hole is given as

$$A = 4\pi(r_+ + a^2) = 4\pi \left[M + \sqrt{M^2 - Q^2 - a^2} + a^2\right] \quad (1.35)$$

Howsoever the interaction of the black hole with matter and fields change the black hole parameters $M, Q, a$ in various ways, the mass and angular momentum of the black hole can even decreased through processes such as Penrose process [18] where the rotational energy can be extracted from a black hole, the total surface area of the black hole can never decrease and if once increased the total area can never be brought to its initial value.

Based on this law the black hole processes can be classified in two groups viz.

a) *Reversible Transformations:* When the area is fixed, a set of parameters $M, Q, a$ after a transformation can again be brought back to their initial set

of values. Such processes are therefore termed as reversible processes since the area does not change in the process.

b) *Irreversible Transformations*: If we change the values of the parameters $M, Q, a$ in such a way that the area is increased then we cannot by any process get back to the same set of these parameters. Such processes are therefore termed as irreversible as the second law of black hole dynamics does not allow further decrease in the surface area of the black hole by any process.

Another concept related to the irreducibility of the surface area of the black hole is the *irreducible mass* inherent for any black hole. The irreducible mass of a black hole is the mass given in terms of the Schwarzschild surface area of a black hole which is

$$A = 4\pi(2M)^2 \qquad (1.36)$$

The irreducible mass therefore is,

$$M_{ir} = (A/16\pi)^{1/2} \qquad (1.37)$$

The final mass in terms of irreducible mass can be expressed as (with $S = Ma$).

$$M = (M_{ir} + Q^2/4M_{ir})^2 + S^2/4M_{ir}^2 \qquad (1.38)$$

Thus the total mass energy of the black hole can be viewed as the sum of its irreducible mass, an electromagnetic energy and a rotational energy. If we remove through some process the rotational energy and the electromagnetic energy from the black hole, the final mass will be reduced to the irreducible mass which will be as expected, the Schwarzschild mass of the black hole.

## 1.4 Types of Black Holes

In terms of spacetime structures, black holes can be either a non rotating Schwarzschild black hole or a rotating Kerr black hole. In astrophysical point of

view the black holes are primarily classified as Stellar black holes, Supermassive black holes, and Premordial black holes. The evidences for each type of these black holes are a key area of study in observational astrophysics. The detection methods and techniques advance with the increase in understanding of the underlying physics and the technological advancements in space based detectors and telescopes. X-ray astronomy and Gamma Ray Bursts observatories provide important necessary clues to sort out the right candidates for black holes in the outer universe. We discuss the physical phenomena that can lead to discoveries of each of these objects and the present day status of the field of black hole detections.

### 1.4.1 Stellar Black Holes

A star is an example of thermo gravity equilibrium where the gravitational pull of the matter of which it is composed, mainly hydrogen, is balanced by the radiation pressure of the nuclear fusion taking place inside the star, mainly hydrogen to helium. A star spends most of its life in this process of converting hydrogen into helium and radiating the energy in the form of radiation pressure and photons. The question arises of what happens whence the star has converted all its hydrogen to helium. The star starts to shrink and heat due to its gravity until a temperature is reached where its helium nuclei start to fuse together and form carbon, and once again another cycle of helium to carbon conversion saves the star from its inward gravitational pull and so on. The process continues till most of its central matter is converted to nickel which is the most stable form of atomic nuclei ceasing any further fusion reactions. Then it would start the final state of the stellar cycle. The star is incapable of further nuclear fusions and thus incapable to avoid its gravitational shrinkage. Its fate is now decided by only one parameter which is its initial mass.

If the initial mass of the star was less than 1.4 times solar mass ($1.4\ M_{\odot}$), then a phenomena known as the *electron degeneracy pressure* comes to the rescue of the and balances the inward gravitational pull of the star to form a stable white dwarf

star. This limit for the electron degeneracy pressure was given by Subramanian Chandrasekhar and is named after him as the *Chandrasekhar limit* [22].

A slightly massive star with the initial mass up to 2-3 times solar mass, saves itself from gravitational collapse by a phenomena known as the *neutron degeneracy pressure*, suggested by Zwicky in the early thirties, and this upper limit on the initial mass of the star is known as the *Oppenheimer-Volkoff limit* [6]. There are also a various phenomena such as steady mass loss, the catastrophic mass ejection and the supernovae explosions which can bring an initially massive star to these limits at its final evolution and thereby saving the star to a white dwarf or a neutron star fate [23].

The massive stars for which the neutron degeneracy pressure can not balance out the gravitational collapse are destined to a fate of a *stellar black hole*. The continuous gravitational collapse causes the star to shrink just to its gravitational radius and its spacetime eventually gets cut from the outside universe to form a hole in the spacetime covering a singularity at the center by the event horizon. The physical implications of this spacetime structure are discussed at length in various topics on this thesis and here we concern ourselves with the astrophysical sense of these objects.

If we want to estimate the number density of these stellar black holes in our galaxy we need to know the birth rate of stars, average age of stars, their death rate, and the ratio of massive stars which can be progenitors of these black holes. With these values at hand we can estimate the birth rate of black holes in the galaxy and the total mass of all the stellar black holes in the galaxy to further estimate the density of black holes in the solar neighborhood. According to the related work on this topic [24], it is estimated that $\sim 1$ percent of the visible mass of the galaxy is in the form of these stellar black holes.

#### 1.4.1.1 Disk Accretion onto Black Holes

To detect a field stellar black hole in the interstellar medium from astronomical distances even with the most powerful telescopes would be something like searching an object of thickness of the size of human hair on the moon from earth with the naked eye! Chances are boldly nil. How does one look for these objects in the solar neighborhood? A let alone black hole lurking in the interstellar medium is never expected to be detected from earth. However if the black hole is part of a binary system, such as a black hole accompanying a star or a black hole surrounded by a interstellar dust cloud we can start to have some positive opinion of detecting one. In order to do so we need to understand the underlying physics of such systems in detail and a good amount of work has been done in the literature discussing all the viable cases [25].

The most assuring evidence that stellar black holes exist comes from the study of X-ray binaries. It was pointed out by Novikov and Zel'dovich [12] that X-rays should be produced by the accretion of gas onto compact objects in binary systems. With the advent of X-ray astronomy, various binary systems were studied in detail and by the determination of orbital motions of these systems it was made possible to determine the mass of the compact objects in the binary system. If the masses of the compact objects were greater than the neutron star upper mass limits they were pointed out to be strong candidates of stellar black holes. Cyg X1 is by far the most probable case for a stellar black hole in our part of the galaxy [14].

### 1.4.2 Supermassive Black Holes

The theory of black holes was primarily developed concerning the problem of stellar fate and long before any stellar black hole candidate was discovered, the mathematical background was already prepared in place to deal with all the physical aspects of these objects and their spacetime. On the contrary, the second class of black holes, supermassive black holes (SMBHs), were only inferred first observationally after the discoveries of active galactic nuclei (AGN), upon the

advancement in Radio, X-Ray, and Gamma Ray observatories in the middle of the last century. The visible universe was now merely a fraction of the universe, which was indeed found to be vibrant in the whole electromagnetic spectrum, once these observatories were largely developed and started to give the observations.

Many new discoveries of objects and physical phenomenon were made with the help of these telescopes enhancing our understanding of the universe many a folds. The most important of these discoveries were the powerful sources of radiations in the radio, infrared, hard ultraviolet, X-ray, and gamma regions of the electromagnetic spectrum, coming from the centers of certain galaxies (AGN). In some cases the full luminosity of the nucleus is million times the luminosity of the quieter galaxies. Quasars, which form a subclass of AGN are the most powerful sources of energy seen in the universe and yet their sizes are inferred to be only a few light hours [26]. Novikov and Zel'dovich [27] first estimated the mass of these AGN and quasars using the luminosity mass relation and inferred masses of the range $\sim 10^7 M_{sun}$. Such large masses and small linear dimensions indicated that there could be supermassive blackholes at the centers of the quasars and AGN [27,28].

Now it is widely accepted that the AGN contain supermassive black holes at their center with accreting gas disks. Presence of directed jets from the nuclei of certain AGN suggests a rotating black hole and there are observational evidences that these jets are accompanied by gyroscopic precision further supporting the claims for a central rotating black hole [29].

The SMBHs are now no more only related with the AGN but are believed to exist in every galactic center including our own [30]. They are now referred to as dormant SMBHs which make the center of each galaxy and have run out of fuel (gas and dust). Observations suggest that galactic nuclei are more populous at higher $z$ epochs [31].Very recent works in this domain are shedding light on the importance of SMBHs at the galactic centers, their role in galaxy formations, and

more importantly a strong correlation between the SMBHs mass and the galaxy size suggests that the SMBHs play a key role in galaxy formation and hence the large scale structure of the universe [32]. The origin of these SMBHs at the galactic nuclei is an open area of present day research and will answer the key questions related to our understanding of the structure formation in the universe.

### 1.4.3 Primordial Black Holes

For black holes of mass $M \ll M_{sun}$ to form, would require a very high density to which the matter must be compressed and therefore these black holes are not expected to form in our contemporary universe. However at the very beginning of the expansion of the universe, the density of the universe was enormously high and it would have been possible that black holes were formed at this highly dense epoch. This idea was put forward by Novikov and Zel'dovich in 1967 [33,34] and later by Stephen Hawking in 1971[35]. Such black holes are called *primordial.* Primordial black holes are important for a process known as Hawking quantum evaporation which require small-mass black holes of $M \approx 5 \times 10^{14} g$ that can evaporate in an observational period of $10^{10}$ years of the history of the universe. These small mass black holes can only be primordial. For stellar and SMBH the quantum evaporation period is much greater than the age of the universe and can be neglected.

Primordial black hole density at the present epoch or at the earlier epochs can give crucial information about the structure formation of the universe. Radiation from primordial black hole at the earlier epoch of their formation could have resulted inhomogeneities which could have perturbed the cosmological nucleosynthesis and played an important role in the present large scale structure formation.

Primordial black holes evaporation (explosion) are also sometimes expected to be the cause behind the Gamma Ray Bursts but there have been no observational evidences till date of such connections [36] and the existence of PBHs.

# Chapter 2

# Spacecraft Trajectory Analysis

The discovery of heliocentric model by Copernicus led to the first era of scientific understanding of the motion of the celestial bodies. Tycho Brahe studied the planetary motions in detail and later Keplar utilized those observational data and came up with empirical laws that are since widely referred as the Keplar laws of planetary motion. Isaac Newton discovered the laws of gravitation and formulated the theory of celestial mechanics which explained the Keplar's laws of planetary motion verifying the Newton's theory of gravitation.

The three laws of planetary motion given by Keplar are stated as under:

1.) Planets follow elliptical orbits with Sun at one of the focus.
2.) The radius vector joining the Sun with the planet sweeps out equal area in equal interval of time.
3.) The square of the period of a planet is proportional to the cube of its average radius.

The study of motion of a spacecraft considered as a particle in the gravitational field of a celestial body is called *astrodynamics* and the subject of the motion of the spacecraft about its center of mass is referred as *attitude control.* Astrodynamics exploits the Newtonian laws of gravity in most of the cases and would use the Einstein's general relativity laws for extreme gravity conditions. The Newtonian laws are a special approximation of the Einstein's general theory

of relativity which is considered by far the most accurate description of laws of motion in the influence of gravity.

## 2.1 General

Newtonian laws of gravity are a good first hand description of the laws of motion of bodies in the influence of gravitational interactions. The laws of gravitation given by Newton in *Principia* are given as

1.) A body would stay at rest or in a state of uniform motion unless acted upon by an external force.
2.) The rate of change of linear momentum is in direction of and proportional to the force applied.
3.) To every action there is an equal and opposite reaction.

In addition the law of gravitation states that two bodies attract one another with a force proportional to the product of their masses $(m_1, m_2)$ and inversely proportional to the square of distance $(r)$ between them, i.e.

$$F = G\frac{m_1 m_2}{r^2} \qquad (2.1)$$

where, $G$ is the universal constant of gravitation, $6.6695 \times 10^{-11}$ $\mathrm{m^3/kg.s^2}$.

The concept of work and energy are elaborated using the Newton's Laws and are required to study the two body problem in detail. The work done on a body is equivalent to the energy stored in the body and is expressed as the scalar sum of product of the force applied and the infinitesimal displacement,

Type equation here.

$$W_{12} = \int_{r_1}^{r_2} \boldsymbol{F}.d\boldsymbol{r}$$

$$= \int_{t_1}^{t_2} m \frac{d\boldsymbol{v}}{dt}.\boldsymbol{v}dt$$

$$= \frac{1}{2}\int_{t_1}^{t_2} m \frac{d}{dt}(\boldsymbol{v}.\boldsymbol{v})dt$$

$$= \frac{1}{2}\, m\,(v_2{}^2 - v_1^2) \qquad (2.2)$$

Thus the work done on a particle is the change in its kinetic energy.

The force is said to be *conservative* if the amount of work done in taking a closed path is zero, i.e.

$$\oint \boldsymbol{F}.d\boldsymbol{r} = 0 \qquad (2.3)$$

The potential energy is defined as the work done by a conservative force in going from a point $\boldsymbol{r}_1$ to a reference point $\boldsymbol{r}_0$ .

$$V(\boldsymbol{r}_1) = \int_{r_1}^{r_0} \boldsymbol{F}.d\boldsymbol{r} \; + V(\boldsymbol{r}_0) \qquad (2.4)$$

The force can thus be expressed as the negative gradient of potential,

$$\boldsymbol{F} = -\nabla \mathrm{V}(\mathbf{r}) \qquad (2.5)$$

The principle of conservation of energy preserves the total energy of a particle as it moves in a conservative field. Another quantity that remains conserved is the total angular momentum which is given as

$$\boldsymbol{L} = \boldsymbol{r} \times (m\boldsymbol{v}) \qquad (2.6)$$

The specific angular momentum is defined as $\boldsymbol{h} = \boldsymbol{r} \times \boldsymbol{v}$.

The constancy of angular momentum requires that $\boldsymbol{r}$ and $\boldsymbol{v}$ remain in the same plane. An important consequence of which is that the orbits in gravitational field are always planar.

## 2.2 The Two Body Problem

The motion of two bodies in the influence of gravitational force between them is termed as the two body problem. The two bodies are considered to have spherical mass distribution and the separation between the bodies is assumed to be large enough compared to their dimensions. This assumption allows considering the bodies as point particles. If $\boldsymbol{R_1, R_2, R_G}$ are the radius vectors of the first and second body and the center of mass respectively, in an inertial frame of reference O. Then the position vector,$\boldsymbol{R_G}$ can be expressed as

$$\boldsymbol{R_G} = \frac{m_1\boldsymbol{R_1} + m_2\boldsymbol{R_2}}{m_1+m_2} \tag{2.7}$$

and the velocity and accelerations will be given as

$$\dot{\boldsymbol{R}}_G = \frac{m_1\dot{\boldsymbol{R}}_1 + m_2\dot{\boldsymbol{R}}_2}{m_1+m_2} \tag{2.8}$$

$$\ddot{\boldsymbol{R}}_G = \frac{m_1\ddot{\boldsymbol{R}}_1 + m_2\ddot{\boldsymbol{R}}_2}{m_1+m_2} \tag{2.9}$$

If $\boldsymbol{r}$ is the position vector of $m_2$ relative to $m_1$ and $\boldsymbol{u}_r$ be the unit vector in this direction, then,

$$\boldsymbol{r} = \boldsymbol{R_2} - \boldsymbol{R_1} \tag{2.10}$$

The gravitational force exerted on $m_2$ by $m_1$ is

$$F_{21} = \frac{Gm_1m_2}{r^2}\ (-\boldsymbol{u}_r\ ) \tag{2.11}$$

The Newton's law of motion in gravitational interaction suggests that this force can be expressed as

$$F_{21} = \frac{Gm_1m_2}{r^2}\ (-\boldsymbol{u}_r\ ) \tag{2.12}$$

$$F_{21} = \frac{Gm_1m_2}{r^2}\ (-\boldsymbol{u}_r\ ) = \ m_2\ddot{\boldsymbol{R}}_{\boldsymbol{2}} \tag{2.13}$$

By the action-reaction principle, $F_{21} = \ -F_{12}$, and so

$$\frac{Gm_1m_2}{r^2}\ (\boldsymbol{u}_r\ ) = \ m_2\ddot{\boldsymbol{R}}_{\boldsymbol{1}} \tag{2.14}$$

Multiplying the first equation by $m_1$ and the second equation by $m_2$ and adding, gives

$$m_1m_2\big(\ \ddot{\boldsymbol{R}}_2 - \ \ddot{\boldsymbol{R}}_{\boldsymbol{1}}\big) = \ -\frac{G(m_1+m_2)}{r^2}\ (m_1 + m_2)\boldsymbol{u}_r \tag{2.15}$$

This can be written in the form

$$\ddot{\boldsymbol{r}} = \ -\frac{\mu}{r^3}\ \boldsymbol{r} \tag{2.16}$$

representing the equation of motion of a two body system under the influence of gravity. Where $\mu$ is the gravitational parameter given by $\mu = G(m_1 + m_2)$ with unit $\mathrm{km^3s^{-2}}$ .

The above equation on cross multiplication with $\boldsymbol{r}$ becomes,

$$\boldsymbol{r} \times \ddot{\boldsymbol{r}} = \ \frac{d}{dt}\left(\boldsymbol{r} \times \frac{d\boldsymbol{r}}{dt}\right) = \frac{d}{dt}\,\boldsymbol{h} = 0 \tag{2.17}$$

This is the expression for the constancy of the angular momentum per unit mass derived from the Newton's laws of gravitation. The cross product of the equation of motion with $\boldsymbol{h}$ would give,

$$\frac{d^2\boldsymbol{r}}{dt^2} \times \boldsymbol{h} = -\frac{\mu}{r^3}\,\boldsymbol{r} \times \boldsymbol{h} = -\frac{\mu}{r^3}\,\boldsymbol{r} \times \left(\boldsymbol{r} \times \frac{d\boldsymbol{r}}{dt}\right) \tag{2.18}$$

using the identity for triple vector products,

$$\frac{d^2\boldsymbol{r}}{dt^2} \times \boldsymbol{h} = \mu \frac{d}{dt}\left(\frac{\boldsymbol{r}}{r}\right) \tag{2.19}$$

since $\boldsymbol{h}$ is a constant the above equation can be directly integrated to give,

$$\frac{d\boldsymbol{r}}{dt} \times \boldsymbol{h} = \frac{\mu}{r}\,(\boldsymbol{r} + r\boldsymbol{e}) \tag{2.20}$$

Taking dot product of the above equation with $\boldsymbol{h}$ will give

$$\boldsymbol{h}.\boldsymbol{e} = 0 \tag{2.21}$$

The vector $\boldsymbol{e}$ is referred as the eccentricity vector and it marks the plane of the orbital motion. The dot product with $\boldsymbol{r}$ of the above equation and using the identity of scalar triple product gives

$$r + \boldsymbol{r}.\boldsymbol{e} = \frac{h^2}{\mu} \tag{2.22}$$

$$r = \frac{h^2/\mu}{1 + e\,cos\theta} \tag{2.23}$$

here $\theta$ is the angle between the eccentricity vector and the radius vector $\boldsymbol{r}$ and is called the true anomaly. The above equation is known as the orbit equation and it mathematically represents the Keplar's first law.

The angular velocity of the position vector is given as $\dot{\theta}$ and the normal component of the velocity will be

$$v_{\perp} = r\dot{\theta} \tag{2.24}$$

The specific angular momentum can be written as $h = rv_{\perp} = r^2\dot{\theta}$

since $$\boldsymbol{h} = \boldsymbol{r} \times \boldsymbol{v} = r\boldsymbol{u}_r \times (v_r\boldsymbol{u}_r + v_{\perp}\boldsymbol{u}_{\perp}) = rv_{\perp}\hat{\boldsymbol{h}} \qquad (2.25)$$

therefore

$$v_{\perp} = \frac{h}{r} = \frac{\mu}{h}(1 + e\,cos\theta) \qquad (2.26)$$

The radial component of the velocity vector is given as

$$v_r = \dot{r} = \frac{dr}{dt} = \frac{\mu}{h}\,e\,sin\theta \qquad (2.27)$$

In a differential time $dt$ the position vector $\boldsymbol{r}$ sweeps out an area $dA$ given by

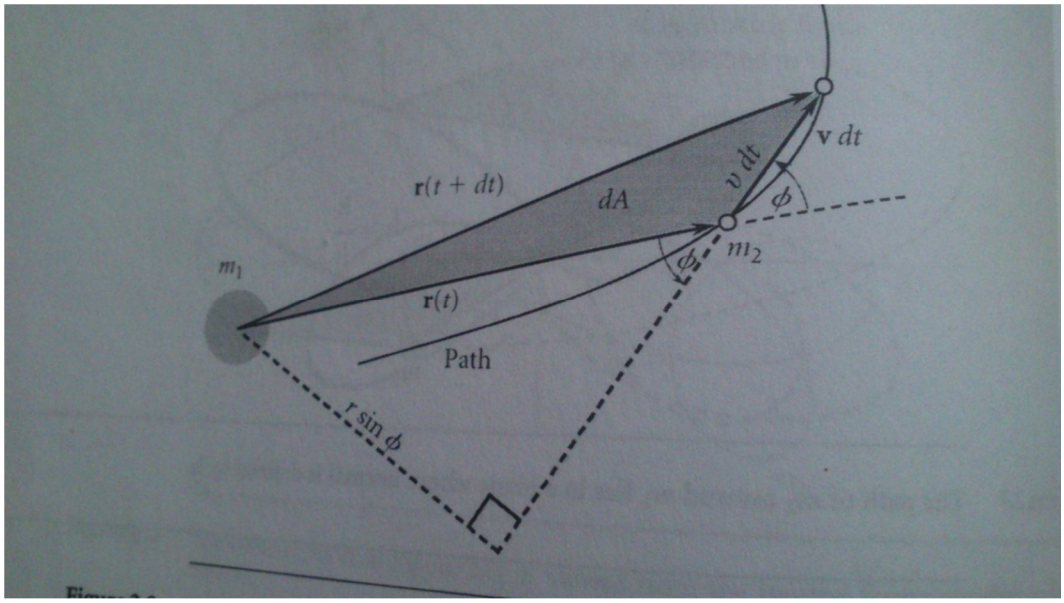


**Fig 2.1** Differntial area swept by vector **r** during interval dt (courtesy H. Curtis)

$$dA = \frac{1}{2} \times \text{base} \times \text{altitude} = \frac{1}{2} \times vdt \times rsin\phi = \frac{1}{2}\,r\,v_{\perp}dt = \frac{1}{2}\,h\,dt \qquad (2.29)$$

or

$$\frac{dA}{dt} = \frac{h}{2} = \text{constant} \qquad (2.30)$$

$\frac{dA}{dt}$ is known as the areal velocity and is a constant of motion and the equation mathematically endorses the second Kepler's law which is that equal areas are swept in equal times.

The line $\theta = 0$ is known as the apse line and the point of closest approach $r_p$ termed as the periapsis is obtained by setting $\theta = 0$ in the orbit equation,

$$r_p = \frac{h^2}{\mu}\frac{1}{1+e} \tag{2.31}$$

At this point of the trajectory the radial component of the velocity vector vanishes.

## 2.2.1 Energy Equation

The Newton's equation of motion given as

$$\ddot{\boldsymbol{r}} = -\frac{\mu}{r^3}\boldsymbol{r} \tag{2.32}$$

is now used to formulate the energy equation by taking dot product with $\dot{\boldsymbol{r}}$ giving,

$$\ddot{\boldsymbol{r}}.\dot{\boldsymbol{r}} = -\frac{\mu}{r^3}\boldsymbol{r}.\dot{\boldsymbol{r}} \tag{2.33}$$

taking first the left-hand side of this equation,

$$\ddot{\boldsymbol{r}}.\dot{\boldsymbol{r}} = \frac{1}{2}\frac{d}{dt}(\dot{\boldsymbol{r}}.\dot{\boldsymbol{r}}) = \frac{1}{2}\frac{d}{dt}(\boldsymbol{v}.\boldsymbol{v}) = \frac{d}{dt}\left(\frac{v^2}{2}\right) \tag{2.34}$$

and for the right-hand side

$$\frac{\mu}{r^3}\boldsymbol{r}.\dot{\boldsymbol{r}} = \mu\frac{r\dot{r}}{r^3} = \mu\frac{\dot{r}}{r^2} = -\frac{d}{dt}\left(\frac{\mu}{r}\right) \tag{2.35}$$

equating the two sides

$$\frac{d}{dt}\left(\frac{v^2}{2} - \frac{\mu}{r}\right) = 0 \tag{2.36}$$

or

$$\frac{v^2}{2} - \frac{\mu}{r} = \epsilon \quad \text{(constant)} \tag{2.37}$$

with $v^2/2$ being the relative kinetic energy per unit mass and $-(\mu/r)$ the potential energy per unit mass of the body $m_2$ in the gravitational field of $m_1$. The above equation represents the principle of conservation of energy conserved along the trajectory. The above equation can also be expressed in terms of the orbital parameters $\mu, h, e$, in which case the equation becomes

$$\epsilon = -\frac{1}{2}\frac{\mu^2}{h^2}(1 - e^2) \tag{2.38}$$

Thus the orbital energy is not an independent orbital parameter. Depending on different $e$ values the different types of trajectories will have different forms of specific energies as discussed in the following subsections.

### 2.2.2 Circular Orbits ($e = 0$)

The circular orbits are defined by zero eccentricity and thus the orbital equation takes on the simple form

$$r = \frac{h^2}{\mu} \tag{2.39}$$

now since $r$ is constant in these orbits $\dot{r} = 0$ and hence $v = v_\perp$ so that the specific angular momentum is $h = rv$ and we have

$$v_{\text{circular}} = \sqrt{\frac{\mu}{r}} \tag{2.40}$$

and since the velocity is constant the time period of the circular orbit will be

$$T_{\text{circular}} = \frac{\text{circumference}}{\text{speed}} = \frac{2\pi r}{\sqrt{\frac{\mu}{r}}} = \frac{2\pi}{\sqrt{\mu}} r^{\frac{3}{2}} \tag{2.41}$$

The specific energy $\epsilon$ of a circular orbit will be

$$\epsilon_{\text{circular}} = -\frac{1}{2}\frac{\mu^2}{h^2} = -\frac{\mu}{2r} \qquad (2.42)$$

The energy of a circular orbit is negative and it increases with the increasing radius. Similarly the velocity of a particle decreases with the increasing radius. For a typical geostationary satellite the radius should be 42,164 km and the velocity of 3.075 km/s.

### 2.2.3 Elliptical Orbits ($0 < e < 1$)

The orbital equation which is given by

$$r = \frac{h^2/\mu}{1+e\,cos\theta} \qquad (2.43)$$

will have the denominator on the r.h.s. always positive and never reaching zero for the eccentricity range $0 < e < 1$ . Thus orbits with this eccentricity range will be bound and are called elliptical or Keplerian orbits. The orbits of all the planets that revolve around the Sun are elliptic and so are the orbits of all the Earth's satellites.

The relative position vector for elliptical orbits remains bound and its minimum and maximum values are termed as the periapsis ($r_p$) and apoapsis ($r_a$) respectively,

Periapsis is given at $= 0$ ,

$$r_p = \frac{h^2}{\mu}\frac{1}{1+e} \qquad (2.43)$$

and the apoapsis is given at $\theta = \pi$

$$r_a = \frac{h^2}{\mu}\frac{1}{1-e} \qquad (2.44)$$

The semi-major axis $a$ is given as

$$2a = r_a + r_p \tag{2.45}$$

substituting the values of $r_a$ and $r_p$ gives

$$a = \frac{h^2}{\mu}\frac{1}{1-e^2} \tag{2.46}$$

and the orbit equation can thus be rewritten in the form

$$r = a\frac{1-e^2}{1+ecos\theta} \tag{2.47}$$

The semi-minor axis $b$ is

$$b = a\sqrt{1-e^2} \tag{2.48}$$

If $x, y$ are the coordinates of a point on the orbit then the equation of the ellipse is given as

$$\frac{x^2}{a^2} + \frac{y^2}{b^2} = 1 \tag{2.49}$$

The specific energy of an elliptic orbit is

$$\epsilon = -\frac{1}{2}\frac{\mu^2}{h^2}(1-e^2) \tag{2.50}$$

and will always be negative and can be rearranged to be given in terms of the semi-major axis

$$\epsilon = -\frac{\mu}{2a} \tag{2.51}$$

The conservation of energy equation for an elliptical orbit can be written as

$$\frac{v^2}{2} - \frac{\mu}{r} = -\frac{\mu}{2a} \tag{2.52}$$

The area of an ellipse given in terms of $a, b$ is $A = \pi ab$. To find the time period of the elliptical orbit the second law of Kepler is employed i.e.

$$\Delta A = \frac{h}{2}\Delta t \tag{2.53}$$

for a complete revolution $\Delta A = \pi ab$ and $\Delta t = T$, thus,

$$T = \frac{2\pi ab}{h} \tag{2.54}$$

which can be re-expressed as

$$T = \frac{2\pi}{\sqrt{\mu}} a^{3/2} \tag{2.55}$$

This equation mathematically represents the third Kepler's law which states that the time period of a planet is proportional to the three-half power of the semi-major axis.

### 2.2.4 Parabolic Trajectories ($e = 1$)

The orbit equation when $e = 1$ is given as

$$r = \frac{h^2}{\mu} \frac{1}{1+\cos\theta} \tag{2.56}$$

The specific energy of a parabolic trajectory will be

$$\epsilon = -\frac{1}{2}\frac{\mu^2}{h^2}(1 - e^2) = 0 \tag{2.57}$$

Such that the conservation of energy for a parabolic trajectory is given as

$$\frac{v^2}{2} - \frac{\mu}{r} = 0 \tag{2.58}$$

This depicts that the velocity on a parabolic path at any point is given as

$$v = \sqrt{\frac{2\mu}{r}} \tag{2.59}$$

If a body is on a parabolic trajectory it will continue moving towards infinity where its velocity becomes zero and it escapes the gravitational field of other body. The escape velocity at a distance $r$ from $m_1$ is therefore given as

$$v_{\text{esc}} = \sqrt{\frac{2\mu}{r}} \tag{2.60}$$

The velocity of a circular orbit is given as

$$v_o = \sqrt{\frac{\mu}{r}} \tag{2.61}$$

Therefore the escape velocity for a circular orbit is

$$v_{\text{esc}} = \sqrt{2}\, v_o \tag{2.62}$$

Or a boost of 41.4 percent is required to escape from a circular orbit.

The flight path angle for a parabolic trajectory is given as

$$\tan\gamma = \frac{e\,sin\theta}{1+e\,cos\theta} = \frac{sin\theta}{1+cos\theta} = \tan\theta/2 \tag{2.63}$$

or the flight path angle of a parabolic trajectory is equal to one half of the true anomaly.

The semi-latus rectum of a conic section is given as

$$p = \frac{h^2}{\mu} \tag{2.64}$$

and the periapsis radius for a parabolic trajectory is simply

$$r_p = \frac{p}{2} \tag{2.65}$$

and the equation of a parabola in cartesian coordinates written in terms of the semi-latus rectum is,

$$x = \frac{p}{2} - \frac{y^2}{2p} \tag{2.66}$$

The parabolic trajectories are rarely found in nature, however some comets have trajectories that approximate a parabola. The parabolic trajectories are interesting from a space-craft point of view as they represent the border line of closed and open trajectories.

### 2.2.5 Hyperbolic Trajectories ($e > 1$)

Meteors that strike the earth and the interplanetary space-probes that leave the earth travel with hyperbolic trajectories relative to the earth. A hyperbolic trajectory is important if we want the escaping body to have some excess speed when it escapes the influence of the other body.

If $e > 1$, the orbit formula

$$r = \frac{h^2}{\mu} \frac{1}{1+e\cos\theta} \tag{2.67}$$

describes the geometry of a hyperbola.

The hyperbolic system consists of two symmetric curves, the curve on the left represents the orbiting body and the curve on the right is its mathematical image. In the case of repulsive forces the right curve will represent the motion of the second body with the first body at the focus of the left curve.

The denominator of the above equation reaches zero when $\cos\theta = -\frac{1}{e}$. This value $\theta_\infty$ is known as the true anomaly of the asymptote as the radial distance at $\theta_\infty$ reaches infinity,

$$\theta_\infty = \cos^{-1}(1/e) \tag{2.68}$$

The periapsis P lies on the apse line where the left hyperbola meets the apse line and the apoapsis A lies on intersection of the right hyperbola with the apse line. The point halfway between periapsis and apoapsis is called the center of the

hyperbola. The asymptotes of the hyperbola are the straight lines which the curve approaches at infinity, meeting at C, and making an angle $\beta$ with the apse line,

where

$$\beta = \pi - \theta_{\infty} = \cos^{-1}(1/e) \tag{2.69}$$

The periapsis point is given by the equation

$$r_p = \frac{h^2}{\mu}\frac{1}{1+e} \tag{2.70}$$

and the apoapsis point is at

$$r_a = \frac{h^2}{\mu}\frac{1}{1-e} \tag{2.71}$$

since $e > 1$ then $r_a$ comes out to be negative that signifies that apoapse lies on the right of the focus F.

The semimajor axis $a$ is given by as

$$2a = -r_a - r_p = -\frac{h^2}{\mu}\left(\frac{1}{1-e} + \frac{1}{1+e}\right) \tag{2.73}$$

or,

$$a = \frac{h^2}{\mu}\frac{1}{e^2-1} \tag{2.74}$$

The semiminor axis is the distance from the periapsis P to the asymptote, measured perpendicular to the apse line and is calculated to be

$$b = a\sqrt{e^2 - 1} \tag{2.75}$$

Another feature of a hyperbola is the aiming radius which is the distance between a asymptote and a parallel line to the focus and is given as

$$\Delta = \left(r_p + a\right) sin\beta = a\, e\, sin\theta_\infty = b \qquad (2.76)$$

Thus the aiming radius equals the length of the semiminor axis of the hyperbola.

The specific energy of a hyperbolic trajectory can be calculated using the energy equation

$$\epsilon = \frac{1}{2}\frac{\mu^2}{h^2}\left(e^2 - 1\right) \qquad (2.77)$$

Substituting the value of $a$ in the above equation gives

$$\epsilon = \frac{\mu}{2a} \qquad (2.78)$$

Therefore the energy of the hyperbolic trajectory is always positive and the conservation of energy for a hyperbolic trajectory is

$$\frac{v^2}{2} - \frac{\mu}{r} = \frac{\mu}{2a} \qquad (2.79)$$

We can find now the speed at which a body will escape to infinity by letting $r = \infty$ in the above equation to obtain the hyperbolic excess speed $v_\infty$,

$$v_\infty = \sqrt{\frac{\mu}{a}} \qquad (2.80)$$

Therefore the energy equation can be alternatively written in the form

$$\frac{v^2}{2} - \frac{\mu}{r} = \frac{v_\infty^2}{2} \qquad (2.81)$$

Substituting the expression for the escape velocity we can further write the energy equation in the form

$$v^2 = v_{\text{esc}}^2 + \text{v}_\infty^2 \qquad (2.82)$$

Thus hyperbolic excess speed is the velocity with which a body escapes the gravity of another body. For interplanetary missions this excess velocity is required with which the probe travels farther as it leaves the sphere of influence of the primary planet.

### 2.2.5 Perifocal Frame

This is the most natural frame of reference for the study of orbits, The origin the $xy$ plane of the frame lies in the plane of the orbit, with the $x$ axis pointing in the direction of periapsis and the $y$ axis perpendicular to the apse line lying in the plane of the orbit. The $z$ axis lies perpendicular to the plane of the orbit and coincides with the direction of the angular momentum $\boldsymbol{h}$,

If $\hat{\boldsymbol{p}}, \hat{\boldsymbol{q}}, \hat{\boldsymbol{w}}$ are the respective unit vectors in the $x, y, z$ directions in the perifocal frame then the radius vector can be written as

$$\boldsymbol{r} = x\hat{\boldsymbol{p}} + y\hat{\boldsymbol{q}} \tag{2.83}$$

and the $z$ unit vector is

$$\hat{\boldsymbol{w}} = \frac{\boldsymbol{h}}{h} \tag{2.84}$$

now $x = rcos\theta$ , $y = rsin\theta$ and the magnitude of $r$ is given by the orbit equation

$$r = (h^2/\mu)[1/(1 + ecos\theta)] \tag{2.85}$$

and the radius vector can be expressed as

$$\boldsymbol{r} = \frac{h^2}{\mu}\frac{1}{1+ecos\theta}\,(cos\theta\,\hat{\boldsymbol{p}} + sin\theta\,\hat{\boldsymbol{q}}) \tag{2.86}$$

The velocity can be found by taking the time derivative of the radius vector $\boldsymbol{r}$

$$\boldsymbol{v} = \dot{\boldsymbol{r}} = \dot{x}\hat{\boldsymbol{p}} + \dot{y}\hat{\boldsymbol{q}} \tag{2.87}$$

where $\dot{x}$ and $\dot{y}$ can be found as

$$\dot{x} = \dot{r}\cos\theta - r\dot{\theta}\sin\theta \quad (2.88)$$

$$\dot{y} = \dot{r}\sin\theta + r\dot{\theta}\cos\theta \quad (2.89)$$

giving

$$\boldsymbol{v} = \frac{\mu}{h}\left[-\sin\theta\hat{\boldsymbol{p}} + (e + \cos\theta)\hat{\boldsymbol{q}}\right] \quad (2.90)$$

This describes the orbital kinematics in the perifocal frame. The next section utilizes the concept of perifocal frame to calculate the Lagrange coefficients which provide a direct method to calculate the radial vector and velocity at later time once the initial values of these two quantities are known.

## 2.2.6 The Lagrange Coefficients

The position and velocity of a body in an orbit at a later time can be calculated from the initial values of these quantities and the coefficients of such a multiplication matrix are known as the Lagrange coefficients. The Lagrange coefficients can be derived in the following manner,

If ( $\boldsymbol{r}_0, \boldsymbol{v}_0$) are the initial set of values at time $t_0$, and( $\boldsymbol{r}, \boldsymbol{v}$ ) the values at a later time $t$. Then in the perifocal frame,

$$\boldsymbol{r}_0 = x_0\hat{\boldsymbol{p}} + y_0\hat{\boldsymbol{q}} \quad (2.91)$$

$$\boldsymbol{v_0} = \dot{x_0}\hat{\boldsymbol{p}} + \dot{y_0}\hat{\boldsymbol{q}} \quad (2.92)$$

and

$$\boldsymbol{r} = x\hat{\boldsymbol{p}} + y\hat{\boldsymbol{q}} \quad (2.93)$$

$$\boldsymbol{v} = \dot{x}\hat{\boldsymbol{p}} + \dot{y}\hat{\boldsymbol{q}} \quad (2.94)$$

The angular momentum $\boldsymbol{h}$ can be written as

$$\boldsymbol{h} = \boldsymbol{r}_0 \times \boldsymbol{v}_0 = \begin{vmatrix} \hat{\boldsymbol{p}} & \hat{\boldsymbol{q}} & \hat{\boldsymbol{w}} \\ x_0 & y_0 & 0 \\ \dot{x} & \dot{y} & 0 \end{vmatrix} = \hat{\boldsymbol{w}}(x_0\dot{y} - y_0\dot{x}) = h\,\hat{\boldsymbol{w}} \qquad (2.95)$$

Unit vectors $\hat{\boldsymbol{p}}, \hat{\boldsymbol{q}}$ can be expressed in terms of the $\boldsymbol{r}_0, \boldsymbol{v}_0, x, y, \dot{x}_0, \dot{y}_0$ and $h$ as,

$$\hat{\boldsymbol{p}} = \frac{\dot{y}_0}{h}\boldsymbol{r_0} - \frac{y}{h}\boldsymbol{v_0} \qquad (2.96)$$

$$\hat{\boldsymbol{q}} = \frac{\dot{x}_0}{h}\boldsymbol{r}_0 + \frac{x_0}{h}\boldsymbol{v}_0 \qquad (2.97)$$

substituting these values of $\hat{\boldsymbol{p}}, \hat{\boldsymbol{q}}$ in the expressions of $\boldsymbol{r}, \boldsymbol{v}$ yields,

$$\boldsymbol{r} = x\left(\frac{\dot{y}_0}{h}\boldsymbol{r_0} - \frac{y}{h}\boldsymbol{v_0}\right) + y\left(\frac{\dot{x}_0}{h}\boldsymbol{r}_0 + \frac{x_0}{h}\boldsymbol{v}_0\right) = \frac{x\dot{y}_0 - y\dot{x}_0}{h}\boldsymbol{r_0} + \frac{-xy_0 + yx_0}{h}\boldsymbol{v_0} \qquad (2.98)$$

$$\boldsymbol{v} = \dot{x}\left(\frac{\dot{y}_0}{h}\boldsymbol{r_0} - \frac{y}{h}\boldsymbol{v_0}\right) + y\left(\frac{\dot{x}_0}{h}\dot{\boldsymbol{r}}_0 + \frac{x_0}{h}\boldsymbol{v}_0\right) = \frac{\dot{x}\dot{y}_0 - \dot{y}\dot{x}_0}{h}\boldsymbol{r_0} + \frac{-\dot{x}y_0 + \dot{y}x_0}{h}\boldsymbol{v_0} \qquad (2.99)$$

or

$$\boldsymbol{r} = f\boldsymbol{r_0} + g\boldsymbol{v}_0 \qquad (2.100)$$

$$\boldsymbol{v} = \dot{f}\boldsymbol{r}_0 + \dot{g}\boldsymbol{v}_0 \qquad (2.101)$$

where

$$f = \frac{x\dot{y}_0 - y\dot{x}_0}{h} \qquad (2.102)$$

$$g = \frac{-xy_0 + yx_0}{h} \qquad (2.103)$$

and

$$\dot{f} = \frac{\dot{x}y_0 - \dot{y}x_0}{h} \tag{2.104}$$

$$\dot{g} = \frac{-\dot{x}y_0 + \dot{y}x_0}{h} \tag{2.105}$$

The functions $f$ and $g$ are known as Lagrange coefficients. The Lagrange coefficients and their time derivatives are functions of time and initial conditions. The conservation of total angular momentum imposes a condition on $f, g, \dot{f}$ and $\dot{g}$,

$$f\dot{g} - \dot{f}g = 1 \tag{2.106}$$

Thus we require any three of the four functions to calculate the position and velocity in an orbit at a later time once the initial values of the position and velocity are given. The Lagrange coefficients can also be expressed in terms of the radius vector and the change in true anomaly,

$$f = 1 - \frac{\mu r}{h^2}\,(1 - cos\Delta\theta) \tag{2.107}$$

$$g = \frac{rr_0}{h} sin\Delta\theta \tag{2.108}$$

$$\dot{f} = \frac{\mu}{h}\frac{1-cos\Delta\theta}{sin\Delta\theta}\left[\frac{\mu}{h^2}(1 - cos\Delta\theta) - \frac{1}{r_0} - \frac{1}{r}\right] \tag{2.109}$$

$$\dot{g} = 1 - \frac{\mu r_0}{h^2}(1 - cos\Delta\theta) \tag{2.110}$$

where $r$ is given as

$$r = \frac{h^2}{\mu}\frac{1}{1+\left(\frac{h^2}{\mu r_0}-1\right)cos\Delta\theta - \frac{hv_{r0}}{\mu}sin\Delta\theta} \tag{2.111}$$

And the initial radial velocity $v_{r0}$ is the projection of $\boldsymbol{v}_0$ onto the direction of $\boldsymbol{r_0}$,

$$v_{r0} = \boldsymbol{v_0}.\frac{\mathbf{r}_0}{r_0} \tag{2.112}$$

with

$$r_0 = \frac{h^2}{\mu}\frac{1}{1+e\ cos\theta_0} \tag{2.113}$$

and

$$v_{r0} = \frac{\mu}{h} e\ sin\theta_0 \tag{2.114}$$

This provides a method to calculate the position and velocity vectors at a given time with the knowledge of the eccentricity and the true anomaly of the initial point.

## 2.3 Restricted Three Body Problem

The two body problem can be completely solved analytically whereas the scenario is not similar for a general three body problem where there exist no analytical solutions. However for special cases it is possible to describe the problem analytically. One such case is the problem of two bodies of masses $m_1, m_2$ circling about a common center of mass and a third body of mass $m$ , negligible compared to $m_1$ and $m_2$ , moving under the combined gravitational influence of $m_1$ and $m_2$. The reference frame is chosen such that the origin lies at the center of mass of the first two bodies with the $x$ axis pointing towards $m_2$ and the $xy$ plane coinciding with the plane of the orbit. In this frame of reference the two bodies $m_1, m_2$ will appear to be at rest, ref Fig 8. Since the mass of the third body is considered to be negligible the problem is referred as restricted three body problem.

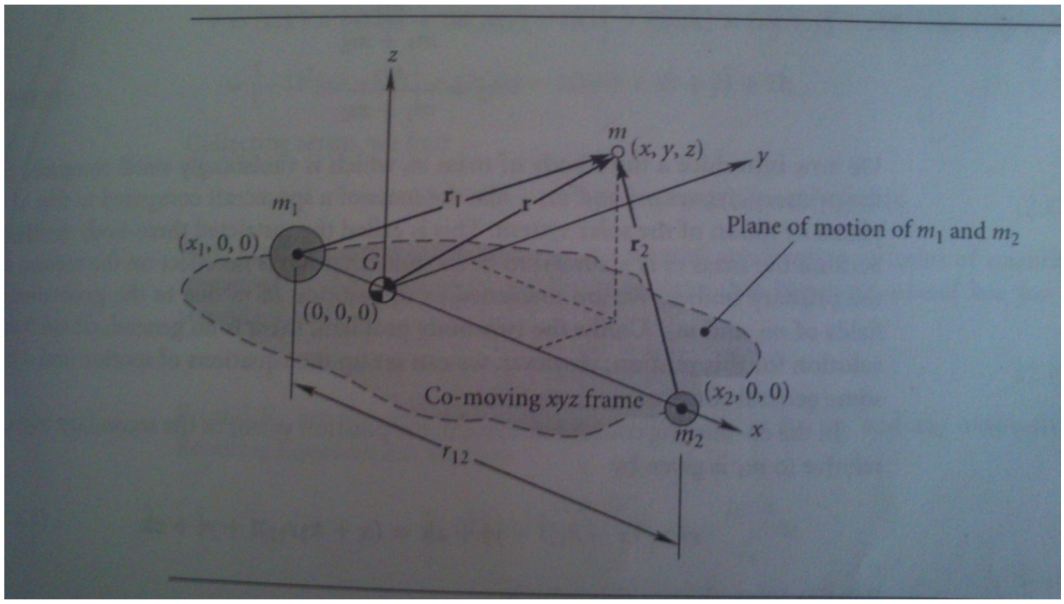


**Fig 2.2** *Illustration of Restricted Three Body Problem (courtesy H. Curtis)*

The inertial angular momentum that is a constant of motion is given by,

$$\boldsymbol{\Omega} = \Omega\,\hat{\boldsymbol{k}} \tag{2.115}$$

where $\Omega = 2\pi/T$ and $T$ is the time period of the circular orbit of the primary bodies, given by the Kepler law,

$$T = 2\pi \frac{r_{12}^{3/2}}{\sqrt{\mu}} \tag{2.116}$$

If $M$ is the total mass of the primary bodies and $x_1, x_2$ their distances from the origin, and if we denote $\pi_1, \pi_2$ as the mass ratios then

$$m_1 x_1 + m_2 x_2 = 0 \tag{2.117}$$

and

$$x_1 = -\pi_2 r_{12} \tag{2.118}$$

$$x_2 = \pi_1 r_{12} \tag{2.119}$$

where $\pi_1 = m_1/(m_1 + m_2)$ and $\pi_2 = m_2/(m_1 + m_2)$.

In the co-moving reference frame, the position of the $m$ relative to $m_1, m_2$ is

$$\boldsymbol{r}_1 = (x - x_1)\hat{\boldsymbol{\imath}} + y\hat{\boldsymbol{\jmath}} + z\hat{\boldsymbol{k}} = (x + \pi_2 r_{12})\hat{\boldsymbol{\imath}} + y\hat{\boldsymbol{\jmath}} + z\hat{\boldsymbol{k}} \qquad (2.120)$$

and

$$\boldsymbol{r}_2 = (x - x_2)\hat{\boldsymbol{\imath}} + y\hat{\boldsymbol{\jmath}} + z\hat{\boldsymbol{k}} = (x - \pi_1 r_{12})\hat{\boldsymbol{\imath}} + y\hat{\boldsymbol{\jmath}} + z\hat{\boldsymbol{k}} \qquad (2.121)$$

The position vector of the secondary body in the co-moving reference frame is

$$\boldsymbol{r} = x\hat{\boldsymbol{\imath}} + y\hat{\boldsymbol{\jmath}} + z\hat{\boldsymbol{k}} \qquad (2.122)$$

However, since the co-moving reference frame is rotating with a constant angular velocity the absolute velocity of the secondary mass can be derived as

$$\dot{\boldsymbol{r}} = \boldsymbol{v}_G + \boldsymbol{\Omega} \times \mathbf{r} + \mathbf{v}_{\text{rel}} \qquad (2.123)$$

Where $\boldsymbol{v}_G$ is the inertial velocity of the center of mass of the primary bodies and $\boldsymbol{v}_{\text{rel}}$ is the velocity of the secondary body in the moving reference frame,

$$\boldsymbol{v}_{\text{rel}} = \dot{x}\hat{\boldsymbol{\imath}} + \dot{y}\hat{\boldsymbol{\jmath}} + \dot{z}\hat{\boldsymbol{k}} \qquad (2.124)$$

The absolute acceleration of the secondary body will be given as

$$\ddot{\boldsymbol{r}} = \boldsymbol{a}_G + \dot{\boldsymbol{\Omega}} \times \boldsymbol{r} + \boldsymbol{\Omega} \times (\boldsymbol{\Omega} \times \boldsymbol{r}) + 2\boldsymbol{\Omega} \times \boldsymbol{v}_{\text{rel}} + \boldsymbol{a}_{\text{rel}} \qquad (2.125)$$

Since the velocity of the moving frame is constant and so is the angular velocity of the center of mass ($\Omega$) in this frame, therefore $\boldsymbol{a}_G = \dot{\boldsymbol{\Omega}} = 0$ and

$$\boldsymbol{a}_{\text{rel}} = \ddot{x}\hat{\boldsymbol{\imath}} + \ddot{y}\hat{\boldsymbol{\jmath}} + \ddot{z}\hat{\boldsymbol{k}} \qquad (2.126)$$

Therefore

$$\ddot{\boldsymbol{r}} = (\ddot{x}\hat{\boldsymbol{\imath}} - 2\Omega\dot{y} - \Omega^2 x)\hat{\boldsymbol{\imath}} + (\ddot{y} + 2\Omega\dot{x} - \Omega^2 y)\hat{\boldsymbol{\jmath}} + \ddot{z}\hat{\boldsymbol{k}} \qquad (2.127)$$

The Newton's second law for the secondary body gives us

$$m\ddot{\boldsymbol{r}} = \boldsymbol{F}_1 + \boldsymbol{F}_2 \tag{2.127}$$

where

$$\boldsymbol{F}_1 = -\frac{\mu_1 m}{r_1^3}\boldsymbol{r}_1 \tag{2.128}$$

and

$$\boldsymbol{F}_2 = -\frac{\mu_2 m}{r_2^3}\boldsymbol{r}_2 \tag{2.129}$$

Or

$$\ddot{\boldsymbol{r}} = -\frac{\mu_1}{r_1^3}\boldsymbol{r}_1 - \frac{\mu_2}{r_2^3}\boldsymbol{r}_2 \tag{2.130}$$

Finally substituting the corresponding values,

$$(\ddot{x} - 2\Omega\dot{y} - \Omega^2 x)\hat{\boldsymbol{\imath}} + (\ddot{y} + 2\Omega\dot{x} - \Omega^2 y)\hat{\boldsymbol{\jmath}} + \ddot{z}\hat{\boldsymbol{k}} = -\frac{\mu_1}{r_1^3}[(x + \pi_2 r_{12})\hat{\boldsymbol{\imath}} + y\hat{\boldsymbol{\jmath}} + z\hat{\boldsymbol{k}}] - \frac{\mu_2}{r_2^3}[(x - \pi_1 r_{12})\hat{\boldsymbol{\imath}} + y\hat{\boldsymbol{\jmath}} + z\hat{\boldsymbol{k}}] \tag{2.131}$$

Equating coefficients,

$$\ddot{x} - 2\Omega\dot{y} - \Omega^2 x = -\frac{\mu_1}{r_1^3}(x + \pi_2 r_{12}) - \frac{\mu_2}{r_2^3}(x - \pi_1 r_{12})$$

$$\ddot{y} + 2\Omega\dot{x} - \Omega^2 y = -\frac{\mu_1}{r_1^3}y - \frac{\mu_2}{r_2^3}y$$

$$\ddot{z} = -\frac{\mu_1}{r_1^3}z - \frac{\mu_2}{r_2^3}z \tag{2.132}$$

These correspond to the analytically derived equation of motions for a restricted three-body problem.

# Chapter 3

# Rotating Kerr Black Holes

The gravitational collapse of a rotating spherical mass would produce a rotating black hole if the radius of the collapsing body reaches the gravitational radius. Such collapses will be more general than a non rotating collapse and would complete the case for all gravitational collapses. The asymmetry inherent in the collapsing body is suggested to be radiated gravitationally and the final outcome is assumed to be a stationary spherically symmetric rotating black hole [14]. All the features of rotating black holes can then be described by the charge, mass and the angular momentum of the black hole.

A complete mathematical description of spacetime around a rotating black hole was provided by Roy Kerr in 1963 [9]. The original paper proved that exact solutions of such geometry were possible and further conclusions led to interesting physical nature of the spacetime behavior in such extreme conditions. The Kerr metric used to describe a rotating black hole is studied using various coordinate systems out of which the Boyer Lindquist coordinates [17] provide an extension to the Schwarzschild coordinates and are the most studied and exploited for the study of rotating spacetime behavior.

A Kerr Black hole can be formed either from the death of a massive star or can exist at the centers of galaxies, the two different types of black holes differ in their formations and mass range but the underlying physics describing the spacetime associated with these objects is expected to be same. The strikingly similar behavior of Kerr spacetime at different scales gives us two different scenarios to study the overall behavior of spacetime in extreme conditions. In the case of supermassive black holes existing at the centers of galaxies the trajectories of the nearby stars can be studied in detail to understand the motion of bodies in Kerr spacetime. The study of the supermassive black hole at the center of the Milky Way exhibits stellar orbits of extremely high eccentricities that orbit the central black hole.

The orbits around the central black hole in Milky Way can provide a test ground of the theory of motion of bodies in Kerr spacetime. Since the nature of the spacetime is similar in both types of black hole one can approximate the case of a satellite revolving around a stellar black hole to that of stars orbiting a supermassive black hole since in both the cases the mass of the secondary body is negligible compared to the mass of the black hole, and the spacetime associated with the black holes are similar to each other only varying in scales.

## 3.1 Kerr Geometry

The spacetime around rotating black holes is described uniquely by the Kerr Metric [9] given by Roy Kerr in 1963. It is the most general form of a space metric which embodies the rotation of spacetime around a gravitational source of an extremely high order of density. The stellar originated black holes with a definite angular momentum fall in the category of Kerr black holes and the spacetime around these black holes can be studied with the aid of the Kerr metric given below in the Boyer-Lindquist coordinates [17],

$$ds^2 = -\frac{\Delta}{\rho^2}[dt - \text{asin}^2\,\theta\ d\phi]^2 + \frac{\sin^2\theta}{\rho^2}[(r^2 + a^2)d\phi - adt]^2 + \frac{\rho^2}{\Delta}dr^2 + \rho^2 d\theta^2 \quad (3.1)$$

or alternatively

$$ds^2 = -\frac{1}{\rho^2}[\Delta - a^2\sin^2\theta]dt^2 + \frac{\sin^2\theta}{\rho^2}[-\Delta a^2\sin^2\theta + (r^2 + a^2)^2]d\phi^2 - 2\frac{(2Mr - Q^2)a\sin^2\theta}{\rho^2}dtd\phi + \frac{\rho^2}{\Delta}dr^2 + \rho^2 d\theta^2 \quad (3.2)$$

where,

$\Delta \equiv r^2 - 2Mr + a^2 + Q^2$

$\rho^2, \Sigma \equiv r^2 + a^2\cos^2\theta$

$a \equiv S/M \equiv$ angular momentum per unit mass (3.3)

The mixed metric coefficients $g_{t\phi}, g_{\phi t}$ are seen to be non zero and the metric is in general a non-diagonal metric irrespective of the choice of the coordinate system. The non vanishing non diagonal components of the Kerr metric introduces new concepts of space-time reversal and static limit which accounts for intriguing new physics in such spacetimes.

The derivation of Kerr Metric is carried out by considering the general form of a spacetime metric and applying the necessary conditions of symmetries and finding the non zero components of the Ricci curvature tensor and utilizing the Einstein equation of General Relativity [16]. Once derived, the metric can be shown to be a unique metric describing rotating spacetime by the theorems of Robinson and Carter [37, 38].

The Kerr metric in Boyer Lindquist coordinates becomes singular at the horizon where the metric coefficient $g_{tt}$ vanishes, and it requires an infinite amount of coordinate time to reach the horizon. Moreover the dragging of inertial frame causes an infinite twisting as one approaches the horizon. This singularity is seen

to be coordinate dependent and can be avoided by choosing a different set of coordinate system called the Kerr coordinates [39] by replacing $t, \phi$ by $\tilde{V}, \tilde{\phi}$ in the following manner,

$$\boldsymbol{d}V = \boldsymbol{d}t + (r^2 + a^2)(\boldsymbol{d}r/\Delta) \tag{3.4}$$

$$\boldsymbol{d}\tilde{\phi} = \boldsymbol{d}\phi + a(\boldsymbol{d}r/\Delta) \tag{3.5}$$

This transformation leads to an infinite suppression of coordinate time $t$ and an infinite untwisting of the angular coordinate $\phi$ in the neighborhood of the horizon. In the Kerr coordinate system the Kerr metric takes on the form

$$ds^2 = -[1 - \rho^{-2}(2Mr - Q^2)]d\tilde{V}^2 + 2drd\tilde{V} + \rho^2 d\theta^2 + \rho^{-2}[(r^2 + a^2)^2 - \Delta a^2 \sin^2\theta]\sin^2\theta d\tilde{\phi}^2 - 2a\sin^2\theta d\tilde{\phi}\, dr - 2a\rho^{-2}(2Mr - Q^2)\sin^2\theta d\tilde{\phi} d\tilde{V} \tag{3.6}$$

The Kerr metric behaves well in the neighborhood of the horizon in the Kerr coordinate system and the inward photon and particle world lines remain singular in this new choice of coordinate system. However the Boyer Lindquist coordinates are used for most of the calculations in Kerr geometry in this work.

The metric coefficients in Boyer Lindquist coordinates are independent of the $t$ and $\phi$ coordinates and thus the spacetime geometry is both time independent and axially symmetric. The independence of the metric coefficients of a coordinate leads to a killing vector associated with that coordinate and these killing vectors are associated with conservation of energy and conservation of the angular momentum. The Killing vectors associated with the Kerr metric are

$$\boldsymbol{\xi}_t = \left(\frac{\partial}{\partial t}\right)_{r,\theta,\phi} = \left(\frac{\partial}{\partial \tilde{V}}\right)_{r,\theta,\tilde{\phi}} \tag{3.7}$$

$$\boldsymbol{\xi}_\phi = \left(\frac{\partial}{\partial \phi}\right)_{t,r,\theta} = \left(\frac{\partial}{\partial \tilde{\phi}}\right)_{\tilde{V},r,\theta} \tag{3.8}$$

The dot products of the killing tensors with each other and themselves give

$$\boldsymbol{\xi}_t.\boldsymbol{\xi}_t = g_{tt} = -(1 - \frac{2Mr - Q^2}{\rho^2})$$

$$\boldsymbol{\xi}_\phi.\boldsymbol{\xi}_\phi = g_{\phi\phi} = \frac{\left[(r^2+a^2)^2 - \Delta a^2 \sin^2\theta\right]\sin^2\theta}{\rho^2} \qquad (3.9)$$

$$\boldsymbol{\xi}_t.\boldsymbol{\xi}_\phi = g_{t\phi} = -\frac{(2Mr-Q^2)a\sin^2\theta}{\rho^2} \qquad (3.10)$$

The Killing vectors have coordinate free meaning and they are associated with the symmetries in the spacetime and so the metric coefficients $g_{tt}, g_{\phi\phi}, g_{t\phi}$ also embody information of the symmetries in spacetime in the Boyer Lindquist coordinate form of the Kerr metric. The Killing vectors scalar products in Kerr coordinates are seen to be

$$\boldsymbol{\xi}_{\tilde{r}}.\boldsymbol{\xi}_{\tilde{r}} = -\left(1 - \frac{2Mr-Q^2}{\rho^2}\right) = g_{\tilde{r}\tilde{r}} = g_{tt} = \boldsymbol{\xi}_t.\boldsymbol{\xi}_t \qquad (3.11)$$

$$\boldsymbol{\xi}_{\tilde{\phi}}.\boldsymbol{\xi}_{\tilde{\phi}} = \frac{\left[(r^2+a^2)^2 - \Delta a^2 \sin^2\theta\right]\sin^2\theta}{\rho^2} = g_{\tilde{\phi}\tilde{\phi}} = g_{\phi\phi} = \boldsymbol{\xi}_\phi.\boldsymbol{\xi}_\phi \qquad (3.12)$$

$$\boldsymbol{\xi}_{\tilde{r}}.\boldsymbol{\xi}_{\tilde{\phi}} = -\frac{(2Mr-Q^2)a\sin^2\theta}{\rho^2} = g_{\tilde{r}\tilde{\phi}} = g_{t\phi} = \boldsymbol{\xi}_t.\boldsymbol{\xi}_\phi \qquad (3.13)$$

which establishes the invariance of the Killing vectors in the two different coordinate systems used to describe the Kerr spacetime. These inherent symmetries in Kerr spacetime leads to the two constants of motion associated with the conservation of energy and the conservation of angular momentum. Another constant of motion in Kerr spacetime was discovered by Brandon Carter [40], using the Hamilton-Jacobi method. These three constants together with the constant associated with the particle rest mass describe the motion of a particle in Kerr geometry in a complete analytical manner. The equations of motion in Kerr geometry are described in detail in the next chapter of this work and we now

focus our attention in detail on the various properties of the Kerr geometry in the following sections.

## 3.2 Properties of Kerr Metric

The interesting features exhibited by the Kerr metric are the concepts of event horizon, frame dragging, static limit, and ergosphere which have been briefly discussed in the introductory chapter. A closer look at these concepts is the motive of this section.

### 3.2.1 The Event Horizon

The event horizon is the boundary of a black hole beyond which it is impossible to get information of an object that make its way to the black hole. A Kerr black hole has its event horizon in the form of a sphere located at a distance

$$r_+ = M + \sqrt{M^2 - a^2 - Q^2} \qquad (3.14)$$

At $r < r_+$ it is impossible to have a motion which does not lead to the singularity lying at the center of the black hole. The event horizon of a black hole thus demarcates the events happening inside and outside of the black hole. It is called an event horizon because the events occurring beyond this region are inaccessible to the outside universe. An event horizon is thus the region in space that clearly separates the black hole from the rest of the universe. The region outside the event horizon are affected by the gravitational pull of the black hole but are considered to be the part of the universe but the region inside the event horizon is not describable by the laws of causality and effects and the meaning of space and time are no more valid the same way inside this region as they are outside the event horizon.

A closed time like circuit is one of the possibilities inside the event horizon where the motion inside the horizon can be chosen in such a form that the time does not flow in such trajectories and thus the time can be stopped inside such

mathematically allowed trajectories which can exist in the region bounded by the event horizon.

It is however not possible for a massive body to enter an event horizon without being crushed by the infinite tidal forces which will tear the integrity of any material to its atomic or subatomic limit. The notion of time and space lose their meaning inside this region and beyond the event horizon the time-like structure of the space time is reversed to a space-like structure with the space and time exchanging their roles even before the event horizon is reached.

The region beyond the event horizon is distinctly disconnected from the outer world and only has mathematical attributes escaping any physical implications. The event horizon of a black hole only physically embodies the singularity at the center of the black hole and demarcates the boundary of the black hole in space. No known matter can exist that can withstand the gravitational forces just near the event horizon, mass gets converted into pure energy upon falling inside a black hole and this energy gets absorbed in the black hole as its gravitational potential energy, causing it to grow in size, as the mass of the black hole is increased by the amount of mass falling inside the event horizon so does its event horizon.

The singularity inside a Kerr black hole is expected to be in the form of a ring in contrast to the singularity inside a Schwarzschild black hole which is expected to be in the form of a point at the center. It can be said that the singularity that exists in the center of a black hole in the form of a ring mathematically embodies the breakage of the physical notions of mass, space and time. The nature of singularity and its mathematics are beyond the scope of this work. The events and regions only outside the event horizon would be of interest in the discussions and analytical treatments of the physics of the spacetime of black holes presented in this work.

### 3.2.2 Frame Dragging

As a Kerr black hole rotates about its axis the region outside the event horizon is also dragged because of this rotation of the black hole and this dragging of space outside a rotating black hole is termed as *frame dragging* as any inertial frame considered in this region will move along with the rotating space of the black hole. The frame dragging is an intuitive concept as even the space is expected to be dragged along with the strong gravitational effects in the vicinity of a black hole. The non vanishing metric coefficient $g_{t\phi}$ implies that the angular coordinate $\phi$ is coupled with the time coordinate $t$ and thus a non zero angular velocity $\omega$ is inherent to the spacetime of a rotating black hole.

For an observer near a rotating black hole, in order to be at rest with respect to the asymptotic Lorentz frame, has to apply a force in the opposite direction of the rotation of the black hole. The dragging of inertial frame causes the space to move along with the black hole and as will be seen in the next subsection there is a region beyond which it is impossible for a body to stay at rest with respect to the asymptotic Lorentz frame no matter what amount of force is applied in the opposite direction of the rotation of the black hole.

For the space craft approaching a rotating black hole in order to be in a controllable orbit will have to take into account the effects of frame dragging to be able to maneuver in the close limits of the rotating black hole. Apart from the strong gravitational pull of the black hole the space craft will also have to adjust itself with the frame dragging caused by the rotation of the black hole. The scope of this work is to carefully take into consideration these forces into the navigation of a space craft which probes the region of such strongly gravitating bodies.

### 3.2.3 Ergosphere and The Static Limit

The region beyond which it is impossible for any observer to be static with respect to the asymptotic Lorentz frame is known as the static limit of the rotating Kerr black hole. This region is mathematically defined by the vanishing of the metric coefficient $g_{tt}$ in the Kerr metric description of the rotating black hole. The metric coefficient $g_{tt}$ in the Kerr metric is given as

$$g_{tt} = \frac{1}{\rho^2}[\Delta - a^2 \sin^2\theta] \quad (3.15)$$

And it vanishes at the $r$ value

$$r = r_e(\theta) = M + \sqrt{M^2 - Q^2 - a^2\cos^2\theta} \quad (3.16)$$

An observer with fixed ( $r, \theta$) with respect to the rotating frame of reference in the vicinity of the black hole will appear to be stationary in this frame of reference of the black hole however locally stationary observer will be rotating with respect to the asymptotic Lorentz frame. The angular velocity of this observer in the asymptotic reference frame will be given as

$$\Omega \equiv \frac{d\phi}{dt} = \frac{d\phi/d\tau}{dt/d\tau} = \frac{u^\phi}{u^t} \quad (3.17)$$

The 4-velovity $\boldsymbol{u}$ of this stationary observer in terms of the Killing vectors can be expressed as

$$\boldsymbol{u} = u^t\left(\frac{\partial}{\partial t} + \frac{\Omega\,\partial}{\partial \phi}\right) = \frac{\xi_t + \Omega\xi_\phi}{|\xi_t + \Omega\xi_\phi|} \quad (3.18)$$

$$= \frac{\xi_t + \Omega\xi_\phi}{\left(-g_{tt} - 2\Omega g_{t\phi} - \Omega^2 g_{\phi\phi}\right)^{1/2}} \quad (3.19)$$

The above expression for the 4-velocity $\boldsymbol{u}$ will be timelike and physically viable for,

$$g_{tt} + 2\Omega g_{t\phi} + \Omega^2 g_{\phi\phi} < 0 \quad (3.20)$$

The above inequality suggests that the allowed values of the angular velocity of the stationary observer should lie between

$$\Omega_{min} < \Omega < \Omega_{max} \quad (3.21)$$

where,

$$\Omega_{min} = \omega - \sqrt{\omega^2 - g_{tt}/g_{\phi\phi}} \tag{3.22}$$

$$\Omega_{max} = \omega + \sqrt{\omega^2 - g_{tt}/g_{\phi\phi}} \tag{3.23}$$

and

$$\omega \equiv \frac{1}{2}(\Omega_{min} + \Omega_{max}) = -\frac{g_{\phi t}}{g_{\phi\phi}} = \frac{(2Mr - Q^2)a}{(r^2+a^2)^2 - \Delta a^2 \sin^2\theta} \tag{3.24}$$

Implying that the stationary observer can only have certain range of angular velocity for it to be a stationary observer at a given $(r, \theta)$ and also that $\Omega_{\text{min}}$ would be zero when $g_{tt}$ vanishes. This implies that at the surface, $g_{tt} = 0$, an observer cannot help itself but to rotate along with the black hole. This is called the *static limit* and the region between $r_e(\theta)$ and $r_+$ is called the *ergosphere* of the black hole.

The ergosphere is a region of spacetime unknown in the realm of observed physical universe. The physics inside the ergosphere has many interesting consequences and it remains an area of unprecedented research in the physics of spacetime. Many questions are posed on the behavior of physical laws in this region that can be one day accessible to the human science. If a spacecraft prepares itself for a black hole probe then the ergosphere can be one of the prime regions of investigation for understanding the physics in extreme high gravitational conditions.

It has been shown in literature that ergosphere can be exploited to extract an almost infinite amount of energy from a rotating black hole. A rotating black hole can be a source of huge amount of energy by carefully exploiting this region by a

process known as Penrose process [18]. If human are some day capable of interstellar travels then a rotating black hole can be a haven for extracting energy for an infinitely large amount of time and thus can be the safest places in colonizing the interstellar space [14].

## 3.3 Effect on Outer Bodies

As a body approaches a black hole the gravitational pull of the black hole gets stronger and a force acts on the body which is directly proportional to the size and mass of the body that it acts to elongate or stretch the body and also sideway suppress the body as it nears the black hole. This force is known as the tidal force of the black hole and it is the major cause of threat for the destruction of any body as it approaches the black hole. Before the body arrives at the event horizon it will be disrupted by these forces causing it to become like a noodle and finally disintegrating into individual atoms and absorbed by the event horizon.

A similar kind of fate is in store for a photon as it approaches the black hole. To an external observer the photon will be infinitely red shifted on its journey to the black hole and finally absorbed at the event horizon.

For a realistic case for a space craft to probe a black hole it is important that the space craft is kept at a considerable distance from the black hole in order to preserve its integrity in view of the tidal forces of the black hole. Depending upon the size and material used for the probe one has to design a mission outside a critical distance of the region outside the black hole that these forces are negligibly small for the structure of the spacecraft.

The tidal forces become more and more important as the spacecraft approaches the black hole, however if we are a safe distance from the black hole the orbits

with fairly constant radial coordinates and we are only considered about the tangential journeys then the effect of tidal forces can be minimized to a greater extent. Depending on the placement of the spacecraft and its motion in the Kerr spacetime a method has to be employed in order to take into account the effect of tidal forces and a means to minimize their effects on the space craft structure.

The Tidal tensor in Kerr spacectime along a general geodesic is calculated in chapter 6. The tidal tensor along the polar orbit in Kerr spacetime is derived in section 6.3.

# Chapter 4

# Particle Trajectory in Kerr Spacetime

A spacecraft in a strong gravitational field has to find the right trajectories or geodesics that can establish the spacecraft in a stable orbit around the gravitating body. A close understanding of such orbits allowed in the Kerr geometry is a first step in this direction. The geodesics in Kerr spacetime are classified as equatorial geodesics or off equatorial geodesics. A general trajectory is off equatorial geodesics and the equations are derived by the Hamiltonian formulism.

## 4.1 Constants of Motion in Kerr Spacetime

Geodesic motion in the equatorial plane in Kerr spacetime has been extensively dealt in theoretical works and a complete analytical solution of the motion of a particle in the Kerr spacetime is provided by the equations derived below[43]. The motion in Kerr spacetime is characterized by the constants of motion which are found to be the energy, angular momentum, rest mass of the particle, and a new constant of motion known as the Carter's constant [40].

Considering a geodesic with affine parameter $\lambda$ and a tangent vector $u^{\mu}$

$$u^{\mu} = \frac{dx^{\mu}}{d\lambda} \equiv \dot{x}^{\mu} \tag{4.1}$$

The tangent vector $u^{\mu}$ is the solution of the geodesic equations

$$u^{\mu} u^{\nu}_{;\mu} = 0 \tag{4.2}$$

which is the manifestation of the Euler-Lagrange equations

$$\frac{d}{d\lambda}\frac{\partial \mathcal{L}}{\partial \dot{x^{\alpha}}} = \frac{\partial \mathcal{L}}{\partial x^{\alpha}} \tag{4.3}$$

where the Lagrangian is given as

$$\mathcal{L}(x^{\mu}, \dot{x}^{\mu}) = \frac{1}{2}\, g_{\mu\nu} \dot{x}^{\mu} \dot{x}^{\nu} \tag{4.4}$$

The *conjugate momentum* $p_{\mu}$ is defined as

$$p_{\mu} \equiv \frac{\partial \mathcal{L}}{\partial \dot{x}^{\mu}} = g_{\mu\nu} \dot{x}^{\nu} \tag{4.5}$$

If the metric $g_{\mu\nu}$ does not explicitly depend on a given coordinate $x^{\mu}$ or in other words is cyclic in the coordinate $x^{\mu}$ then the corresponding conjugate momentum $p_{\mu}$ is a constant of motion related to the Killing vector tangent to the corresponding coordinate lines. The Kerr metric in Boyer Lindquist coordinates as well as in Kerr coordinates is independent of the coordinates $t$ and $\phi$ and thus the corresponding $p_t$ and $p_{\phi}$ are constants of motion,

$$p_t = \dot{x}_t \equiv u_t = const \tag{4.6}$$

and

$$p_\phi = \dot{x}_\phi \equiv u_\phi = const \tag{4.7}$$

The geodesics in Kerr spacetime are naturally characterized by the two constants of motion

$$E = -p_t \tag{4.8}$$

and

$$L = p_\phi \tag{4.9}$$

The third constant of motion $\kappa$ which also represents the conserved mass of the test particle, is related with the metric and the 4 velocity $u^\mu$ through

$$g_{\mu\nu}u^\mu u^\nu = \kappa \tag{4.10}$$

where

$$\kappa = -1 \quad \text{for timelike geodesics}$$

$$\kappa = 0 \quad \text{for null geodesics}$$

$$\kappa = 1 \quad \text{for spacelike geodesics} \tag{4.11}$$

The fourth constant of motion, Carter's constant was derived by Brandan Carter in 1966 [40,41] and has been discussed in the later section. The origin of the

constant is not completely understood and has been suggested to be linked to a Killing tensor related to the Boyer Lindquist coordinates $r$ and $\theta$ [42].

## 4.2 Equatorial Geodesics in Kerr Spacetime

Equatorial geodesics correspond to motion restricted to the $\theta = \pi/2$ plane. The existence of such orbits can be shown by showing that the above equation is a solution of the Euler-Lagrange equations.

The Lagrangian in Kerr spacetime will be

$$\mathcal{L} = \frac{1}{2}\, g_{\mu\nu}\dot{x}^{\mu}\dot{x}^{\nu} = \frac{1}{2}\left\{-\left(1-\frac{2Mr}{\Sigma}\right)\dot{t}^{2} - \frac{2Mr}{\Sigma}\, a\sin^{2}\theta \dot{t}\,\dot{\phi} + \frac{\rho}{\Delta}\,\dot{r}^{2} + \rho\,\dot{\theta}^{2} + \left[r^{2} + a^{2} + \frac{2Mra^{2}}{\Sigma}\sin^{2}\theta\right]\sin^{2}\theta\,\dot{\phi}^{2}\right\} \qquad (4.12)$$

the $\theta$ component of the Euler-Lagrange's equation becomes

$$\frac{d}{d\lambda}\left(g_{\theta\mu}\dot{x}^{\mu}\right) = \frac{d}{d\lambda}\left(\Sigma\dot{\theta}\right) = \Sigma\ddot{\theta} + \Sigma_{,\mu}\dot{x}^{\mu}\dot{\theta} = \frac{1}{2}g_{\mu\nu,\theta}\dot{x}^{\mu}\dot{x}^{\nu} \qquad (4.13)$$

Opening the right hand side using the Einstein summation rule gives

$$\frac{1}{2}g_{\mu\nu,\theta}\dot{x}^{\mu}\dot{x}^{\nu} = \frac{1}{2}\left\{\Sigma_{,\theta}\left(\frac{\dot{r}^{2}}{\Delta} + \dot{\theta}^{2}\right) + 2\,sin\theta cos\theta(r^{2}+a^{2})\dot{\phi}^{2} - \frac{2Mr}{\Sigma^{2}}\rho_{,\theta}\left(a\sin^{2}\theta\,\dot{\phi} - t\right)^{2} + \frac{4Mr}{\Sigma}\left(a\sin^{2}\theta\,\dot{\phi} - \dot{t}\right)2a\,sin\theta cos\theta\dot{\phi}\right\} \qquad (4.14)$$

for $\theta = \pi/2$ the equation reduces to

$$\ddot{\theta} = -\frac{2}{r}\dot{r}\dot{\theta} \qquad (4.15)$$

Therefore if $\dot{\theta} = 0$ and $\theta = \pi/2$ at $\lambda = 0$ then for $\lambda > 0$, $\dot{\theta} \equiv 0$ and $\equiv \pi/2$ . Thus a geodesic which starts in the equatorial plane remains at the equatorial plane for all times, establishing that the equatorial geodesics are planar in form.

On the equatorial plane, $\rho = r^2$, therefore the metric coefficients can be expressed as

$$g_{tt} = -\left(1 - \frac{2M}{r}\right) \tag{4.16}$$

$$g_{t\phi} = -\left(\frac{2Ma}{r}\right) \tag{4.17}$$

$$g_{rr} = \frac{r^2}{\Delta} \tag{4.18}$$

$$g_{\phi\phi} = r^2 + a^2 + \frac{2Ma^2}{r} \tag{4.19}$$

and

$$E = -g_{t\mu}u^{\mu} = \left(1 - \frac{2M}{r}\right)\dot{t} + \frac{2Ma}{r}\dot{\phi} \tag{4.20}$$

$$L = g_{\mu\phi}u^{\mu} = -\frac{2Ma}{r}\dot{t} + \left(r^2 + a^2 + \frac{2Ma^2}{r}\right)\dot{\phi} \tag{4.21}$$

The above equations for $\dot{t}$ and $\dot{\phi}$ can be solved by defining

$$A \equiv 1 - \frac{2M}{r} \tag{4.22}$$

$$B \equiv \frac{2Ma}{r} \tag{4.23}$$

$$C \equiv r^2 + a^2 + \frac{2Ma^2}{r} \tag{4.24}$$

to write

$$E = A\dot{t} + B\dot{\phi} \tag{4.25}$$

$$L = -B\dot{t} + C\dot{\phi} \tag{4.26}$$

Also noting that $AC + B^2 = \left(1 - \frac{2M}{r}\right)\left(r^2 + a^2 + \frac{2Ma^2}{r}\right) + \frac{4M^2a^2}{r^2} = r^2 - 2Mr + a^2 = \Delta$.

Furthermore,

$$CE - BL = [AC + B^2]\dot{t} = \Delta\dot{t} \tag{4.27}$$

$$AL + BE = [AC + B^2]\dot{\phi} = \Delta\dot{\phi} \tag{4.28}$$

Or

$$\dot{t} = \frac{1}{\Delta}\left[\left(r^2 + a^2 + \frac{2Ma^2}{r}\right)E - \frac{2Ma}{r}L\right] \tag{4.29}$$

$$\dot{\phi} = \frac{1}{\Delta}\left[\left(1 - \frac{2M}{r}\right)L + \frac{2Ma}{r}E\right] \tag{4.30}$$

The equation for the radial component can be derived by using

$$g_{\mu\nu}u^\mu u^\nu = \kappa \tag{4.32}$$

$$= -A\dot{t}^2 - 2B\dot{t}\dot{\phi} + C\dot{\phi}^2 + \frac{r^2}{\Delta}\dot{r}^2 \tag{4.33}$$

$$= -\left[A\dot{t} + B\dot{\phi}\right]\dot{t} + \left[-B\dot{t} + C\dot{\phi}\right]\dot{\phi} + \frac{r^2}{\Delta}\dot{r}^2 \tag{4.34}$$

$$= -E\dot{t} + L\dot{\phi} + \frac{r^2}{\Delta}\dot{r}^2 \tag{4.35}$$

Therefore,

$$\dot{r}^2 = \frac{\Delta}{r^2}\left(E\dot{t} - L\dot{\phi} + \kappa\right) = \frac{1}{r^2}[CE^2 - 2BLE - AL^2] + \frac{\kappa\Delta}{r^2} \tag{4.36}$$

The polynomial $[CE^2 - 2BLE - AL^2]$ has zeros at

$$V_\pm = \frac{BL \pm \sqrt{B^2L^2 + ACL^2}}{C} = \frac{L}{C}[B \pm \sqrt{\Delta}] \tag{4.37}$$

So the radial equation can now be written as

$$\dot{r}^2 = \frac{C}{r^2}(E - V_+)(E - V_-) + \frac{\kappa\Delta}{r^2} \quad (4.38)$$

$$= \frac{(r^2+a^2)^2 - a^2\Delta}{r^4}(E - V_+)(E - V_-) + \frac{\kappa\Delta}{r^2} \quad (4.39)$$

and

$$V_\pm = \frac{2Mar \pm r^2\sqrt{\Delta}}{(r^2+a^2)^2 - a^2\Delta}L \quad (4.40)$$

These are the complete set of equations required to describe the motion of a particle or photon in the equatorial plane of the Kerr black hole. In the Schwarzschild limit where → 0 ,

$$V_+ + V_- \propto a \to 0, \quad (4.41)$$

and

$$V_+V_- \to \frac{L^2\Delta}{r^4} \quad (4.42)$$

If we define ≡ $V_+V_-$ , the equations can be reduced to the expected form

$$\dot{r}^2 = E^2 - V(r), \quad (4.43)$$

where

$$V(r) = -\frac{\kappa\Delta}{r^2} + \frac{L^2\Delta}{r^4} = \left(1 - \frac{2M}{r}\right)\left(-\kappa + \frac{L^2}{r^2}\right) \quad (4.44)$$

Recalling that $\kappa = -1$ for time like geodesics, $\kappa = 0$ for null geodesics and $\kappa = 1$ for spacelike geodesics. A general description on the stability of the orbits in Kerr spacetime was primarily carried out by James Bardeen et al [44].

## 4.3 The General Equations of Geodesic motion in Kerr Spacetime

The general geodesics are studied using the Hamiltonian Jacobi formulism as it will be seen that this approach leads to an additional constant of motion discovered by Brandon Carter and thereby termed as the Carters constant. This constant is not associated with any spacetime symmetry and is a result of the separable of variable method used in the Hamiltonian Jacobi approach.

The Lagrangian in terms of the spacetime metric is expressed in the following manner

$$\mathcal{L}(x^{\mu}, \dot{x}^{\mu}) = \frac{1}{2} g_{\mu\nu} \dot{x}^{\mu} \dot{x}^{\nu} \tag{4.45}$$

and the conjugate momenta associated with a given coordinate can be derived using

$$p_{\mu} = \frac{\partial \mathcal{L}}{\partial \dot{x}^{\mu}} = g_{\mu\nu} \dot{x}^{\nu} \tag{4.46}$$

the above expression can be inverted to obtain $\dot{x}^{\mu}$ in terms of $p_{\mu}$ as

$$\dot{x}^{\mu} = g^{\mu\nu} p_{\nu} \tag{4.47}$$

The Hamiltonian is defined as

$$H(x^{\mu}, p_{\nu}) = p_{\mu} \dot{x}^{\mu}(p_{\nu}) - \mathcal{L}(x^{\mu}, \dot{x}^{\mu}(p_{\nu})) \tag{4.48}$$

and with the above equations would take the form

$$H = \frac{1}{2} g^{\mu\nu} p_{\mu} p_{\nu} \tag{4.49}$$

The geodesic equations in Hamiltonian formulism are given as

$$\dot{x}^{\mu} = \frac{\partial H}{\partial p_{\mu}} \tag{4.50}$$

$$\dot{p}_{\mu} = -\frac{\partial H}{\partial x^{\mu}} \tag{4.51}$$

A forth constant of motion can now be derived by using the Hamiltonian-Jacobi approach [45]. The action function associated with the Hamiltonian function is defined as

$$S = S(x^{\mu}, \lambda) \tag{4.52}$$

and is a solution of the *Hamilton-Jacobi* equation

$$H\left(x^{\mu}, \frac{\partial S}{\partial x^{\mu}}\right) + \frac{\partial S}{\partial \lambda} = 0 \tag{4.53}$$

If $S$ has to be a solution of the above equation then

$$\frac{\partial S}{\partial x^{\mu}} = p_{\mu} \tag{4.54}$$

Thus the solution of the Hamilton –Jacobi equation provides with the conjugate momenta in terms of four constants and can provide the necessary solutions of the geodesic equations.

The Hamiltonian and the two constants known in this case are

$$H = \frac{1}{2} g^{\mu\nu} p_{\mu} p_{\nu} \tag{4.55}$$

$$p_t = -E \tag{4.56}$$

$$p_{\phi} = L \tag{4.57}$$

thus the function $S$ can now be written as

$$S = -\frac{1}{2}\kappa\lambda - Et + L\phi + S^{r\theta}(r, \theta) \tag{4.58}$$

Assuming a separable solution for the function $S^{r\theta}$ the above equation can be written as

$$S = -\frac{1}{2}\kappa\lambda - Et + L\phi + S^{r}(r) + S^{\theta}(\theta) \tag{4.59}$$

Using the inverse metric and its coefficients

$$g^{\mu\nu} = -\frac{1}{\Delta\Sigma}\left[(r^2+a^2)\frac{\partial}{\partial t}+a\frac{\partial}{\partial\phi}\right]^2+\frac{1}{\Sigma\sin^2\theta}\left[\frac{\partial}{\partial\phi}+a\sin^2\theta\frac{\partial}{\partial t}\right]^2+\frac{\Delta}{\Sigma}\left(\frac{\partial}{\partial r}\right)^2+\frac{1}{\Sigma}\left(\frac{\partial}{\partial\theta}\right)^2 \quad (4.60)$$

The Hamilton-Jacobi equation can be expressed as

$$-\kappa+\frac{\Delta}{\Sigma}\left(\frac{dS^{(r)}}{dr}\right)^2+\frac{1}{\Sigma}\left(\frac{dS^{(\theta)}}{d\theta}\right)^2-\frac{1}{\Delta}\left[r^2+a^2+\frac{2Mra^2}{\Sigma}\sin^2\theta\right]E^2+\frac{4Mra}{\Sigma\Delta}EL+\frac{\Delta-a^2\sin^2\theta}{\Sigma\Delta\sin^2\theta}L^2=0 \quad (4.61)$$

or

$$-\kappa(r^2+a^2\cos^2\theta)+\Delta\left(\frac{dS^{(r)}}{dr}\right)^2+\left(\frac{dS^{(\theta)}}{d\theta}\right)^2-\left[\frac{\left(r^2+a^2\right)^2}{\Delta}-a^2\sin^2\theta\right]E^2+\frac{4Mra}{\Delta}EL+\left(\frac{1}{\sin^2\theta}-\frac{a^2}{\Delta}\right)L^2=0 \quad (4.62)$$

alternatively,

$$\Delta\left(\frac{dS^{(r)}}{dr}\right)^2-\kappa r^2-\frac{\left(r^2+a^2\right)^2}{\Delta}E^2+\frac{4Mra}{\Delta}EL-\frac{a^2}{\Delta}L^2+a^2E^2+L^2 \quad (4.63)$$

$$=-\left(\frac{dS^{(\theta)}}{d\theta}\right)^2+\kappa a^2\cos^2\theta+a^2\cos^2\theta\,E^2-\frac{\cos^2\theta}{\sin^2\theta}L^2 \quad (4.64)$$

In the above equation the LHS does not depend on $\theta$ and the RHS does not depend on $r$ and thus the two sides can be equated to a constant, such that

$$\left(\frac{dS^{(\theta)}}{d\theta}\right)^2-\cos^2\theta\left[(\kappa+E^2)a^2-\frac{1}{\sin^2\theta}L^2\right]=C \quad (4.65)$$

$$=\Delta\left(\frac{dS^{(r)}}{dr}\right)^2-\kappa r^2-\frac{\left(r^2+a^2\right)^2}{\Delta}E^2+\frac{4Mra}{\Delta}EL-\frac{a^2}{\Delta}L^2+a^2E^2+L^2 \quad (4.66)$$

$$=\Delta\left(\frac{dS^{(r)}}{dr}\right)^2-\kappa r^2+(L-aE)^2-\frac{1}{\Delta}\left[E(r^2+a^2)-La\right]^2=-C \quad (4.67)$$

and now defining the functions $R(r)$ and $\Theta(\theta)$ as

$$R(r) \equiv \Delta[-C + \kappa r^2 - (L - aE)^2] + [E(r^2 + a^2) - La]^2 \quad (4.68)$$

$$\Theta(\theta) \equiv C + \cos^2\theta \left[(\kappa + E^2)a^2 - \frac{1}{\sin^2\theta} L^2\right] \quad (4.69)$$

Then

$$\left(\frac{dS^{(\theta)}}{d\theta}\right)^2 = \Theta \quad (4.70)$$

$$\left(\frac{dS^{(r)}}{dr}\right)^2 = \frac{R}{\Delta^2} \quad (4.71)$$

and the solution of the Hamilton-Jacobi equation has now the form

$$S = -\frac{1}{2}\kappa\lambda - Et + L\phi + \int \frac{\sqrt{R}}{\Delta} dr + \int \sqrt{\Theta}\, d\theta \quad (4.72)$$

The equations of motion in Kerr spacetime can be written as a quadrature

$$\Sigma\, d\theta/d\lambda = \pm\sqrt{\Theta} \quad (4.73)$$

$$\Sigma\, dr/d\lambda = \pm\sqrt{R} \quad (4.74)$$

$$\Sigma\, d\phi/d\lambda = -(aE - L/\sin^2\theta) + (a/\Delta)[E(r^2 + a^2) - La] \quad (4.75)$$

$$\Sigma dt/d\lambda = -a(aE\, sin^2\theta - L) + (r^2 + a^2)\Delta^{-1}[E(r^2 + a^2) - La] \quad (4.76)$$

The signs of the functions $\sqrt{R}$ and $\sqrt{\Theta}$ can be chosen arbitrarily but once chosen have to be further consistent.

With the help of the above equations it is possible to describe the trajectory of a free particle as it enters the Kerr spacetime, the above equations are the free particle equations which are seen to be completely solvable because of the fourth constant of motion discovered using the Hamilton-Jacobi approach to the Kerr Metric.

For a spacecraft with a specific mass and required rocket thrusts it can be possible for the spacecraft to maneuver over the Kerr region with the knowledge of these geodesics. It is the aim of this work to study the trajectories and the necessary external forces required to carry a spacecraft mission in such extreme gravitational regions.

The above equations of motion in Kerr spacetime can be numerically integrated and it thus becomes possible for spacecrafts in such regions to obtain a trajectory and by the use of sufficient rocket thrusts an orbit can be established around the rotating black hole.

## 4.4 Keplerian Spherical Orbits in Kerr Spacetime

The above equations of geodesics in Kerr spacetime can be numerically solved for varied initial conditions. The various orbits for different eccentricities and different inclinations are plotted for a rotating black hole of 10 $M_{\odot}$ with angular parameter $a = 0.5M$ [67]. The initial launching distance from the centre of the Boyer Lindquist coordinate system is kept at $1000\ M$.

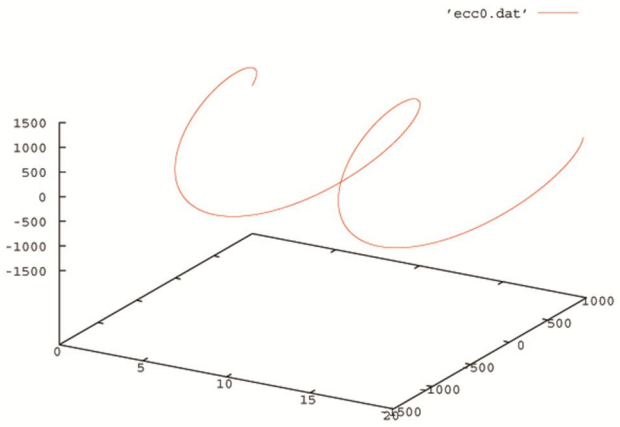


**Fig 4.1** Trajectory of a particle in the Kerr spacetime at a distance of $1000M$ and eccentricity 0 ($a = 0.5$)

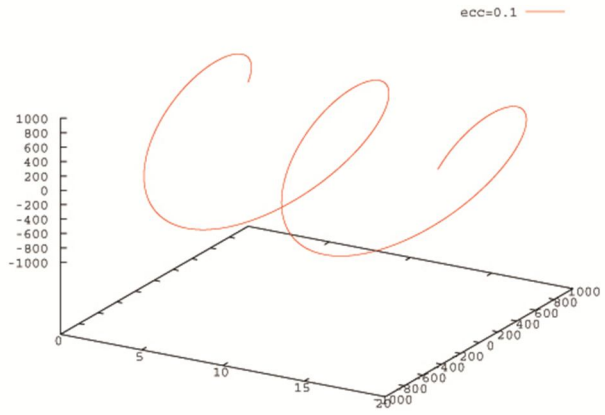


***Fig 4.2*** Trajectory of a particle in the Kerr spacetime at a distance of $1000M$ and eccentricity $0.1$ ($a = 0.5$).

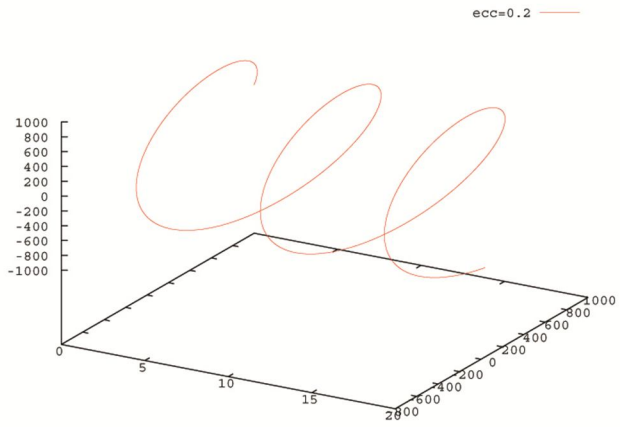


**Fig 4.3** Trajectory of a particle in the Kerr spacetime at a distance of $1000M$ and eccentricity $0.2$ ($a = 0.$)

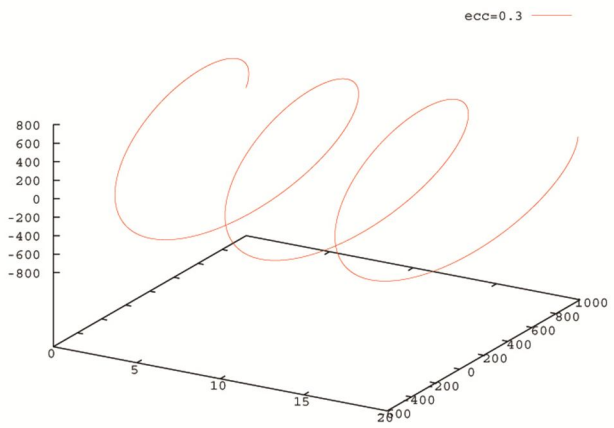


**Fig 4.4** Trajectory of a particle in the Kerr spacetime at a distance of $1000M$ and eccentricity 0.3 ($a = 0.5$)

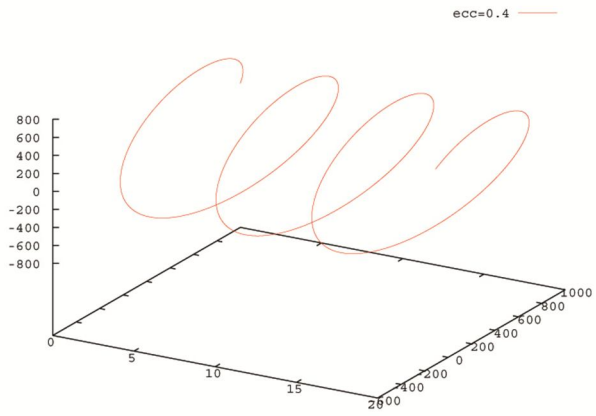


**Fig 4.5** Trajectory of a particle in the Kerr spacetime at a distance of $1000M$ and eccentricity 0.4 ($a = 0.5$)

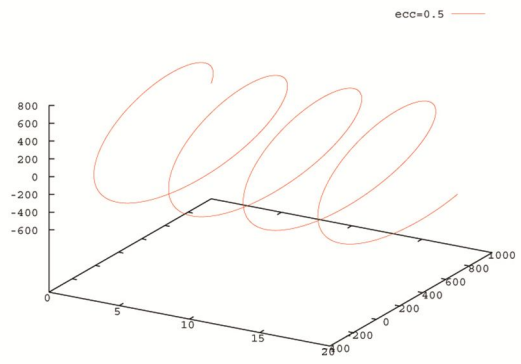


**Fig 4.6** Trajectory of a particle in the Kerr spacetime at a distance of $1000M$ and eccentricity 0.5 ($a = 0.5$)

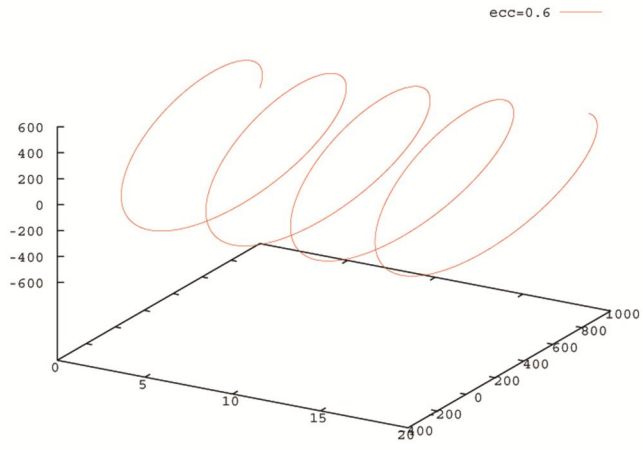


**Fig 4.7** Trajectory of a particle in the Kerr spacetime at a distance of $1000M$ and eccentricity 0.6 ($a = 0.5$)

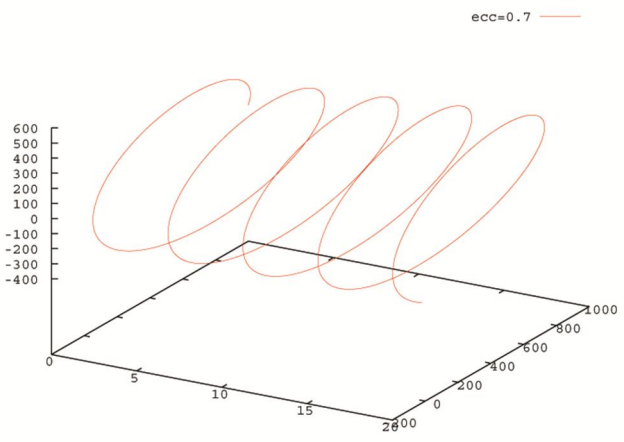


**Fig 4.8** Trajectory of a particle in the Kerr spacetime at a distance of $1000M$ and eccentricity 0.7 ($a = 0.5$)

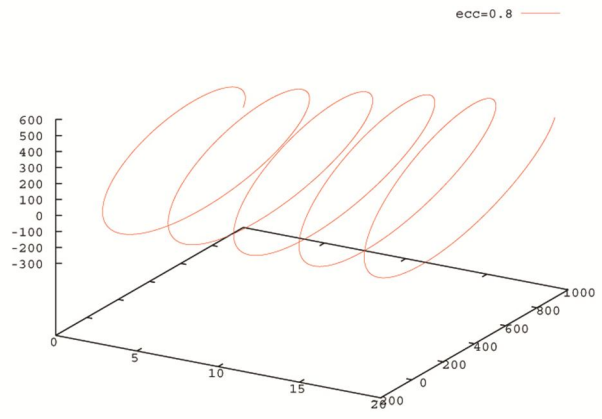


**Fig 4.9** Trajectory of a particle in the Kerr spacetime at a distance of $1000M$ and eccentricity 0.8 ($a = 0.5$)

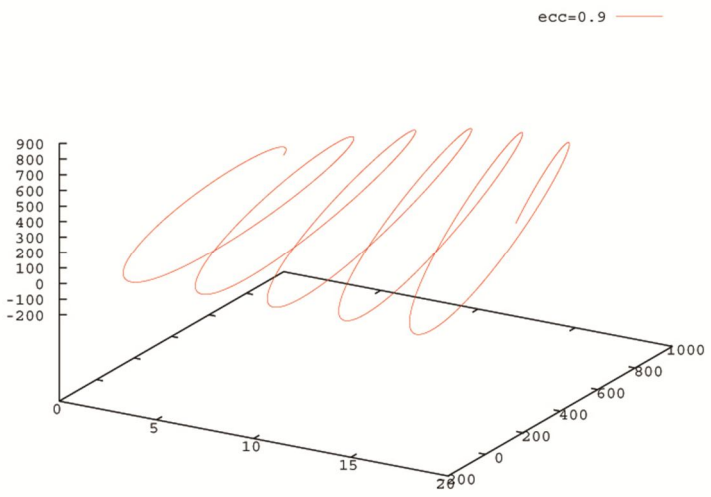


**Fig 4.10** Trajectory of a particle in the Kerr spacetime at a distance of $1000M$ and eccentricity 0.9 ($a = 0.5$)

As seen from the above patterns, for the same amount of time in coordinate frame, the number of orbits increases with an increase in the eccentricity of the orbit. This can be explained as with the increase in eccentricity of the orbit, the corresponding energy associated with the orbit also increases and least being for the circular orbit for zero eccentricity. With the increase in energy associated with an orbit the corresponding velocity increases and the particle takes an increasing number of rotation about the black hole centre.

# Chapter 5

# Polar Orbits in Kerr Spacetime

The discovery of Carter's constant of motion in Kerr spacetime led to the complete analytic solution of the case of a particle motion in rotating curved spacetimes. Polar orbits in Kerr spacetime would be the ones that cross the axis of rotation of the black hole and because of the rotation of spacetime such orbits experience an advancement of the ascending node [46]. The equations of motion for the polar orbits can be deduced for the orbital angle $\theta = 0$.

Let $x^{\mu}$ be the Boyer Lindquist coordinates in which the Kerr metric is written as

$$ds^2 = -\left(1 - \frac{2Mr}{\Sigma}\right) dt^2 - 2\left(\frac{2Mr}{\Sigma}\right) a \sin^2\theta \; dt \, d\phi + \left(\frac{\Sigma}{\Delta}\right) dr^2 + \Sigma d\theta^2 + \left(\frac{A}{\Sigma}\right) \sin^2\theta \, d\phi^2 \qquad (5.1)$$

where

$$\Sigma = r^2 + a^2 \cos^2\theta \tag{5.2}$$

$$\Delta = r^2 + a^2 - 2Mr \tag{5.3}$$

$$A = (r^2 + a^2)^2 - \Delta a^2 \sin^2\theta \tag{5.4}$$

The equations of motion obtained by Carter using the Hamilton Jacobi formulism are given as follows, if $x^a(\tau)$ is the coordinate image of the timelike geodesic $C(\tau)$ followed by a particle of rest mass $\mu$, then the vector $u^a = \dot{x}^2 = dx^a/d\tau$ will satisfy the quadrature equations :

$$\dot{t} = (\Delta\Sigma)^{-1}(AE - 2Mar\Phi) \tag{5.5}$$

$$\Sigma^2\dot{r}^2 = [(r^2 + a^2)E - a\phi]^2 - \Delta(\mu^2 r^2 + K) \tag{5.6}$$

$$\Sigma^2\dot{\theta}^2 = K - \mu^2 a^2 \cos^2\theta - \left(aEsin\theta - \frac{\Phi}{sin\theta}\right)^2 \tag{5.7}$$

$$\dot{\phi} = \Delta^{-1}\left[\left(\frac{2Mr}{\Sigma}\right)aE + \frac{\left(1-\frac{2Mr}{\Sigma}\right)\Phi}{\sin^2\theta}\right] \tag{5.8}$$

Where $\Phi, E$ and $K$ are the projection of the angular momentum along the symmetric axis, energy at infinity of the particle, and the Carter's constant respectively.

For the orbit represented by the $C(\tau)$ to be polar, it has to intersect the symmetric axis of the Kerr spacetime, since this axis consists of points for which $sin\theta = 0$ , hence from the third equation above, $\Phi = 0$ , is a necessary condition for an orbit to be polar in the Kerr spacetime. Or in other words, for a particle to follow a polar orbit, it is necessary that the particle in Kerr spacetime has a null angular momentum.

The equations of motion for polar orbits are then expressed as

$$\dot{t} = AE/\Delta\Sigma \tag{5.9}$$

$$\Sigma^2\dot{r}^2 = R(r) = (r^2 + a^2)^2[E^2 - V^2(r)] \tag{5.10}$$

$$\Sigma^2\dot{\theta} = Q - a^2(1 - E^2)\cos^2\theta \tag{5.11}$$

$$\dot{\phi} = 2MaEr/\Delta\Sigma \tag{5.12}$$

Where the effective potential V is given as

$$V^2 = \Delta(K + r^2)/(r^2 + a^2)^2 \tag{5.13}$$

and

$$Q = K - a^2E^2 \tag{5.14}$$

The effective potential $V^2(r)$ is plotted with the radius for different values of K and it is seen that bound orbits can exist for $K$ values greater than 8.

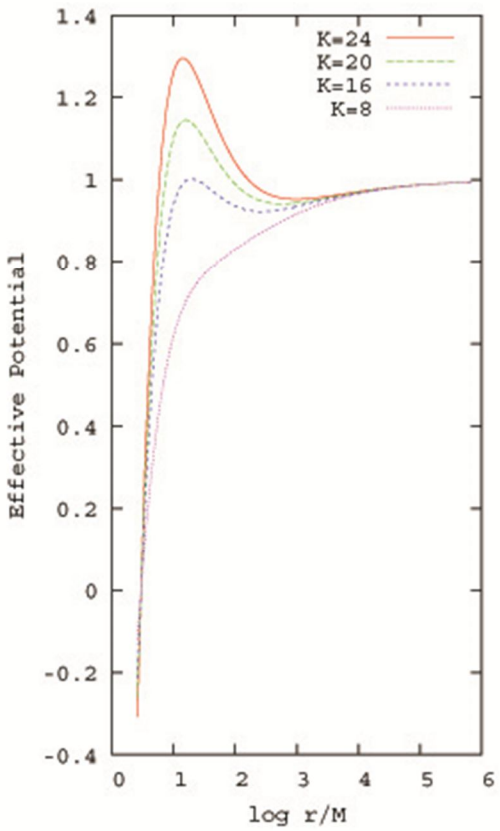


**Fig 5.1***:* Effective potential *vs* log *r/M* for Kerr spacetime, for four different values of Carter's constant.

## 15.1 Spherical Polar Orbits in Kerr spacetime

The spherical polar orbits for which the radial vector remains constant throughout the orbit can be expressed by replacing the $r$ equation as $\partial r/\partial\tau = 0$.

$$\Sigma^2\dot{r}^2 = R(r) = (r^2 + a^2)^2[E^2 - V^2(r)] = 0 \qquad (5.15)$$

The above equations are solved numerically for the case $r = 10M$, when the energy of the test particle is $E = 0.956$ and the Carter's constant $K = 14.783$ for a rotating blackhole with angular momentum $a = 0.8M$.

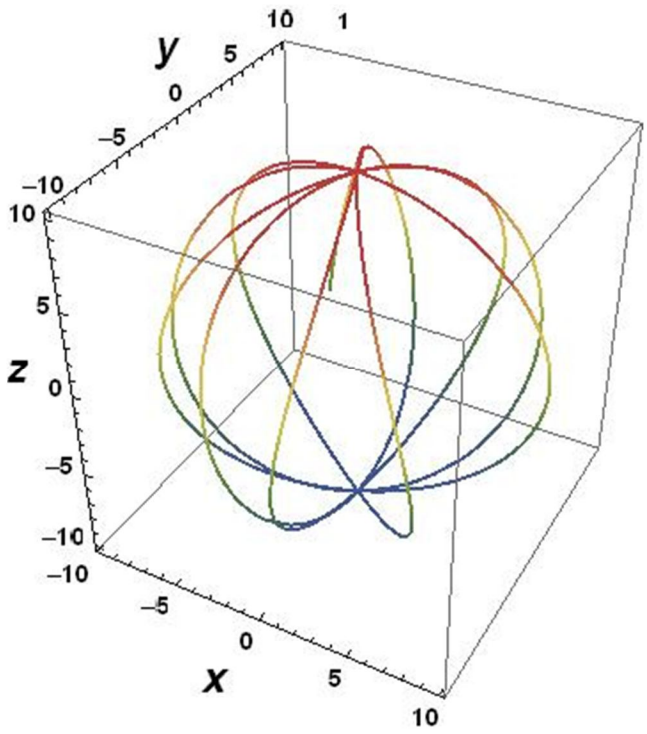


**Fig 5.2a** : Temporal evolution of a spherical polar orbit in the x-y-z space.

The results are plotted in the three dimensional space and the particle is observed to be following a polar orbit which rotates due to the frame dragging. Since the orbit lies on a sphere of fixed radius, such orbits are termed as spherical polar orbits in Kerr spacetime.

The energy and the Carters constants for a spherical polar orbit are given as

$$E^2 = \Delta(r^2 + K)/(a^2 + r^2)^2 \qquad (5.16)$$

and

$$K = (Mr^4 - a^2r^3 - 3Ma^2r^2 + a^4r)/(r^3 - 3Mr^2 + a^2r + Ma^2) \qquad (5.17)$$

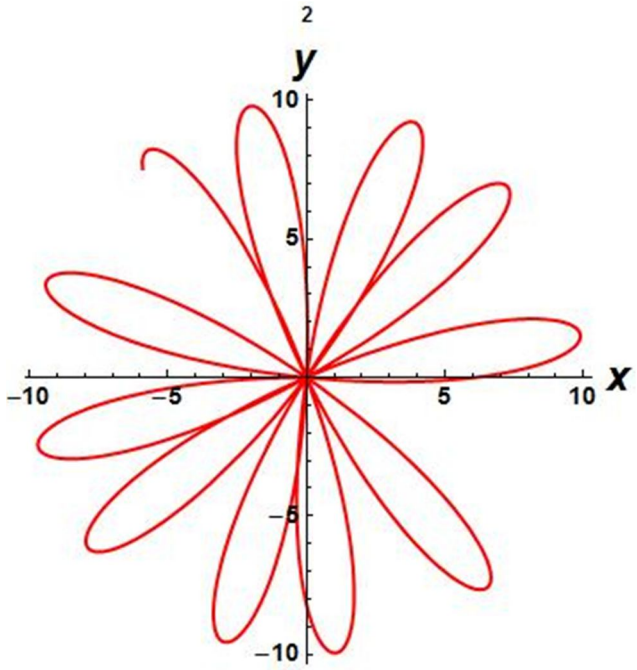


**Fig 5.2b** : Spherical polar orbits in the x-y plane.

The spherical polar orbits have been plotted for different radii with their corresponding E and K values and have been verified to hold good upto large radii of $1000M$, which is the proposed range of orbits for spacecrafts in Kerr spacetime in this study.The variation of $\theta$ and $\phi$ coordinates with respect to the proper time gives the following linear increase for both the coordinates, fig *5.3*.

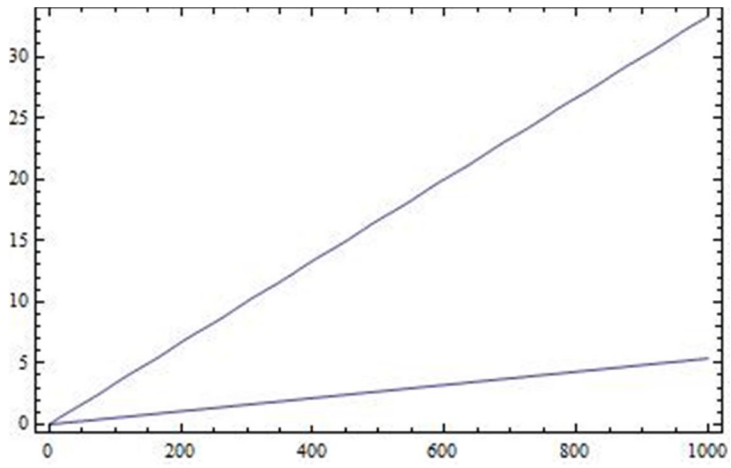


**Fig. 5.3***:* Variation of $\theta, \phi$ coordinates with respect to $\tau$ for an orbit of radius $10M$.

## 5.2 Frame Dragging of Polar Orbits

The rotation of the spacetime inherent in the Kerr geometry will force the lines of nodes of bound orbits of the non-equatorial orbits to advance in the sense of the rotating black hole. Therefore the advancement of the nodal point (where the particle's orbit intersects the equatorial plane) coincides with the rotation of the black hole. This effect is known as the Lense and Thirring effect [51].An experiment to measure this effect due to the rotation of the Earth has been proposed and is known as the Stanford Gyroscope Experiment [52] based on the method proposed by Schiff [53].

From the last two equations of motion in polar orbit, the rate of change of the coordinate $\phi$ with the coordinate $\theta$ can be written as

$$\frac{d\phi}{d\theta} = \frac{2MaEr}{\Delta\,\Theta^{1/2}}$$

$$= \frac{2MaEr}{\Delta\,\mathrm{Q}^{1/2}(1-\mathrm{k}^2\cos^2\theta)} \qquad (5.18)$$

where

$$k^2 = a^2\Gamma^2/Q \qquad (5.19)$$

and

$$\Gamma^2 = 1 - E^2 \qquad (5.20)$$

For the cases, $E^2 < 1$, $k$ is also less than 1, and the above equation can be integrated to give the solutions in the form,

$$\phi = \phi_0 + \frac{2MaEr}{\Delta\,\mathrm{Q}^{1/2}}F(\theta,k) \qquad (5.21)$$

Where $F(\theta,k)$ is the elliptical integral of the first kind and is defined as

$$F(\theta,k) = \int_0^{\theta}(1-k^2\cos^2\theta)^{1/2}\,d\theta \qquad (5.22)$$

In the approximation, $k \ll 1$, the integral can be solved to give the final change of the coordinate $\phi$ per revolution as [49]

$$\delta\phi = \frac{4\pi MaEr}{\Delta\, Q^{1/2}}\left(1 + \frac{k^2}{4} + \frac{3}{26}k^4 + O(k^6)\right) \qquad (5.23)$$

This is a typical result of the dragging effect associated with rotating bodies and the effect vanishes for the non rotating black holes as for such cases $a = 0$ and hence $\delta\phi = 0$.

## 5.3 Non Spherical Polar Orbits

The radial equation corresponding to the polar orbits in Kerr spacetime is given as

$$\rho^4\dot{r} = R(r) = (r^2 + a^2)\left(E^2 - V^2(r)\right) \qquad (5.24)$$

If $r_0$ is the radius of a spherical orbit and a double root of the function $R(r)$,

$$R(r) = (r - r_0)^2 G(r) \qquad (5.25)$$

where

$$G(r) = -\Gamma^2 r^2 + 2(M - \Gamma^2 r_0)r - a^2 Q/r_0^2 \qquad (5.26)$$

If the energy of the particle now varies from $E$ to $E_0$, then the radial equation can be written as

$$R(r) = (r^2 + a^2)[E^2 - E_0^2 + E_0^2 - V^2(r)]$$

$$= (r^2 + a^2)(E^2 - E_0^2) + (r - r_0)^2 G(r) \qquad (5.27)$$

The turning points of the radial coordinate can be given by

$$(r_1 - r_0)^2 = (r_1^2 + a^2)(E^2 - E_0^2)/G(r) \qquad (5.28)$$

For small differences in the energy the points $r_1$ will lie close to $r_0$ , and the radial function can be expressed as

$$R(r) \approx -G(r_0)[(r_1 - r_0)^2 - (r - r_0)^2] \tag{5.29}$$

such that

$$\int \frac{dr}{\sqrt{R(r)}} \approx [-G(r_0)]^{-1/2} \frac{\sin^{-1}(r-r_0)}{|r_1-r_0|} \tag{5.30}$$

The above equations yield the approximate solution for the radial motion of the particle as its orbit oscillates between the radial values $r_0 + \Delta r$ and $r_0 - \Delta r$ where $(\Delta r = |r_1 - r_0|)$ [50].

Alternatively, when the double root of the equation $R(r) = 0$, is associated with the interval $r_1 < r_0 < r_2$ , and the function $G(r_0) > 0$

$$R(r) = \Gamma^2(r - r_0)^2(r - r')(r'' - r) \tag{5.31}$$

substituting

$$x = (r - r_0)^{-1} \tag{5.32}$$

$$I_0(r) = \int \frac{dr}{R^{1/2}} = \int dr\ [(r - r_0)^2 G]^{-1/2} = -\int dx/X^{1/2} \tag{5.33}$$

where

$$X(x) = \alpha + \beta x + \gamma x^2 \tag{5.34}$$

$$\alpha = -\Gamma^2 \tag{5.35}$$

$$\beta = 2(M - 2\Gamma^2 r_0) = \Gamma^2(r' + r'' - 2r_0) \tag{5.36}$$

$$\gamma = G(r_0) = \Gamma^2(r_0 - r')(r'' - r_0) \tag{5.37}$$

and

$$I_0 = -(1/\gamma)^{1/2} \ln(\beta + 2\gamma x + \gamma^2 X^{1/2}) \text{ if } G(r_0) > 0$$

$$= (-1/\gamma)^{1/2} \sin^{-1}(2\gamma x + \beta)/\Gamma^2(r'' - r') \text{ if } G(r_0) < 0 \qquad (5.38)$$

If $G(r)$ vanishes at $r_0$ it would imply that $r_0$ coincides with either one value of $r'$or $r''$, which would give

$I_0 = \pm\frac{2}{|\Gamma|(r''-r_0)}\left(\frac{r''-r}{r-r_0}\right)^{1/2}$ if $r'' = r_0$ and similarly ,

$$I_0 = \pm\frac{2}{|\Gamma|(r'-r_0)}\left(\frac{r'-r}{r-r_0}\right)^{1/2} \text{ if } r'' = r_0. \qquad (5.39)$$

The above integrals give the analytic solutions for the near spherical polar orbits and can be evaluated to identify the non spherical polar orbits associated with a spherical polar orbit of radius $r_0$.

## 5.5 Precession of Gyroscope

The calculations for the change in the spin of the gyroscope as it completes a rotation of the Kerr black hole has been possible using the equations of parallel transport in Kerr geometry by J.-A. Marck [54]. A further study of parallel transport in polar orbits has been given by Tsoubelis et al. [54] For a gyroscope falling freely along the path $\mathsf{C}(\tau)$, that of the polar orbit, the spin vector $S(\tau)$ will be parallel transported along the geodesic. If an orthonormal tetrad is constructed, $\{\lambda_{(a)}\}$ , which is parallelly transported along the geodesic then the spin of the gyroscope in this reference frame would stay constant and $S^{(0)} = 0$.

Considering the base $\{e_a\}$ such that,

$$\boldsymbol{e}_0 = \left(\frac{A}{\Sigma\Delta}\right)^{1/2}\partial_t + \left[\frac{2Mar}{(A\Sigma\Delta)^{\frac{1}{2}}}\right]\partial_\phi \qquad (5.40)$$

$$\boldsymbol{e}_1 = \left(\frac{\Delta}{\Sigma}\right)^{1/2}\partial_r \qquad (5.41)$$

$$\boldsymbol{e}_2 = \left(\frac{1}{\Sigma}\right)^{1/2}\partial_\theta \qquad (5.42)$$

$$\boldsymbol{e}_3 = \left(\frac{\Delta}{a}\right)^{\frac{1}{2}} \left(\frac{1}{\sin\theta}\right) \partial_\phi \tag{5.43}$$

The Kerr metric in this base would now take the form

$$ds^2 = \eta_{ab} \boldsymbol{e}^a \otimes \boldsymbol{e}^b \tag{5.44}$$

where $\eta_{ab} = \text{diag}(-1,+1,+1,+1)$ and $\boldsymbol{e}^a$ are the one-form dual to $\boldsymbol{e}_a$. Now according to the set of geodesic equations in Kerr spacetime for polar orbits, the vectors

$$\boldsymbol{e}_{\hat{0}} = P\boldsymbol{e}_0 + Q\boldsymbol{e}_2 \tag{5.45a}$$

$$\boldsymbol{e}_{\hat{1}} = \boldsymbol{e}_1 \tag{5.45b}$$

$$\boldsymbol{e}_{\hat{2}} = Q\boldsymbol{e}_0 + P\boldsymbol{e}_2 \tag{5.45c}$$

$$\boldsymbol{e}_{\hat{3}} = \boldsymbol{e}_3 \tag{5.45d}$$

would form a comoving frame along the geodesic $\mathrm{C}(\tau)$, where

$$P = \left(\frac{A}{\Sigma\Delta}\right)^{1/2} E \tag{5.46}$$

and

$$Q = \Sigma^{1/2}\dot{\theta} \tag{5.47}.$$

This base is not defined well on the symmetry axis as $\sin\theta = 0$ and thus there is a coordinate singularity in the Boyer Lindquist coordinate system. This coordinate singularity can be avoided by choosing another coordinate system which is known as the Kerr-Schild coordinate system $(x_0, x, y, z)$ which is well behaved on the symmetry axis. In this coordinate system the Kerr metric on the symmetric axis is given as

$$ds^2 = -\left[1 - \frac{2Mz}{z^2+a^2}\right] d(x^0)^2 + \left[1 - \frac{2Mz}{z^2+a^2}\right]^{-1} dz^2 + dx^2 + dy^2 \qquad (5.48)$$

Therefore as $\sin\theta \to 0$

$$\boldsymbol{e}_0 \to [1 - 2Mz/(z^2 + a^2)]^{-1/2}\partial_{x^0} \qquad (5.49a)$$

$$\boldsymbol{e}_1 \to [1 - 2Mz/(z^2 + a^2)]^{1/2}\partial_z \qquad (5.49b)$$

$$\boldsymbol{e}_2 \to \cos\phi\,\partial_x + \sin\phi\,\partial_y \qquad (5.49c)$$

$$\boldsymbol{e}_3 \to -\sin\phi\,\partial_x + \cos\phi\,\partial_y \qquad (5.49d)$$

Thus if the initial direction along which the orbit emerges from the $z$-axis is set, it is possible to join the orthonormal base $\{\boldsymbol{e}_a\}$ to a unique coordinate-tied tetrad there. Assuming that initially $\phi = 0$, the gyroscope will return after one rotation to the starting point on the $z$-axis along a direction which is given as

$$\phi = \frac{4\pi MaEr}{\Delta\, Q^{1/2}}\left(1 + \frac{k^2}{4} + \frac{3}{26}k^4 + O(k^6)\right) \qquad (5.50)$$

which is derived earlier, equation (*5.23*) .

Making use of the Marck's [47] construction of parallelly transported orthonormal tetrad along a geodesic in Kerr spacetime to express the set of vectors $\{\lambda_{(a)}\}$ in terms of the base $\{\boldsymbol{e}_{\hat{a}}\}$.

$$\boldsymbol{\lambda}_{(0)} = \boldsymbol{e}_{\hat{0}} \qquad (5.51a)$$

$$\boldsymbol{\lambda}_{(1)} = \cos\Psi(\tau)\boldsymbol{\lambda}'_{(1)} - \sin\Psi(\tau)\boldsymbol{\lambda}'_{(3)} \qquad (5.51b)$$

$$\boldsymbol{\lambda}_{(2)} = P\left(\frac{1}{KA}\right)^{\frac{1}{2}}(r^2 + a^2)\, a\cos\theta\, \boldsymbol{e}_{\hat{1}} - \left(\frac{\Delta}{KA}\right)^{1/2} a\, r\sin\theta\, \boldsymbol{e}_{\hat{2}} - Q\left(\frac{1}{KA}\right)^{\frac{1}{2}}(r^2 + a^2) r\boldsymbol{e}_{\hat{3}} \qquad (5.51c)$$

$$\boldsymbol{\lambda}_{(3)} = \sin\Psi(\tau)\boldsymbol{\lambda}'_{(1)} + \cos\Psi(\tau)\,\boldsymbol{\lambda}'_{(3)} \qquad (5.51d)$$

where the angle $\Psi(\tau)$ is given by the equation

$$\dot{\Psi} = EK^{1/2}(K - a^2)/(r^2 + K)(K - a^2\cos^2\theta) \qquad (5.52)$$

and

$$\boldsymbol{\lambda}'_{(1)} = \alpha P\left(\frac{1}{KA}\right)^{\frac{1}{2}}(r^2 + a^2)r\boldsymbol{e}_{\hat{1}} + \beta\left(\frac{\Delta}{KA}\right)^{1/2} a^2\sin\theta\cos\theta\ \boldsymbol{e}_{\hat{2}} + \beta Q\left(\frac{1}{KA}\right)^{\frac{1}{2}}(r^2 + a^2)\ a\ \cos\theta\ \boldsymbol{e}_{\hat{3}} \qquad (5.53)$$

$$\boldsymbol{\lambda}'_{(3)} = \beta Q\left[\frac{\Sigma}{A(K+a^2)}\right]^{\frac{1}{2}}(r^2 + a^2)\boldsymbol{e}_{\hat{2}} - \beta\left[\frac{\Sigma\Delta}{A(K+r^2)}\right]^{1/2} a\sin\theta\ \boldsymbol{e}_{\hat{3}} \qquad (5.54)$$

where

$$\alpha^2 = \beta^{-2} = (K - a^2\cos^2\theta)/(K + r^2) \qquad (5.55)$$

If $\Psi(0) = 0$ and $S^{\hat{\imath}}(0)$ are the components of the gyroscope's spin at the beginning, then when the gyroscope returns to the starting point after one complete latitude oscillation, the components of the spin vector in the comoving frame $\{\boldsymbol{e}_{\hat{\imath}}\}$will have changed to $S^{\hat{\imath}}(T_\tau)$ where

$$S^{\hat{\imath}}(T_\tau) = R^{\hat{\imath}}_{\hat{\jmath}}S^{\hat{\jmath}}(0) \qquad (5.56)$$

where the matrix $R^{\hat{\imath}}_{\hat{\jmath}}$ given as

$$R^{\hat{\imath}}_{\hat{\jmath}} = \begin{pmatrix} 1 + (\cos\Psi - 1)\cos^2 Z & -\sin\Psi\cos Z & (\cos\Psi - 1)\sin Z\cos Z \\ \sin\Psi\cos Z & \cos\Psi & \sin\Psi\sin Z \\ (\cos\Psi - 1)\sin Z\cos Z & -\sin\Psi\sin Z & 1 + (\cos\Psi - 1)\sin^2 Z \end{pmatrix} \qquad (5.57)$$

and

$$\cot Z = \left(\frac{a}{r}\right)(K + r^2)^{\frac{1}{2}}/(K - a^2)^{1/2} \qquad (5.58)$$

The interpretation as given in [55] is that in each revolution of the gyroscope about the gravitating center its spin rotates by an angle Ψ around an axis which is inclined by an angle $Z$ relative to $\boldsymbol{e}_{\hat{1}}$ and lies in the $\boldsymbol{e}_{\hat{1}} - \boldsymbol{e}_{\hat{3}}$ plane of the comoving frame $\{\boldsymbol{e}_{\hat{i}}\}$. During the same interval the frame $\{\boldsymbol{e}_{\hat{i}}\}$ itself rotates with respect to the $x - y - z$ coordinate system by an angle $\phi$ about the $z$-axis which coincides with the vector $\boldsymbol{e}_{\hat{1}}$ at the beginning and end of the cycle.

The precession of the gyroscope in the polar orbit can be a measure of the properties of the black hole if a satellite is made to revolve in such geodesics. This effect can be directly measured with respect to the asymptotic Lorentz frame and can provide a useful technique for the navigation of spacecrafts in the Kerr spacetime.

## 5.6 Numerical Simulation of Spherical Polar Orbits

Orbits of different radii ranging from $(5 - 2000)M_{\odot}$, are shown in figure 5.4 (*a*)-(*f*), for a black hole of 1 $M_{\odot.}$ and $a = 0.8M_{\odot}$.The first graph of the set plots $\theta\ vs\ \tau$ and $\phi\ vs\ \tau$,and the second 3D plot traces the trajectory of the particle in the spherical polar orbit. With the increase in radius of the spherical polar orbit, the trajectory spans lesser spherical surface but gets confined to a ring of decreasing width.

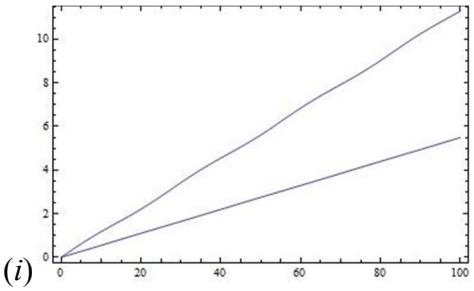


(*i*)

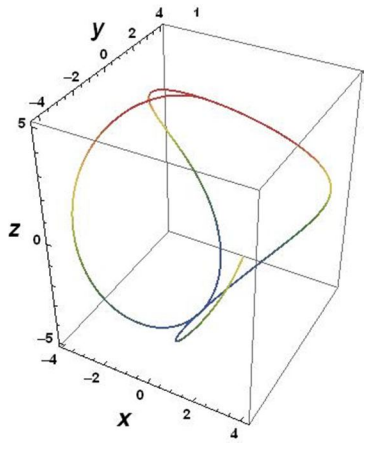


(*ii*)

**Fig:5.4a** *:* The above plots show (*i*) variation of $\theta$ and $\phi$ coordinates of the Boyer Lindquist coordinates system for a spherical polar orbit at $r = 5M_{\odot}$, the top line represents $\theta(\tau)$ and the second line represents $\phi(\tau)$, the graph indicates that the variations are significant for both the cases of $\theta(\tau)$ and $\phi(\tau)$ in lower orbits in Kerr spacetime.(*ii*) Trajectory of a particle in Kerr orbit at $r = 5M_{\odot}$.

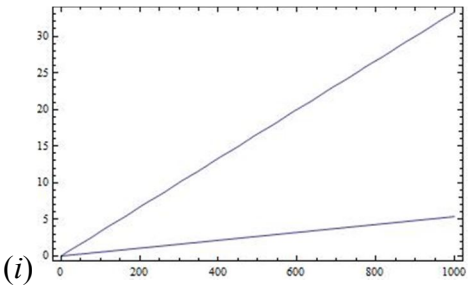


(*i*)

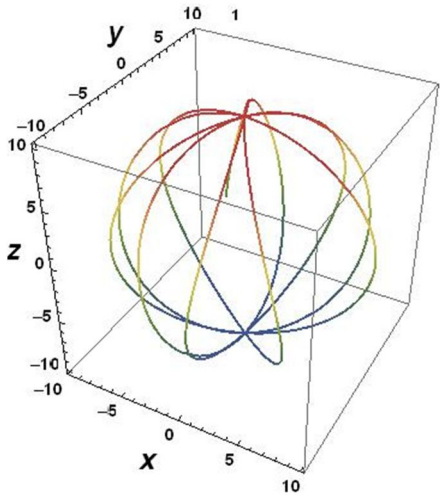


(*ii*)

**Fig:** ***5.4b*** The above plots show ($i$) variation of $\theta$ and $\phi$ coordinates of the Boyer Lindquist coordinates system for a spherical polar orbit at $r = 10M_{\odot}$, the top line represents $\theta(\tau)$ and the second line represents $\phi(\tau)$, the graph indicates that the variations are significant for the cases of $\theta(\tau)$ and lesser variation for $\phi(\tau)$ on increasing the size of orbit from $r = 5M_{\odot}$-$10M_{\odot}$ in Kerr spacetime.($ii$) Trajectory of a particle in Kerr orbit at $r = 10M_{\odot}$. The orbit are suggested to rotate greater in lower spherical polar orbit.

($i$)

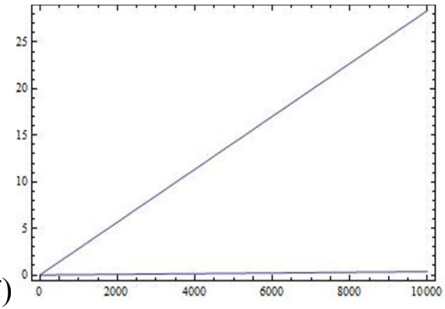


($ii$)

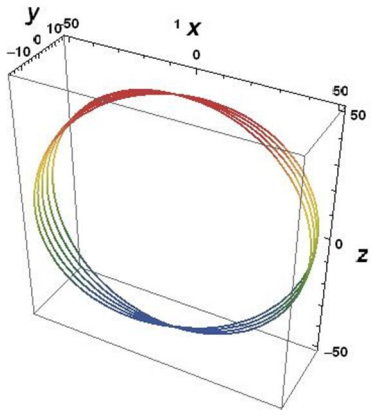


**Fig: 5.4c** The above plots show ($i$) variation of $\theta$ and $\phi$ coordinates of the Boyer Lindquist coordinates system for a spherical polar orbit at $r = 50M_{\odot}$, the top line represents $\theta(\tau)$ and the second line represents $\phi(\tau)$, the graph indicates that the variation is significant for the case of $\theta(\tau)$ and further less variation in $\phi(\tau)$ on increasing the size of orbit from $r = 10M_{\odot}$-$50M_{\odot}$ in Kerr spacetime.($ii$) Trajectory of a particle in Kerr orbit at $r = 50M_{\odot}$. The orbits are very less rotated in the $\phi$ direction, implying decrease in the Lense Thirring effect.

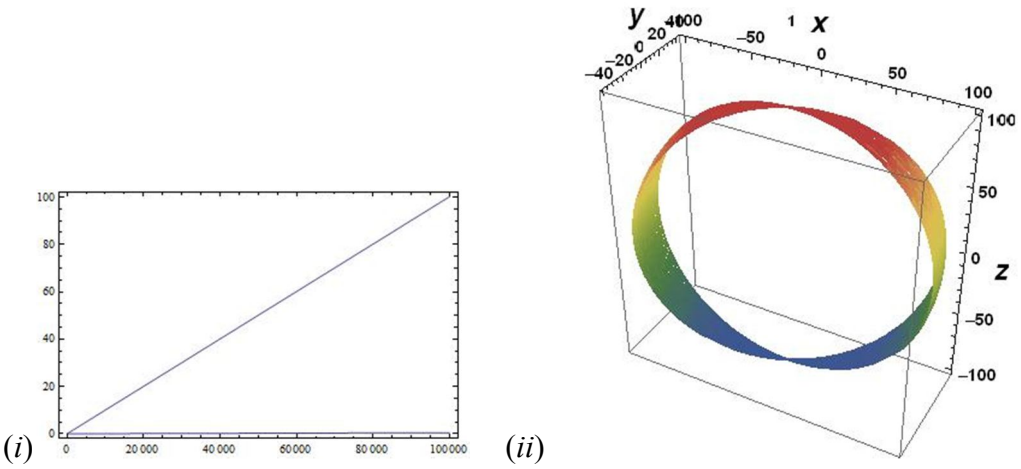


**Fig 5.4d:** The above plots show (*i*) variation of $\theta$ and $\phi$ coordinates of the Boyer Lindquist coordinates system for a spherical polar orbit at $r = 100M_{\odot}$, the top line represents $\theta(\tau)$ and the second line represents $\phi(\tau)$, the graph indicates that the variation is significant for the cases of $\theta(\tau)$ and further less variation in $\phi(\tau)$ on increasing the size of orbit from $r = 50M_{\odot}$-$100M_{\odot}$ in Kerr spacetime.(*ii*) Trajectory of a particle in Kerr orbit at $r = 100M_{\odot}$. The orbits are very less rotated in the $\phi$ direction.

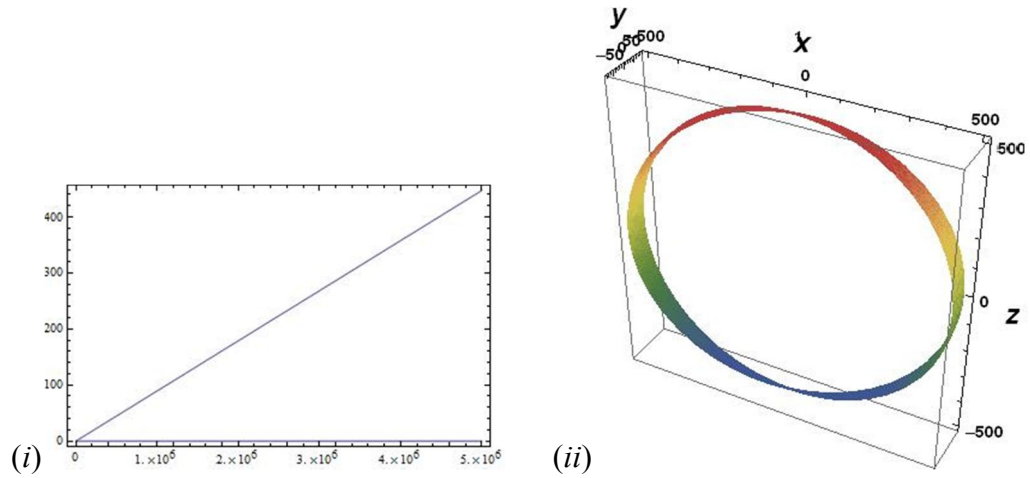


**Fig 5.4e** : The above plots show (*i*) variation of $\theta$ and $\phi$ coordinates of the Boyer Lindquist coordinates system for a spherical polar orbit at $r = 500M_{\odot}$, the

top line represents $\theta(\tau)$ and the second line represents $\phi(\tau)$, the graph indicates that the variation is significant for the cases of $\theta(\tau)$ and further less in $\phi(\tau)$ on increasing the size of orbit from $r = 100M_{\odot}$-$500M_{\odot}$ in Kerr spacetime.($ii$) Trajectory of a particle in Kerr orbit at $r = 500M_{\odot}$. The orbits are less rotated in the $\phi$ direction.

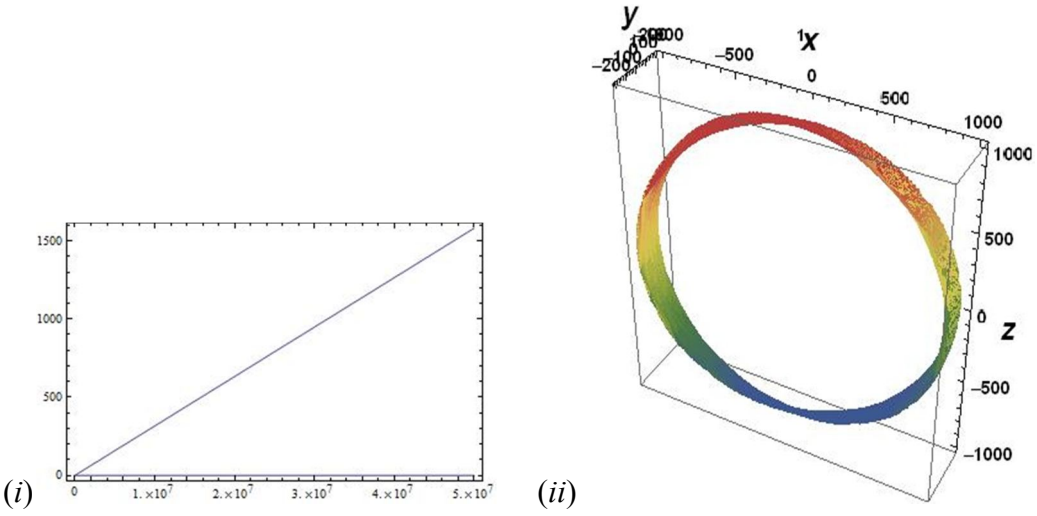


**Fig 5.4f :** The above plots show ($i$) variation of $\theta$ and $\phi$ coordinates of the Boyer Lindquist coordinates system for a spherical polar orbit at $r = 1000M_{\odot}$, the top line represents $\theta(\tau)$ and the second line represents $\phi(\tau)$, the graph indicates that the variation is significant for the cases of $\theta(\tau)$ and further less variation in $\phi(\tau)$ on increasing the size of orbit from $r = 500M_{\odot}$-$1000M_{\odot}$ in Kerr spacetime.($ii$) Trajectory of a particle in Kerr orbit at $r = 1000M_{\odot}$. The orbits are very less rotated in the $\phi$ direction.

The above simulations are run for greater time steps with increasing radii. The energy and Carter's constants and corresponding time periods is shown in table 6.1. The polar orbits at large radii in Kerr spacetime approach the Keplerian polar orbits in the field of a non rotating gravitational source.

# Chapter 6

# Relativistic Effects on the Spacecraft in Kerr Spacetime: Tidal Tensor and Time Dilation

The motion of a spacecraft in the Kerr spacetime would be accompanied by the tidal forces present due to the strong curvature of spacetime. The amount of tidal forces felt by the spacecraft will be dependent on the finite size and mass of the spacecraft as well as on the velocity of the spacecraft. A necessary quantity to be evaluated would be the tidal tensor $C_{ij}$ related with the curvature tensor $R_{abcd}$ of the spacetime of the black hole. The curvature tensor for the Kerr spacetime can be once calculated if one has a set of parallel propagated vectors along the desired trajectory $\mathsf{C}(\tau)$. This can be achieved by making use of the Marck's construction [47] as described in the previous chapter for the motion of the gyroscope in Kerr spacetime.

## 6.1 Parallel Transport in Kerr Geometry

It was first shown by Marck [54] that the equations of parallel transport applied to an orthonormal tetrad along a given geodesic in Kerr spacetime can be analytically solved using the geodesic equations set by Carter [41].

The Kerr metric in Boyer Lindquist coordinates is expressed as

$$ds^2 = -\left(1-\frac{2Mr}{\Sigma}\right)dt^2 - 2\left(\frac{2Mr}{\Sigma}\right)a\sin^2\theta\ dt\,d\phi + \left(\frac{\Sigma}{\Delta}\right)dr^2 + \Sigma d\theta^2 + \left(\frac{A}{\Sigma}\right)\sin^2\theta\ d\phi^2 \qquad (6.1)$$

where

$$\Sigma = r^2 + a^2 \cos^2\theta \tag{6.2}$$

$$\Delta = r^2 + a^2 - 2Mr \tag{6.3}$$

$$A = (r^2 + a^2)^2 - \Delta a^2 \sin^2\theta \tag{6.4}$$

The equations of geodesics as given by Carter [54] are

$$\dot{t} = (\Delta\Sigma)^{-1}(AE - 2Mar\Phi) \tag{6.5a}$$

$$\Sigma^2\dot{r}^2 = [(r^2 + a^2)E - a\phi]^2 - \Delta(\mu^2 r^2 + K) \tag{6.5b}$$

$$\Sigma^2\dot{\theta}^2 = K - \mu^2 a^2 \cos^2\theta - \left(aEsin\theta - \frac{\Phi}{sin\theta}\right)^2 \tag{6.5c}$$

$$\dot{\phi} = \Delta^{-1}\left[\left(\frac{2Mr}{\Sigma}\right)aE + \frac{\left(1-\frac{2Mr}{\Sigma}\right)\Phi}{\sin^2\theta}\right] \tag{6.6d}$$

where $\Phi$, $E$ and $K$ being the projection of the angular momentum along the symmetric axis, energy at infinity of the particle, and the Carter's constant respectively.

The canonical symmetric orthonormal tetrad introduced by Carter is given by

$$\boldsymbol{w}^{(0)} = (\Delta/\Sigma)^{1/2}(dt - a\sin^2\theta\, d\phi) \tag{6.7a}$$

$$\boldsymbol{w}^{(1)} = (\Sigma/\Delta)^{(1/2)}dr \tag{6.7b}$$

$$\boldsymbol{w}^{(2)} = \Sigma^{\frac{1}{2}}\, d\theta \tag{6.7c}$$

$$\boldsymbol{w}^{(3)} = \left(\frac{sin\theta}{\Sigma^{\frac{1}{2}}}\right)(a\, dt - (r^2 + a^2)d\phi\,) \tag{6.7d}$$

In such a basis the Kerr metric takes on the form

$$ds^2 = \eta_{(a)(b)}\boldsymbol{w}^{(a)}\boldsymbol{w}^{(b)} \tag{6.8}$$

where $\eta$ = diag (-1,+1,+1,+1) is the Minkowsky flat spacetime metric.

The Riemann tensor (Weyl Tensor) for the Kerr metric can be expressed as [56, p97]

$$\Omega^{(1)}{}_{(2)} = -I_1 \boldsymbol{w}^{(1)} \wedge \boldsymbol{w}^{(2)} + I_2 \boldsymbol{w}^{(0)} \wedge \boldsymbol{w}^{(3)}$$

$$\Omega^{(0)}{}_{(3)} = -I_1 \boldsymbol{w}^{(0)} \wedge \boldsymbol{w}^{(3)} + I_2 \boldsymbol{w}^{(1)} \wedge \boldsymbol{w}^{(2)}$$

$$\Omega^{(0)}{}_{(1)} = -2I_1 \boldsymbol{w}^{(1)} \wedge \boldsymbol{w}^{(0)} + 2\, I_2 \boldsymbol{w}^{(2)} \wedge \boldsymbol{w}^{(3)}$$

$$\Omega^{(3)}{}_{(2)} = -2I_1 \boldsymbol{w}^{(2)} \wedge \boldsymbol{w}^{(3)} - 2\, I_2 \boldsymbol{w}^{(1)} \wedge \boldsymbol{w}^{(0)}$$

$$\Omega^{(0)}{}_{(2)} = I_1 \boldsymbol{w}^{(2)} \wedge \boldsymbol{w}^{(0)} + I_2 \boldsymbol{w}^{(1)} \wedge \boldsymbol{w}^{(3)}$$

$$\Omega^{(3)}{}_{(1)} = I_1 \boldsymbol{w}^{(1)} \wedge \boldsymbol{w}^{(3)} - I_2 \boldsymbol{w}^{(2)} \wedge \boldsymbol{w}^{(0)} \qquad (6.9)$$

where $\Omega^{(a)}{}_{(b)} = \left(\frac{1}{2}\right) \mathbb{C}^{(a)}{}_{(b)(c)(d)}\, \boldsymbol{w}^{(c)} \wedge \boldsymbol{w}^{(d)}$ is the curvature 2-form and the functions $I_1$ and $I_2$ are defined as

$$I_1 = \left(\frac{Mr}{\Sigma^3}\right)(r^2 - 3a^2 \cos^2\theta) \qquad (6.10)$$

and

$$I_2 = \left(\frac{Ma\cos\theta}{\Sigma^3}\right)(3r^2 - a^2 \cos^2\theta) \qquad (6.11)$$

In order to construct an orthonormal tetrad $\boldsymbol{\lambda} = (\lambda_0, \lambda_1, \lambda_2, \lambda_4)$ which can be parallel transported along the geodesic one can chose $\lambda_0$ to be the unit vector tangent to the geodesic and its components can be written as

$$\lambda_0^{(0)} = (1/\Sigma\Delta)^{1/2}\,(E(r^2 + a^2) - a\Phi) \qquad (6.12a)$$

$$\lambda_0^{(1)} = (\Sigma/\Delta)^{1/2}\dot{r} \qquad (6.12b)$$

$$\lambda_0^{(2)} = \Sigma^{1/2}\,\dot{\theta} \qquad (6.12c)$$

$$\lambda_0^{(3)} = (1/\Sigma)^{1/2}(a\,\sin\theta - \Phi/\sin\theta\,) \qquad (6.12d)$$

The second vector is constructed using the Killing-Yano tensor that exists for the Kerr spacetime and which satisfies the equation

$$\nabla_\rho f_{\mu\nu} + \nabla_\nu f_{\mu\nu} = 0 \qquad (6.13)$$

The above equation implies that [57], the vector $\boldsymbol{L}$ defined by

$$L^\mu = f^\mu{}_\nu\,\lambda_0{}^\nu \qquad (6.14)$$

will be parallel propagated along the geodesic and also orthogonal to $\lambda_0$.

Since $L^{(a)}L_{(a)} = K$, the second unit vector can be chosen as $\left(\frac{1}{K}\right)^{\frac{1}{2}}\boldsymbol{L}$, and its components as given by Marck will be

$$\lambda_2^{(0)} = (\Sigma/K\Delta)^{1/2}a\cos\theta\,\dot{r} \qquad (6.15a)$$

$$\lambda_2^{(1)} = (1/K\Sigma\Delta)^{1/2}\,a\cos\theta\,(E(r^2 + a^2) - a\Phi) \qquad (6.15b)$$

$$\lambda_2^{(2)} = -(1/K\Delta)^{1/2}\,r\,(a\,E\sin\theta - \Phi/\sin\theta) \qquad (6.15c)$$

$$\lambda_2^{(3)} = (\Sigma/K)^{1/2}r\dot{\theta} \qquad (6.15d)$$

From the above two vectors it is possible to generate another set of vectors $\tilde{\boldsymbol{\lambda}}_1$ and $\tilde{\boldsymbol{\lambda}}_2$ such that they form a complete orthonormal basis when taken in conjugation with $\boldsymbol{\lambda}_0$ and $\boldsymbol{\lambda}_2$,

$$\tilde{\boldsymbol{\lambda}}_1^{(0)} = \alpha\,(\Sigma/K\Delta)^{1/2}\, r\,\dot{r} \tag{6.16a}$$

$$\tilde{\boldsymbol{\lambda}}_1^{(1)} = \alpha(1/K\Sigma\Delta)^{1/2}\, r\,(E(r^2 + a^2) - a\Phi) \tag{6.16b}$$

$$\tilde{\boldsymbol{\lambda}}_1^{(2)} = \beta\,(1/K\Sigma)^{1/2}\, a\cos\theta\;(aE\sin\theta - \Phi/\sin\theta) \tag{6.16c}$$

$$\tilde{\boldsymbol{\lambda}}_1^{(3)} = -\beta(\Sigma/K)^{\frac{1}{2}} a\cos\theta\,\dot{\theta} \tag{6.16d}$$

and

$$\tilde{\boldsymbol{\lambda}}_3^{(0)} = \alpha(1/\Sigma\Delta)^{1/2}(E(r^2 + a^2) - a\Phi) \tag{6.17a}$$

$$\tilde{\boldsymbol{\lambda}}_3^{(1)} = \alpha(\Sigma/\Delta)^{1/2}\dot{r} \tag{6.17b}$$

$$\tilde{\boldsymbol{\lambda}}_3^{(2)} = \beta\Sigma^{1/2}\,\dot{\theta} \tag{6.17c}$$

$$\tilde{\boldsymbol{\lambda}}_3^{(3)} = \beta(1/\Sigma)^{1/2}(aE\sin\theta - \Phi/\sin\theta) \tag{6.17d}$$

where

$$\alpha^2 = \frac{1}{\beta^2} = (K - a^2\cos^2\theta)/(r^2 + K) \tag{6.18}$$

The new vectors here obtained are not parallel propagated and can be related by a single time-dependent rotation angle $\Psi$ to the new orthonormal unit vectors $\boldsymbol{\lambda}_1$ and $\boldsymbol{\lambda}_2$ chosen in the same plane in such a way that the acceleration is null or

$$\lambda_0{}^{\mu}\nabla_{\mu}\lambda_k{}^{\nu} = 0 \tag{6.19}$$

is satisfied for $k\ \forall\ 0,1,2,3$.

thus

$$\boldsymbol{\lambda}_1 = \tilde{\boldsymbol{\lambda}}_1\cos\Psi - \tilde{\boldsymbol{\lambda}}_3\sin\Psi \tag{6.20a}$$

$$\boldsymbol{\lambda}_3 = \tilde{\boldsymbol{\lambda}}_1\sin\Psi + \tilde{\boldsymbol{\lambda}}_3\cos\Psi \tag{6.20b}$$

and the rotation angle Ψ can be expressed in the following manner

$$\Psi = \frac{K^{\frac{1}{2}}}{\Sigma}\left\{\frac{E(r^2+a^2)-a\Phi}{r^2+K} + a\frac{(\Phi - \mathrm{a\ E}\sin^2\theta)}{K-a^2\cos^2\theta}\right\} \qquad (6.21)$$

The set of vectors $\boldsymbol{\lambda}$ forms thus an orthonormal set of parallel propagated vectors and it becomes possible to express the Riemann tensor and hence the tidal tensor associated with the given geodesic in Kerr spacetime.

## 6.2 Tidal Tensor

The tidal tensor is a measure of the relative acceleration of two test particles moving in the neighborhood of a timelike geodesic, it is a necessary quantity to be evaluated to estimate the tidal forces imposed on a body following a geodesic in Kerr spacetime. The tidal tensor requires a set of parallel propagated orthogonal vectors along the given geodesic, in terms of these vectors it is possible to express the tidal tensor in Kerr geometry [58].

The components of tidal tensor are given as

$$C_{ij} = \mathbb{C}_{(a)(b)(c)(d)}\lambda_0{}^{(a)}\lambda_i{}^{(b)}\lambda_0{}^{(c)}\lambda_j{}^{(d)} \qquad (6.22)$$

Using the expressions for Weyl Tensor given in the last section one can calculate the components of the tidal tensor in the Kerr geometry. For any orthonormal set of tetrad $\boldsymbol{\lambda}$, for $i \neq j$-

$$C_{ij} = 3\{(\lambda_0^{(0)}\lambda_i^{(1)} - \lambda_0^{(1)}\lambda_i^{(0)})(\lambda_0^{(1)}\lambda_j^{(0)} - \lambda_0^{(0)}\lambda_j^{(1)}) + (\lambda_0^{(2)}\lambda_i^{(3)} - \lambda_0^{(3)}\lambda_i^{(2)})(\lambda_0^{(2)}\lambda_j^{(3)} - \lambda_0^{(3)}\lambda_j^{(2)})\}I_1 - 3\{(\lambda_0^{(0)}\lambda_i^{(1)} - \lambda_0^{(1)}\lambda_i^{(0)})(\lambda_0^{(2)}\lambda_j^{(3)} - \lambda_0^{(3)}\lambda_j^{(2)}) + (\lambda_0^{(0)}\lambda_i^{(1)} - \lambda_0^{(1)}\lambda_i^{(0)})(\lambda_0^{(2)}\lambda_j^{(3)} - \lambda_0^{(3)}\lambda_j^{(2)})\}I_2 \qquad (6.23)$$

And for $i = j$

$$C_{ii} = \left[1 - 3\left\{\left(\lambda_0^{(0)}\lambda_i^{(1)} - \lambda_0^{(1)}\lambda_i^{(0)}\right)^2 - \left(\lambda_0^{(2)}\lambda_i^{(3)} - \lambda_0^{(3)}\lambda_i^{(2)}\right)^2\right\}\right] I_1 - 6(\lambda_0^{(0)}\lambda_i^{(1)} - \lambda_0^{(1)}\lambda_i^{(0)})(\lambda_0^{(2)}\lambda_i^{(3)} - \lambda_0^{(3)}\lambda_i^{(2)})I_2 \quad (6.24)$$

In the particular case of the tetrad defined earlier the components of the tidal tensor are evaluated and are given as

$$C_{11} = \left\{1 - 3\frac{ST(r^2 + a^2\cos^2\theta)}{K\Sigma^2}\cos^2\Psi\right\} I_1 + 6ar\cos\theta\frac{ST}{K\Sigma^2}\cos^2\Psi\, I_2 \quad (6.25a)$$

$$C_{12} = \{-ar\cos\theta\,(S+T)I_1 + (a^2\cos^2\theta\, S - r^2\, T)I_2\}3\frac{(ST)^{\frac{1}{2}}}{K\Sigma^2}\cos\Psi \quad (6.25b)$$

$$C_{13} = \{(a^2\cos^2\theta - r^2)I_1 + 2ar\cos\theta\ I_2\}3\frac{ST}{K\Sigma^2}\cos\Psi\sin\Psi \quad (6.25c)$$

$$C_{22} = \left(1 + 3\frac{r^2T^2 - a^2\cos^2\theta\, S^2}{K\Sigma^2}\right)\mathrm{I}_1 - 6ar\cos\theta\frac{ST}{K\Sigma^2}\ I_2 \quad (6.26d)$$

$$C_{23} = \{-ar\cos\theta\,(S+T)I_1 + (a^2\cos^2\theta\, S - r^2T)I_2\}3\frac{(ST)^{\frac{1}{2}}}{K\Sigma^2}\sin\Psi \quad (6.26e)$$

$$C_{33} = \left\{1 - 3\frac{ST(r^2 - a^2\cos^2\theta)\sin^2\Psi}{K\Sigma^2}\right\} I_1 + 6ar\ \cos\theta\frac{ST}{K\Sigma^2}\sin^2\Psi\ I_2$$

(*6.26f*)

where $S = r^2 + K$ and $T = K - \cos^2\theta$.

The above equations for the tidal tensor hold good for any general geodesic in Kerr spacetime.

Along the equatorial plane the tidal tensor takes on the form,

$$C_{11} = \{1 - 3\frac{(r^2 + K)}{r^2}\cos^2\Psi\}\frac{M}{r^3} \quad (6.27a)$$

$$C_{22} = \left(1 + 3\frac{K}{r^2}\right)\frac{M}{r^3} \quad (6.27b)$$

$$C_{33} = \left\{1 - 3\frac{(r^2 + K)}{r^2}\sin^2\Psi\right\}\frac{M}{r^3} \quad (6.27c)$$

$$C_{13} = -3\frac{(r^2+K)}{r^5} M \cos\Psi \sin\Psi \tag{6.27d}$$

and the angle Ψ for the equatorial orbit is given by

$$\Psi = \frac{EK^{\frac{1}{2}} - aK^{\frac{1}{2}}}{(r^2+K)(aE-\Phi)} \tag{6.28}$$

The tidal tensor for the particular cases of motion along the symmetry axis and along the polar orbit is calculated in the following sections.

## 6.3 Tidal Tensor on the Symmetry Axis

The Kerr metric in Boyer Lindquist coordinates is not well defined at the symmetric axis ($\theta = 0$), to avoid this coordinate singularity another coordinate system is utilized to express the Kerr metric, this coordinate system is known as the Kerr- Schild coordinate system $(T, x, y, z)$ and the Kerr metric is written as

$$ds^2 = -dT^2 + dx^2 + dy^2 + dz^2 + \frac{2Mr^3}{r^4 + a^2z^2} \times \left\{-dT + \frac{1}{r^2+a^2}[r(xdx + ydy) + a(xdy - ydx)]\frac{z}{r} + dz\right\}^2 \tag{6.29}$$

where the function $r(x, y, z)$ is given by

$$\frac{x^2+y^2}{r^2+a^2} + \frac{z^2}{r^2} = 1 \tag{6.30}$$

The relation between the two coordinate systems is given as

$$dT = dt - (2Mr/\Delta)dr \tag{6.31a}$$

$$d\psi = d\phi - \frac{2Mar}{(r^2+a^2)\Delta} dr \tag{6.31b}$$

$$x = (r^2 + a^2)^{\frac{1}{2}} \sin\theta \cos\psi \tag{6.31c}$$

$$y = (r^2 + a^2)^{\frac{1}{2}} \sin\theta \cos\psi \tag{6.31d}$$

$$z = r\cos\theta \tag{6.31e}$$

In the Kerr Schild coordinates the symmetry axis of the Kerr spacetime is thus defined by the conditions

$$x = y = 0, |z| = r \tag{6.32}$$

On the axis the metric takes the form

$$ds^2 = -dT^2 + dx^2 + dy^2 + dz^2 + \frac{2Mr}{(z^2+a^2)}(-dT + dz)^2 \tag{6.33}$$

The motion on the axis can be analysed using the method of null vectors in Kerr geometry first proposed in [59],from equation (*6.18*) the vector $l_c$ given as

$$l_c := \left(-1, \frac{rx-ay}{r^2+a^2}, \frac{ry+ax}{r^2+a^2}, \frac{z}{r}\right) \tag{6.34}$$

is a null vector with respect to the Minkowski metric, such that

$$\eta^{ab} l_a l_b = 0 \tag{6.35}$$

and the Kerr metric $g_{ab}$ can be expressed as

$$g_{ab} = \eta_{ab} + 2ML^2 l_a l_b \tag{6.36}$$

where

$$L^2 := r^3/(r^4 + a^2 z^2) \tag{6.37}$$

Considering a particle confined on the symmetric axis with a fixed $z$, the tetrad given as

$$e_{\hat{0}}{}^a = \left[\frac{z^2+a^2}{\Delta}\right]^{1/2} \delta_0^a \tag{6.38a}$$

$$e_{\hat{1}}{}^a = \delta_1{}^a \tag{6.38b}$$

$$e_{\hat{2}}{}^a = \delta_2{}^a \tag{6.38c}$$

$$e_{\hat{3}}{}^{a} = \left[\frac{\Delta}{z^2+a^2}\right]^{1/2} \left[\delta_3{}^{a} - \left(\frac{2Mz}{\Delta}\right)\delta_0^a\right] \qquad (6.38d)$$

would form an orthonormal tetrad which is non rotating with respect to the asymptotic Lorentz frame.

The four acceleration of the above frame can be calculated using the results [59]

$$a^a = e_{\hat{0}}{}^{a}{}_{;b} e_{\hat{0}}{}^{b} = \frac{Mz(z^2-a^2)H}{r(z^2+a^2)} e_{\hat{3}}{}^{a} \qquad (6.39a)$$

$$e_{\hat{1}}{}^{a}{}_{;b} e_{\hat{0}}{}^{b} = -\frac{2MarH}{(z^2+a^2)^2} e_{\hat{2}}{}^{a} \qquad (6.39b)$$

$$e_{\hat{2}}{}^{a}{}_{;b} e_{\hat{0}}{}^{b} = \frac{2MarH}{(z^2+a^2)^2} e_{\hat{1}}{}^{a} \qquad (6.39c)$$

$$e_{\hat{3}}{}^{a}{}_{;b} e_{\hat{0}}{}^{b} = \frac{Mz(z^2-a^2)H}{r(z^2+a^2)} e_{\hat{0}}{}^{a} \qquad (6.39d)$$

where

$$H = \left[\frac{z^2+a^2}{\Delta}\right]^{1/2} \qquad (6.40)$$

This shows that the static frame above described is rotating with an angular velocity,

$$\Omega_S{}^{a} = -\frac{2MarH}{(z^2+a^2)^2}\, e_{\hat{3}}{}^{a} \qquad (6.41)$$

relative to a frame of reference of *inertial guidance gyroscopes* carried along the symmetry of axis. Eliminating the factor $H$ which represents the ratio $(dt/d\tau_s)$ of the asymptotic to the static frame proper time, one gets the angular velocity of the gyroscopes rotating with respect to the asymptotic Lorentz frame,

$$\Omega_G{}^{a} = \frac{2Mar}{(z^2+a^2)^2} e_{\hat{3}}{}^{a} \qquad (6.42)$$

Therefore for a spacecraft moving on the axis of symmetry of the Kerr black hole, the gyroscope tied to the center of mass of the spacecraft will rotate with an

angular velocity $\Omega_G^a$ with respect to the fixed stars. This measure of the rotation of the gyroscope will provide a measure of the distance from the black hole if the black hole parameters are known in advance.

The components of the tidal tensor on the symmetry axis are obtained by calculating the Christoffel symbols and thus the Riemann tensor using the null vector in Kerr Schild coordinates given in [48,59]

$$C_{(i)(j)} = \text{diag}(I_1, I_1, -2I_2) \tag{6.43}$$

where

$$I_1 = \frac{Maz(z^2-3a^2)}{(z^2+a^2)^3} \tag{6.44a}$$

and

$$I_2 = \frac{Maz(a^2-3z^2)}{r(z^2+a^2)^3} \tag{6.44b}$$

Of the few key features of the motion along the symmetry axis one of the important is that if $a^2 > 3M^2/4$ then beyond the $|z| < 3^{1/2}a$ the direction of the tidal forcres are reversed and for a spacecraft in this region it is an advantageous region as the spacecraft can possibly maneuver over the black hole without getting swallowed by the blackhole [48].

## 6.4 Tidal Tensor along the Spherical Polar Orbit

The tidal tensor can be calculated on a geodesic if one can obtain a parallel propagated tetrad along the given geodesic. To obtain the tidal tensor components on the spherical polar orbits as described in the previous chapter which are the geodesics of interest for the spacecraft point of view, it becomes possible to estimate the tidal forces felt by the spacecraft as it moves along the polar orbit.

To obtain the parallel propagated tetrad along the spherical polar orbit, one can use the formulism used as in [47], the necessary condition for the spacecraft to

obtain a spherical polar orbit is that $\Phi = 0$ together with the spherical polar orbit conditions $\theta = 0$, and $\dot{r}$ , under these values the parallel propagated tetrad can be expressed as,

$$\lambda_0^{(0)} = \left(\frac{1}{\Delta\Sigma}\right)^{1/2} E(r^2 + a^2) \tag{6.45a}$$

$$\lambda_0^{(1)} = 0 \tag{6.45b}$$

$$\lambda_0^{(2)} = \Sigma^{1/2}\dot{\theta} \tag{6.45c}$$

$$\lambda_0^{(3)} = 0 \tag{6.45d}$$

second vector given by

$$\lambda_2^{(0)} = 0 \tag{6.46a}$$

$$\lambda_2^{(1)} = \left(\frac{1}{K\Sigma\Delta}\right)^{1/2} a\, E(r^2 + a^2) \tag{6.46b}$$

$$\lambda_2^{(2)} = 0 \tag{6.46c}$$

$$\lambda_2^{(3)} = \left(\frac{\Sigma}{K}\right)^{1/2} r\dot{\theta} \tag{6.46d}$$

The rest of the two vectors are given using the function $\Psi$ and the vectors $\tilde{\boldsymbol{\lambda}}_1$ and $\tilde{\boldsymbol{\lambda}}_3$ where

$$\tilde{\lambda}_1^{(0)} = 0 \tag{6.47a}$$

$$\tilde{\lambda}_1^{(1)} = \alpha\left(\frac{1}{K\Sigma\Delta}\right)^{1/2} r\, E(r^2 + a^2) \tag{6.47b}$$

$$\tilde{\lambda}_1^{(2)} = 0 \tag{6.47c}$$

$$\tilde{\lambda}_1^{(3)} = -\beta\left(\frac{\Sigma}{K}\right)^{1/2} a\,\dot{\theta} \tag{6.47d}$$

and

$$\tilde{\lambda}_3^{(0)} = \alpha \left(\frac{1}{\Sigma\Delta}\right)^{\frac{1}{2}} E(r^2 + a^2) \qquad (6.48a)$$

$$\tilde{\lambda}_3^{(1)} = 0 \qquad (6.48b)$$

$$\tilde{\lambda}_3^{(2)} = \beta\Sigma^{1/2}\dot{\theta} \qquad (6.48c)$$

$$\tilde{\lambda}_3^{(3)} = 0 \qquad (6.48d)$$

where $\alpha, \beta$ are as given in equation (*6.11e*),

The vectors $\boldsymbol{\lambda}_1$ and $\boldsymbol{\lambda}_3$ can now be expressed in terms of the function $\Psi$ as

$$\boldsymbol{\lambda}_1 = \tilde{\boldsymbol{\lambda}}_1 \cos\Psi - \tilde{\boldsymbol{\lambda}}_3 \sin\Psi \qquad (6.49a)$$

$$\boldsymbol{\lambda}_3 = \tilde{\boldsymbol{\lambda}}_1 \sin\Psi + \tilde{\boldsymbol{\lambda}}_3 \cos\Psi \qquad (6.49b)$$

where the function $\Psi$ for the spherical polar orbit will be given by

$$\dot{\Psi} = \frac{K^{1/2}}{\Sigma}\frac{E(r^2 + a^2)}{(r^2 + K)}$$

$$= \frac{K^{1/2}\Delta^{1/2}}{\Sigma}(r^2 + K)^{1/2} \qquad (6.50)$$

since for spherical polar orbits,

$$E^2 = \Delta(r^2 + K)/(a^2 + r^2)^2 \qquad (6.51)$$

and also,

$$K = (Mr^4 - a^2r^3 - 3Ma^2r^2 + a^4r)/(r^3 - 3Mr^2 + a^2r + Ma^2) \qquad (6.52)$$

The Tidal tensor $C_{ij}$ can now be evaluated using equation (*6.16*), the results obtained are,

$$C_{11} = \left[1 - 3\left\{\alpha^2\left(\frac{1}{\Sigma^2\Delta^2K}\right)r^2E^4(r^2+a^2)^4\cos^2\Psi - \left(\frac{1}{K}\right)\beta^2\Sigma^2\dot{\theta}^4a^2\cos^2\Psi\right\}\right]I_1 + 6\left(\frac{E^2(r^2+a^2)^2ra\dot{\theta}\cos^2\Psi}{\Delta K}\right)I_2 \quad (6.53a)$$

$$C_{22} = \left[1 - 3\left\{\frac{1}{\Delta^2\Sigma^2K}a^2E^2(r^2+a^2)^2 - \frac{\Sigma^2}{K}r^2\dot{\theta}^2\right\}\right]I_1 - 6\left(\frac{\Sigma}{K\Delta^{\frac{1}{2}}}aEr(r^2+a^2)\dot{\theta}^2\right)I_2 \quad (6.53b)$$

$$C_{33} = \left[1 - 3\left\{\left(\frac{\alpha E^2(r^2+a^2)^2r\,sin\Psi}{\Delta\Sigma K^{\frac{1}{2}}}\right)^2 - \left(\frac{\Sigma\beta}{K^{\frac{1}{2}}}\dot{\theta}a\sin\Psi\right)^2\right\}\right]I_1 + 6\left(\frac{E^2(r^2+a^2)^2ra\,\dot{\theta}^2\sin^2\Psi}{\Delta K}\right)I_2$$

$$C_{12} = -3\left\{\frac{\alpha rE^2(r^2+a^2)\sin\Psi}{\Delta^2\Sigma^2K} + \frac{\Sigma^2ar\dot{\theta}^4\beta\cos\Psi}{K}\right\}I_1 - 3\left\{\frac{E^2(r^2+a^2)\alpha r^2\cos\Psi}{\Delta K} - \frac{\beta a^2E^2(r^2+a^2)^2\dot{\theta}^2\cos\Psi}{\Delta K}\right\}I_2 \quad (6.53d)$$

$$C_{21} = -3\left\{\frac{\alpha rE^4(r^2+a^2)^4\cos\Psi}{\Delta^2\Sigma^2K} + \frac{\beta\Sigma^2ar\,\dot{\theta}^4\cos\Psi}{K}\right\}I_1 - 3\left\{\frac{\alpha rE^2(r^2+a^2)\dot{\theta}^2\sin\Psi}{\Delta K} - \frac{\beta a^2E^2(r^2+a^2)^2\dot{\theta}^2\cos\Psi}{\Delta K}\right\}I_2 \quad (6.53e)$$

$$C_{13} = 3\left\{-\frac{\alpha^2r^2E^4(r^2+a^2)^4\sin^2\Psi}{\Delta^2\Sigma^2K^{\frac{1}{2}}} + \frac{\beta^2\Sigma^2\dot{\theta}^4a^2\sin\Psi\cos\Psi}{K}\right\}I_1 + 6\left\{\frac{E^2(r^2+a^2)ar\dot{\theta}\sin\Psi\cos\Psi}{\Delta K^{\frac{1}{2}}}\right\}I_2 \quad (6.53f)$$

$$C_{31} = 3\left\{\frac{\alpha^2r^2E^4(r^2+a^2)^4\sin\Psi\cos\Psi}{\Delta^2\Sigma^2K} + \frac{\Sigma^2\beta^2a^2\dot{\theta}^4\sin\Psi\cos\Psi}{K}\right\}I_1 \quad (6.53g)$$

$$C_{23} = -3\left\{\frac{\alpha E^4\left(r^2+a^2\right)^4 r\sin\Psi}{\Delta^2\Sigma^2 K} + \frac{\Sigma^2\beta a r\,\dot{\theta}^4\sin\Psi}{K}\right\} I_1 + 6\left\{\frac{E^2\left(r^2+a^2\right)^2 a^2\beta\sin\Psi}{\Delta K}\right\} I_2$$

$$C_{32} =$$

$$3\left\{\frac{\alpha E^4\left(r^2+a^2\right)^4 a r\sin\Psi}{\Delta^2\Sigma^2 K} + \frac{\Sigma^2\dot{\theta}^4\beta\, a r\sin\Psi}{K}\right\} I_1 -$$

$$3\left\{\frac{E^2\left(r^2+a^2\right)^2\alpha r^2\dot{\theta}^2}{\Delta K}\;\; \frac{E^2\left(r^2+a^2\right)^2\alpha r\sin\Psi}{\Delta\Sigma K^{\frac{1}{2}}}\right\} I_2 \qquad (6.53i)$$

## 6.5 Time Dilation in Spherical Polar Orbits

The time period in B-L coordinate time for spherical polar orbits is given as [60]

$$T_t =$$

$$4E\left[r/\Delta Q^{1/2}\right]\left[r^3 + a^2(2M+r)\right]K(k) + 4EQ^{\frac{1}{2}}(1-E^2)^{-1}[K(k)-E(k)] \quad (6.54)$$

And the proper time period in the satellite frame is,

$$T_\tau =$$

$$4\left(r^2/Q^{1/2}\right)K(k) + 4Q^{\frac{1}{2}}(1-E^2)^{-1}[K(k)-E(k)] \qquad (6.55)$$

The Energy associated with the spherical orbit, Carter's constant, dragging effect, Time period in distant Lorentz frame, and the Time period in satellite frame,are numerically evaluated for orbits of different radii for a given angular parameter $a$ $(0.8M_{\odot})$.

| $r$ | $E$ | $K$ | $\delta\phi$ | $T_t$ (s) | $T_\tau$(s) | $\Psi(T_\tau)$ |
|---|---|---|---|---|---|---|
| 5 | 0.858737 | 11.096 | 22.1835 | 1795.11 | 62.6137 | 15.4549 |
| 10 | 0.907527 | 13.9856 | 10.3287 | 6505.01 | 206.874 | 18.0825 |
| 50 | 0.98017 | 53.1529 | 3.96097 | 309533 | 2257.48 | 17.4193 |
| 100 | 0.985147 | 103.074 | 2.76519 | $1.72836\times10^{6}$ | 6335.95 | 17.254 |
| 500 | 0.996408 | 503.015 | 1.22491 | $9.56962\times10^{7}$ | 70369 | 17.115 |
| 1000 | 0.998501 | 1003.01 | 0.865146 | $5.40717\times10^{8}$ | 198863 | 17.0973 |
| 2000 | 0.99925 | 2003 | 0.611401 | $3.05701\times10^{9}$ | 562228 | 17.0884 |

**Table 6.1 :** Energy, Carter's constant, $\delta\phi$ and Time Periods $T_t, T_\tau$ for spherical orbits of different radii for a Kerr black hole with $a = 0.8M_\odot$

It is observed that an increase in the radius of the spherical orbit is followed by a decrease in $\delta\phi$. The finite difference between the two time periods suggests that the spacecraft in Kerr region will be subjected to a considerable amount of time dilation effect for each orbit around the black hole,compared to the time in the the asymptotic Lorentz frame. It has been observed numerically that the stable spherical orbit corresponding to a given angular parameter $a$ for a black hole of fixed mass, there exist a critical radius $r_c$ below which the equations of spherical polar orbits do not have solutions. This critical radius is $2.6707\ M_\odot$ for a black hole of mass $10M_\odot$ with angular parameter $a = 0.8M_\odot$.

However there is found to be a region with $r > r_c$ such that the coordinate time on the spacecraft is nearly zero and even negative compared to the finite time period

in the Asymptotic Lorentz frame. Just above these last stable spherical orbits it is possible to obtain a trajectory which is nearly a closed time circuit (CTC), even though the region is outside the event horizon in physically accessible space.

# Chapter 7

# Stellar Polar Orbits in Super Massive Kerr Black Hole At Galactic Centre: Case Study

The stellar orbits around the central black hole in the Milky-way provide a testing ground for the theory of the Kerr black hole. It is assumed that the Milky way has a rotating supermassive black hole at its center in the Sgr A* direction and the stars near the Milky way centre rotate in the direction of the rotation of the central black hole. The stellar orbits in close vicinity of the central supermassive black hole are the objectives of study of the GRAVITY experiment [61].

## 7.1 Stellar Orbits in the central arc second of the Milky way

Observation of stellar orbits in the central arcsecond of Milky way has provided the evidence of the existence of a supermassive black hole at its center [62,63,64]. The location and properties of the central black hole can be estimated with the observed stellar orbits near the central region. The stars nearest the black hole are seen to be young B-Main Sequence stars and the radial velocities and orbital parameters of these central stars are given in [65,Table 1,2].

Stellar orbits in a Supermassive black hole spacetime can be analyzed by assuming that the mass of the star is negligible compared to the mass of the SMBH. In such a scenario the star orbiting the black hole can be considered as a free particle, and the equations of time-like geodesic motion in Kerr spacetime can be extended to such systems. This analogy brings the between the two cases

of spacecraft motion in Stellar black hole region and stellar orbits in SMBH to be described by the same governing equations.

Analysis of stellar orbits in rotating Kerr SMBH can provide an insight in the general case of a particle motion in Kerr spacetime. The central arcsecond of the galactic center thus provides one with a method to study the dynamics of a particle in compact strong gravitational regions.

The Supermassive black hole at the center of the galaxy has been identified with the help of the stellar orbits near the central region. Orbits of various inclinations and eccentricities have been discovered in this region and monitoring such stars over a period of two decades has helped in estimating the parameters of the SMBH at the galactic center.

The types of stars present in the central region raise a number of questions on the origin and formation of stars in such extreme gravitational conditions. The tidal forces are expected to be high as to disrupt the stellar formation in these regions and thus the presence of stellar objects in these regions contradicts the standard models of stellar formation.

Though the strong evidences of a black hole at the center of the galaxy is provided by analyzing the orbits of such stars, the fine details of the exact orientation and the Kerr parameter $a$ of the central black hole are to be provided by further carefully analyzing these orbits in time. The stellar polar orbits would rotate in the sense of the black hole due to the Lense Thirring effect.

Figure 7.1 shows the expected orbits of the central stars as they are observed between the years 1995-2005. The orbits of these stars reveal the presence of an in---visible source in the form of a SMBH.

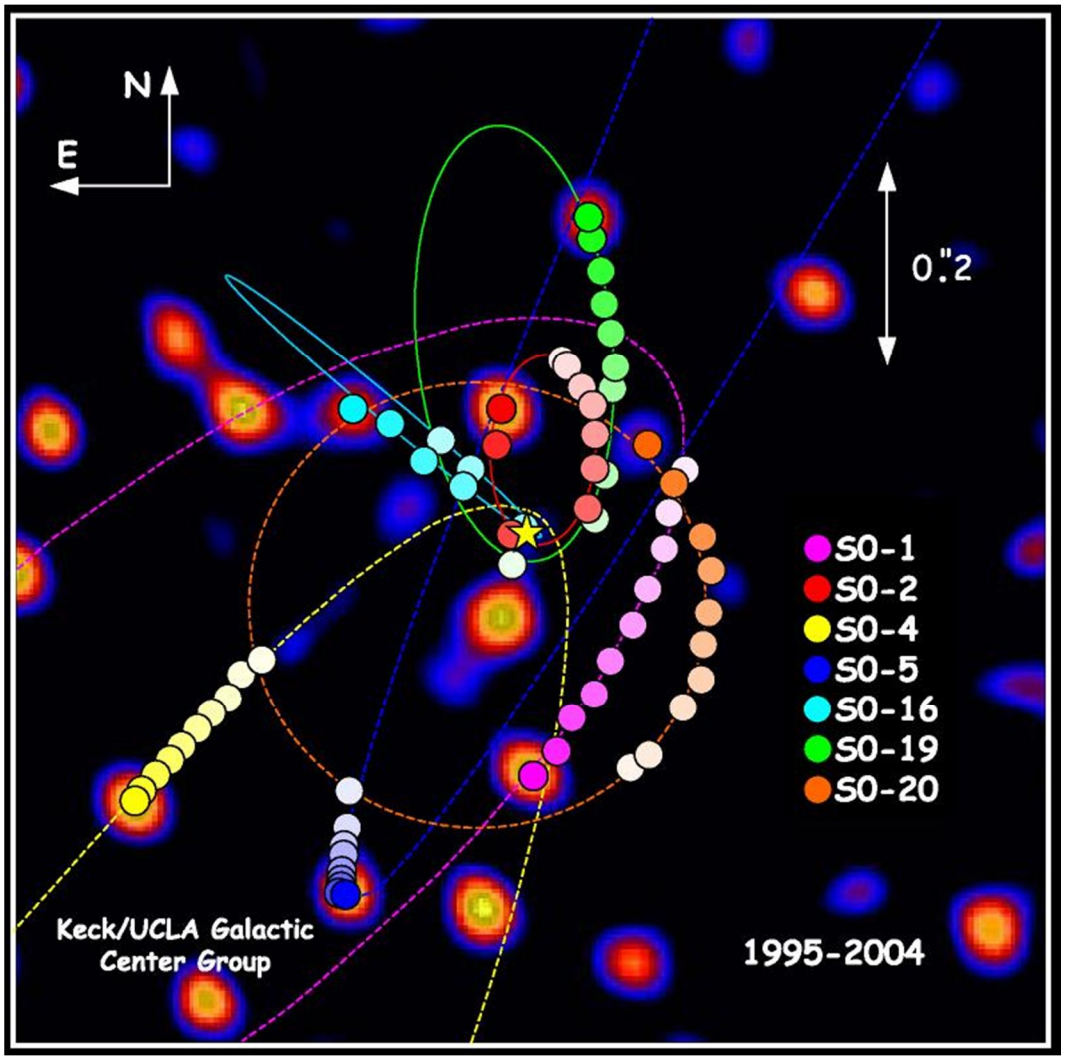


**Fig 7.1** Stellar orbits in the central arc second of the Milky way. (*Courtesy Keck/UCLA Galactic Center Group.*)

The orbital period of the S stars in this region are given in the following table[65] and the minimum time period is that of star S02 estimated to b 15.24 years.

| Star | S1 | S02 | S8 | S12 | S13 | S14 |
|---|---|---|---|---|---|---|
| Orbital Period (y) | 94.1 | 15.24 | 67.2 | 54.4 | 36 | 38 |

*Table 7.1* Orbital Periods of S stars in the galactic central arc second.

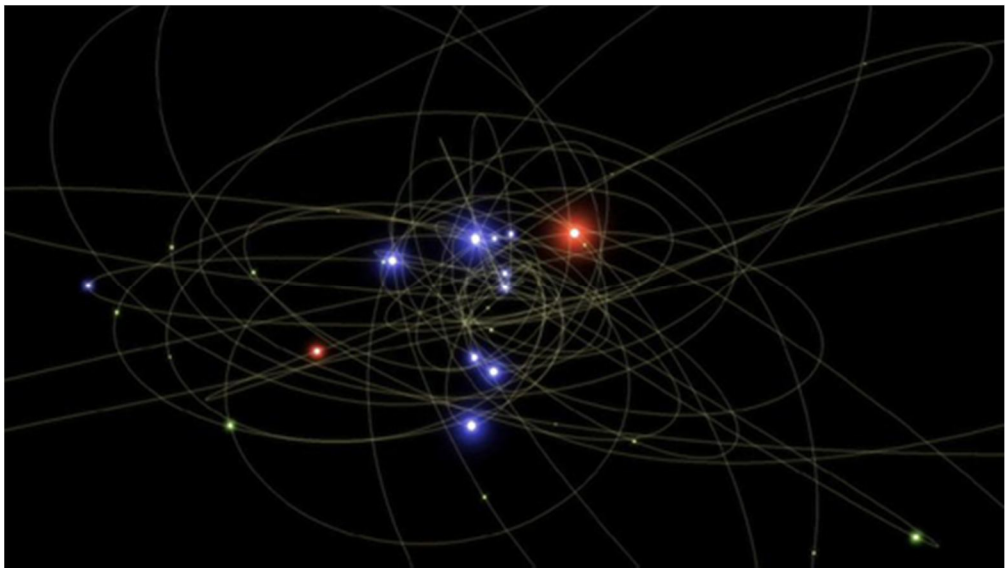

**Fig 7.2.** Image of stars in the Sgr A* region. (*Courtesy Keck/UCLA Galactic Center Group.*)

The stellar orbits in Sgr A* region is an active region of research and with the advancement of time the observations will provide more details on these strong gravitational field orbits and would directly verify the results of the General Theory of Relativity. A major observation re

garding these orbits would be the measure of the gravitomagnetic effects of the Kerr spacetime on these orbits.

## 7.2 Dragging Effect in Stellar Spherical Polar Orbits

The effect of the rotation of black hole can be directly measured in the form of the dragging effect on the orbit of the stars in the concerned region. The dragging effect to be measured over subsequent orbits of a star could be a precise measure of the Kerr parameter $a$ and the mass of the central black hole once the orbital parameters are identified for various orbits in the Sgr A* region.

The dragging effect is estimated for spherical orbits of different radii for three different sets of Kerr parameter $a$ in the tables given below considering the mass of the Black hole to be $4.06 \times 10^6 M_\odot$.

| Radius $r(M_\odot)$ | Energy $E$ | Predicted dragging $(^\circ/revolution)$ |
|---|---|---|
| 10 | 0.914094 | 8.96682 |
| 50 | 0.980425 | 0.738849 |
| 100 | 0.990103 | 0.257866 |
| 200 | 0.995025 | 0.0905654 |

**Table 7.2** Energy associated and the corresponding frame dragging effect for different radii for a SMBH of mass $4.06 \times 10^6 M_\odot$ and Kerr parameter $a = 0.52 M_\odot$.

| Radius $r(M_\odot)$ | Energy $E$ | Predicted dragging $(^\circ/revolution)$ |
|---|---|---|
| 10 | 0.913852 | 14.0191 |
| 50 | 0.980425 | 1.08546 |
| 100 | 0.990103 | 0.375389 |
| 200 | 0.995025 | 0.131232 |

**Table 7.3** Energy associated and the corresponding frame dragging effect for different radii for a SMBH of mass $4.06 \times 10^6 M_\odot$ and Kerr parameter $a = 0.75 M_\odot$.

| Radius $r(M_{\odot})$ | Energy $E$ | Predicted dragging $(^{\circ}/revolution)$ |
|---|---|---|
| 10 | 0.913527 | 19.9481 |
| 50 | 0.980425 | 1.40598 |
| 100 | 0.990103 | 0.480763 |
| 200 | 0.995025 | 0.16714 |

**Table 7.4** Energy associated and the corresponding frame dragging effect for different radii for a SMBH of mass $4.06 \times 10^6 M_{\odot}$ and Kerr parameter $a = 0.95 M_{\odot}$.

The Kerr parameter substantially governs the dragging effect which increases with increase in $a$. The recent X-ray Flares from the galactic center reveal the Kerr parameter to be $a = 0.9939$ [66]. The high angular momentum of the rotating black hole at the centre of the galaxy could render the dragging effect in a measurable regime in the near future.

# CONCLUSION

The geodesic equations in Kerr spacetime have been analytically derived and numerically solved to show various possible orbits in Kerr spacetime. The spherical polar orbits are taken as a case study and are suggested to be the suitable orbits for a spacecraft mission in Kerr spacetime. The Kerr Metric can be approximated for orbits in strong gravitating regions of compact objects such as the neutron stars and white dwarf stars. The effect of rotation of the spacetime is studied under the heading of frame dragging. The effect of frame dragging is studied for a gyroscope moving along a polar orbit and on the axis of symmetry. The tidal tensor for the spherical polar orbit is calculated for the Kerr spacetime. The relativistic effects of tidal forces and time dilation along a spherical polar orbit are analyzed. The case of stellar orbits in SMBH at the centre of Milky Way is studied and an analogy has been predicted to exist in between the two scenarios in Kerr spacetime. The Kerr spacetime is numerically analyzed for describing the timelike trajectories for spacecrafts in regions outside $(r > 10M_{BH})$ a stellar black hole and for the motion of stars and compact objects in close vicinity of the galactic central supermassive black hole.

# REFRENCES


[1] WHEELER, J.A.: 1968, *Phi Beta Kapper Journal* "*The American Scholar",*Vol.37, No.2, Spring 1968, pp.248.

[2] SCHWARZSCHILD, K.:1916*, Sitzber. Deut. Akad. Wiss. Berlin*, K1. Math-Phys. Tech.,s.189.

[3] CHANDRASHEKHAR, S.:1931, *Astrophysical Journal*. **74,** 81.

[4] LANDAU, L.D.: 1932, *Physikalische Zeitschrift Sowjetunion* **1**, 285.

[5] BAADE, W and F. ZWICKY: 1934, *Proc. Nat. Acad. Sci*. **20,** 254.

[6] OPPENHEIMER, J.R. and G.VOLKOFF: 1939, *Phys. Rev*. **55**, 374.

[7] OPPENHEIMER, J.R. and H. SNYDER : 1939, *Phys Rev*. **56**, 455.

[8] KRUSKAL, M.D.: 1960, *Phys. Rev*. **119**, 1743.

[9] KERR, R.P.:1963, *Phys. Rev. Letts.* **11**, 237.

[10] MISNER, C.W., K.S.THORNE, and J.A.WHEELER :1973, *Gravitation*, Freeman, San Francisco.

[11] HEWISH and OKOYE, S. E.:1965, *Nature* **207**, 4992.

[12] ZEL'DOVICH, Y.B. and I.D.NOVIKOV: 1966, *Astron. Zh.* **43**, 758.

[13] GIACONNI, R., H.GURSKY, F.R.PAOLINI, and B.B. ROSSI: 1962, *Phys.Rev.Lett.***9**, 439.

[14] THORN K.S.: 1994, *Black holes and time warps: Einstein's outrageous legacy,* W.W. Nortan and Co., New York.

[15] Webpage *CHANDRA X-RAY OBSERVATORY*: www.chandra.harward.edu

[16] CHANDRASHEKHAR, S.: 1983, *The Mathematical Theory of Black Holes*, Oxford University Press, New York.

[17] BOYER, R.H and R.W.LINDQUIST: 1967, *J. Math Phys*. **8**, 265.

[18] PENROSE, R. and R.M.FLOYD.: 1971, *Nature Phys. Sci*.,229, 177-9

[19] ISRAEL, W.:1971, *Gen. Rel. & Grav*.**2,** 53

[20] HAWKING, S.W. :1971, *Phys. Rev. Lett*. **26,**1344.

[21]HAWKING, S.W.:1972 *Commun. Math. Phys*. **25**,152.

[22]SHAPIRO, S.L. and S.A. TEUKOLSKY: 1983, "*Black Holes, White Dwarfs, and Neutron Stars. The Physics of Compact Objects"*. Wiley-Interscience, New York.

[23] KIPPENHANH, R. and A. WEIGERT: 1990, "*Stellar Structures and Evolution"*, Springer-Verlag

[24] NOVIKOV, I.D. and K.S.THORNE: 1973 "*Black holes, Les Astres Occults"*, Gordon and Breach Science Publishers.

[25] LAMB, F.K.:1991, in D.M. Lambert (ed.), "*Frontiers of Stellar Evolution*" Astronomical Society of the Pacific.

[26] PETERSON, B.M.:1997, *Active Galactic Nuclei*, Cambridge Univ. Press

[27] ZEL'DOVICH, Y.B. and I.D.NOVIKOV:1964, *Sov. Phys. Doklady* **158**,811.

[28] SALPETER, E.:1964, *Astrophys. J.* **140**, 796.

[29] REES, M.: 1996, in O.Lahv, E.Terlevich, and R.J. Terlevich (eds.). *Gravitational Dynamics*, Cambridge Univ. Press

[30] REES, M.: 1990, Science **247**, N4944, 16 February, p.817

[31] COMASTRI, A :.2011, *The Astrophysical Journal*, 741(2),91.

[32] COLPI M. et al. Joint Evolution of Black Holes and Galaxies, *Taylor and Francis*, 2006.

[33] ZEL'DOVICH, Y.B and I.D.NOVIKOV:1967, Astr. Zh. **10**, 602

[34] ZEL'DOVICH, Y.B and I.D.NOVIKOV:1967, *Relativistic Astrophysics*, Nauka, Moscow.

[35] HAWKING, S.W.: 1971, *Mon. Not. RAS* **152**, 75

[36] CLINE, D.B. and W.HONG: 1992, *Astrophys. J*. **401,** L57

[37] CARTER, B., 1972, *Phys. Rev. Letters*, **26**, 331-3.

[38] ROBINSON, D.C., 1975, *Phys. Rev. Letters,***34**, 905-6.

[39] PENROSE, R., 1969, *Rev. Nuovo Cim.* **1**, 252.

[40] CARTAR, B. 1966, *Phys. Rev.* **141,** 1242-7.

[41] CARTAR, B. 1968, *Phys. Rev.* **174,** 1559-70.

[42] WALKER,M. and R.PENROSE,1970,*Commun. Math. Phys.***18**,265.

[43] FERRARI,V. , Geodesic Motion in Kerr Spacetime, *Sapienza Universita' di Roma*.

[44] BARDEEN, J.,W.H.PRESS, S.A.TEUKOLSKY, 1972,*Astrophysical Journal*,**178**,347.

[45]Goldstein, H. *Classical Mechanics*.

[46] STOGHIANIDIS,E. and D.TSOUBELIS, 1987, *General Relativity and Gravitation*, Vol,**19**,No.12.

[47] MARCK, J.A.,1983, *Proc. R. Soc. Lond*. A 385.431-438.

[48] STOGHIANIDIS,E. and D.TSOUBELIS, 1988, *General Relativity and Gravitation*, Vol,**20**,No.1.

[49] CINDRA, J.L, 1989, *Class.Quantum Grav*. **6**, 857-865.

[50] STOGHIANIDIS,E. and D.TSOUBELIS, 1986*, Phys.Lett.A*, **116**, No.5,213

[51] LENSE,J and H.THIRRING, 1918, *Phys.Z*. **19**,156.

[52] PATTEN, R.A VAN and C.W.F EVERITT, 1976, *Phys. Rev. Lett,* **336**,629.

[53] SCHIFF,L.I.,.1960,*Phys. Rev. Lett*, **4**,215

[54] MARCK,J. -A, 1982 C*.r.hebd. Seanc. Acad. Sci., Paris* I **295**, 185.

[55] TSOUBELIS,D., A.ECONOMOU and E.STOGHIANDIS,1986,*Phys.Lett.A*, **118**,No.3,113.

[56] CARTER, B. 1973, In *Black holes* (ed. C.de Witt & B. de Witt). New York : Gordon and Breach.

[57] PENROSE, R. 1973 *Ann. N.Y. Acad. Sci*. **224**,125.

[58] PIRANI,F.A.E. 1956, *Acta phys. Pol.* **15**, 389.

[59] FARIDI, A.M. (1986), *Gen. Rel. Grav*. **18**,271.

[60] TSOUBELIS, D., et al, 1987, *Phys. Rev. D*, **36**, **4**, 1045-1052.

[61] EISENHAUER, F., *GRAVITY: The AO- Assisted, Two Object Beam Combiner Instrument for VLTI*, astro-ph/0508607.

[62] GHEZ, A. M. et al.,1998, *Astrophys. J*., **509**, 678-686.

[63] SCHODEL, R., et al , 2002, *Nature*, **419**, 694-696.

[64] GHEZ A.M., et al :2005, *The Astrophysical Journal*, **620**:744–757.

[65] EISENHAUER, F. et al,:2005, *The Astrophysical Journal* 628 , 246-259.

[66] ASCHENBACH, B. et al. 2004, *Astron. Astrophys* **417** pp 71-78.

[67] BELL S. C. 1995 : *Computers in Physics* 9, 281 (1995).

# Appendix A

# Mathematica Code for Spherical Polar Orbits and Lense Thirring Effect

```
M=1;

r=10*M;

a= 0.8* M;

Δ=(r^2 + a^2 )-2*M*r ;

Σ=r^2 + (a^2 )*Cos[θ[τ]]^2;

A = (r^2 + a^2 )^2 - Δ *(a^2 )*Sin[θ[τ]]^2;

K=(M*r^4  +(a^2)*r^3 - 3*M*(a^2)*r^2 -a^4*r)/(r^3-

3*M*(r^2)+(a^2)*r +M*a^2)

E=Δ*(K + r^2)/(r^2 +a^2 )^2

Φ=0.0;

k=(a/r^2)*(r^4-M*r^3 + 2*(a^2)+a^4)/(r^4+2*(a^2)*r^2 -

4*M*(a^2)*r +a^4);

h=(a^2)/K;

μ=1;

min=0.01;

max=500;

Q=K -(a^2)*E^2

deltaphi=(2*M*a*E*r*(Pi/2)*(1+(k^2)/4)*(360)/(2*Pi*Δ*(
Q^0.5)))

Tt=4*E*(r/Δ*Q^(0.5))*(r^3 +(a^2)*(2*M
```

```
+r))*EllipticK[k]+4*E*Q^(0.5)*(1-E^2)^(-
1)*(EllipticK[k] -EllipticE[k])
Ttau=4*(r^2/Q^(0.5)) EllipticK[k] +4*Q^(0.5)*(1-
E^2)^(-1) (EllipticK[k]-EllipticE[k])
EllipticK[k];
EllipticE[k];
Ψ = 4*E*r^2*((K-
a^2)/((K*Q)^(0.5)*(K+r^2)))*EllipticK[k]-4*E*((K-
a^2)/(K*Q)^(0.5))*(EllipticK[k] - EllipticPi[h,k])
s=NDSolve[
          {
   t'[τ]==(Δ*Σ)^(-1)*(A*E-2 M*a*r*Φ),
*   (θ'[τ])^2 □(K -(μ^2)*a^2*Cos[θ[τ]]^2 -(a*E
Sin[θ[τ]]-Φ/Sin[θ[τ]])^2)/(Σ^2),
   ϕ'[τ]==Δ^(-1) ((2 M*r/Σ))*a*E +(1-
2*M*r/Σ)*Φ/Sin[θ[τ]]^2,
   θ[0]==0,
   t[0]□0,
   ϕ[0]==0
    },
          {t,θ,ϕ},
          {τ,min,max}]
gos =Plot[{θ[τ],ϕ[τ]}/.s[[1]], {τ,min,max},Frame→True]
```

```
ParametricPlot3D[{r*Sin[θ[τ]] Cos[ϕ[τ]],
                  r*Sin[θ[τ]] Sin[ϕ[τ]],
                  r*Cos[θ[τ]]}/.s[[1]],
{τ,min,max},ColorFunction→"DarkRainbow",PlotStyle→Thi
c
k,MeshStyle→Directive[Red],PlotLabel→"1",LabelStyle→{
B
old,FontFamily-
>"Helvetica",FontSize→14},AxesLabel→{Style[x,24],Styl
e
[y,24],Style[z,24]}]
ParametricPlot[{r*Cos[ϕ[τ]]*Sin[θ[τ]],
                  r*Sin[ϕ[τ]]*Sin[θ[τ]]}/.s[[1]],
{τ,min,max},PlotStyle→{Red,Thick},MeshStyle→Directive
[
Red],PlotLabel→"2",LabelStyle→{Bold,FontFamily-
>"Helvetica",FontSize→14},AxesLabel→{Style[x,24],Styl
e
[y,24]}]
gos=ParametricPlot[{r*Cos[ϕ[τ]]*Sin[θ[τ]],
                   r*Sin[ϕ[τ]]*Sin[θ[τ]]}/.s[[1]],
{τ,min,max},PlotStyle→{Red,Thick},MeshStyle→Directive
[
Red],PlotLabel→"2",LabelStyle→{Bold,FontFamily-
>"Helvetica",FontSize→14},AxesLabel→{Style[x,24],Styl
e
```

```
[y,24]}]

gos= ParametricPlot3D[{r*Sin[θ[τ]] Cos[ϕ[τ]],

                       r*Sin[θ[τ]] Sin[ϕ[τ]],

                       r*Cos[θ[τ]]}/.s[[1]],

{τ,min,max},ColorFunction→"DarkRainbow",PlotStyle→Thi
c

k,MeshStyle→Directive[Red],PlotLabel→"1",LabelStyle→{
B

old,FontFamily-

>"Helvetica",FontSize→14},AxesLabel→{Style[x,24],Styl
e

[y,24],Style[z,24]}]
```

# Appendix B

# Fortran code for plot of Effective Potential in Kerr Metric

```
    implicit none

    integer i, N

    parameter (N=50000)

    real r(N),V,t(N),tau(N),E,K,M,a,h,D,S,Ap,theta(N)

    real phi(N)

    M=1.0
```

```
      a=0.8*M

      E=0.976

      K=24.0

      r(1) = 1.51*M

      theta(1)=0.0

      phi(1)=0.0

      h =0.1


      do i =1,N-1


      S= r(i)**2.0 + a**2.0*Cos(theta(i))**2.0

      D = r(i)**2.0-2.0*M*r(i)+a**2.0

      Ap= (r(i)**2.0 + a**2.0)**2.0 - a**2.0*D*Sin(theta(i))**2.0

       V = D*(K + r(i)**2.0)/(r(i)**2.0 + a**2.0)**2.0


c      K= (M*r(i)**4.0-a**2.0*r(i)**3.0 - 3.0*M*a**2.0*r(i)**2.0 +

c     & a**4.0*r(i))/(r(i)**3.0-3.0*M*r(i)**2.0 + a**2.0*r(i) + M*a**2.0)


c       E = D*(r(i)*2.0 + K)/(a**2.0 + r(i)**2.0)
```

```
 tau(i+1) = tau(i) + h


  r(i+1)= r(i) + h*((r(i)**2.0  +a**2.0)**2.0
&     *(E**2.0 - V)/S**2.0)**(0.5)


   theta(i+1) = theta(i) + h*((K-(a**2.0)*E**2.0 -
& a**2.0*(1-E**2.0)*cos(theta(i))**2.0)/S**2.0)**(0.5)


  phi(i+1) = phi(i) + h*(2*M*a*E*r(i)/(D*S))




  write(6,*) r(i), E,V,K
  write(1,*) r(i),E
  write(2,*) r(i),K
  write(3,*) log(r(i)/M), V


    enddo
```

```
      end
```

# Appendix C

# Fortran code for spherical polar orbit using Euler Method for differential equations

```
      implicit none
      integer i, N
      parameter (N= 3000)
      real r, t(N), tau(N), theta(N), phi(N),M,E,K,a,S,Ap,D,h
      open(unit = 1, file= 'sphericalpolarorbit.dat' )

      M= 1
      a =0.8*M
      r =10*M
      E = D*(K + r**2.0)/(r**2.0 + a**2.0)**2.0
      K = (M*r**4.0 + a*r**2.0 - 3.0*M*a**2.0*r**2.0
     &   +a**4.0)/(r**3.0 - 3.0*M*r(i)**2 + a**2.0*r+ M*a**2.0)
      tau(1)=0.0
      theta(1)=0.0
```

```
      phi(1)= 0.0

      h= 0.1


     do i = 1,N


      S= r**2.0 + (a**2.0)*cos(theta(i))**2.0

      D= r**2.0 + a**2.0 - 2*M*r

      Ap = (r**2.0 + a**2.0)**2.0 - D*(a**2.0)*sin(theta(i))**2.0


     tau(i+1)= tau(i) + h


    t(i+1)=t(i)+ h*(A*E/(D*S))


    theta(i+1) = theta(i) + h*((K-(a**2.0)*E**2.0 -
   & a**2.0*(1-E**2.0)*cos(theta(i))**2.0)/S**2.0)**(0.5)


    phi(i+1) = phi(i) + h*(2*M*a*E*r/(D*S))
```

```
      write(6,*) tau(i),t(i),theta(i),phi(i)
      write(1,*) r*sin(theta(i))*cos(phi(i)),
     & r*sin(theta(i))*sin(phi(i)),r*cos(theta(i))

      enddo
      end
```